Ministry of Education and Science of Ukraine

Ministry of Economy of Ukraine

Ukrainian State University of Railway Transport

State Enterprise "Ukrainian Scientific Railway Car Building Research Institute"

I.E. MARTYNOV, A.V. TRUFANOVA, O.M. SAFRONOV

AXLEBOX ROLLER BEARINGS FOR RAILWAY VEHICLES: DESIGN AND CALCULATIONS

Monograph

2022

UDC *629.4.027.115*

Recommended for publication by the Scientific and Technical Council of the State Enterprise «Ukrainian Scientific Railway Car Building Research Institute» (Minutes No. 2 dated December 22, 2022)

Reviewers:

D.Sc., Professor of the Department «Wagons and Wagon Facilities» of the Ukrainian State University of Science and Technology Muradian Leontii Abramovych

D.Sc., Professor of the Department «Electric transport and diesel locomotives construction» of the National Technical University «Kharkiv Polytechnic Institute»

Masliiev Viacheslav Heorhiievych

Axlebox roller bearings for railway vehicles: design and calculations: monograph / I.E. Martynov, A.V. Trufanova, O.M. Safronov

ISBN 978-966-97716-7-4

This monograph is a set of studies that naturally combines the original theoretical developments of the authors concerning the increasing the reliability of axle box bearings by solving applied problems of creating samples of state-of-the-art machinery with the best operational characteristics. The joint work of the authors resulted into the introduction of serial industrial production of the competitive and highly reliable rolling-contact bearings of the new generation for wheel pairs of domestic passenger and freight cars.

The monograph is intended for scientists and engineering and technical staff of the bearing industry and railway transport, engaged in research, calculations, testing and design of roller bearings. The results of the work can be used in the design of roller bearings that take significant dynamic radial and axial loads, as well as machines of heavy modes of operation (lifting, road, mining machines).

ISBN 978-966-97716-7-4 **UDC *629.4.027.115***

INTRODUCTION

Roller bearings are used in all branches of mechanical engineering. The operational characteristics of bearings largely determine the technological level of mechanical engineering development and product competitiveness. This is especially relevant for domestic railway vehicles, which provide a powerful passenger transit and freight flow through the territory of Ukraine. Therefore, the production and operation of innovative bearings of the new generation with increased reliability for railway transport is becoming a strategic objective, the implementation of which guarantees the economic independence of Ukraine.

Rolling-contact bearings of wheel sets for railway rolling stock are referred to bearing assembly of machines with heavy operation modes, where cylindrical, tapered and spherical roller bearings are used to absorb high dynamic loads. Nowadays, the vast majority of the fleet of domestic freight and passenger cars is equipped with cylindrical roller bearings.

But the development of rolling-contact bearings for wheel-sets and locomotives is often based on conventional mechanical engineering techniques, without proper analysis and evaluation of the quality of their design, which would provide a scientifically sound choice of the most effective design and technological solutions. Existing ways to enhance the efficiency of the roller bearings of the wheel pairs of railcars are aimed at solving local problems of upgrading their design while improving primarily the contact endurance of the rings and rolling elements. In order to effectively solve the problem of enhancing the technical level of such bearings, it is necessary to systematically improve their basic parameters, at the same time the increase of some ones will not contribute to the deterioration of others.

This monograph is a set of studies that naturally combines the original theoretical developments of the authors relative to increasing the reliability of axle box bearings by solving applied problems of creating samples of state-of-the-art machinery with the best operational characteristics. The joint work of the authors resulted into the introduction of serial industrial production of the competitive and highly reliable rolling-contact bearings of the new generation for wheel pairs of domestic passenger and freight cars.

The monograph is intended for scientists and engineering and technical staff of the bearing industry and railway transport, engaged in research, calculations, testing and design of roller bearings. The results of the work can be used in the design of roller bearings that take significant dynamic radial and axial loads, as well as machines of heavy modes of operation (lifting, road, mining machines).

The authors thank the reviewers for their attention, valuable scientific advice and comments.

1. ANALYSIS OF THE MAIN TRENDS IN THE DEVELOPMENT OF AXLEBOX BEARING ASSEMBLIES DESING

The history of the development of railway transport shows that the first locomotives and wagons were equipped with plain friction bearings. In comparison with them, the advantages of roller bearings are not in doubt [61]. The main ones are as follows:

• reduction in specific resistance to motion and, as a consequence, reduction in fuel or electricity consumption by locomotives;

• the possibility of increasing the speed and weight of trains, which increases the train-handling and carrying capacity of railways;

• reduction in resistance to movement at the start of moving in 7 - 10 times; the value of resistance does not depend on the parking time and outside air temperature;

• a sharp reduction in the amount of axle boxes maintenance in operation, which allows to significantly reduce the technical engineering staff;

• significant reduction in the use of non-ferrous metals;

• great savings in lubricants, as well as the complete elimination of the cost of lining materials and the need for seasonal oil change;

•greater reliability and durability of roller bearings compared to plain friction bearings, which made it possible to increase the length of nonstop runs of railway vehicles and change the system of repair and maintenance.

Roller bearings were first used in railway rolling stock more than 100 years ago. In the first axle box assemblies, which appeared in 1903 in Germany (Fig. 1.1) and in 1907 in Sweden, ball bearings were used. Operating experience has shown that ball bearings have a low load capacity and the load-bearing capacity of such bearings is very low [35].Therefore, already in 1913 in Germany cylindrical roller bearings were first used in the axle boxes of rolling stock. The most successful was the axle box DVF type (Fig. 1.2), in which the rollers were released from the axial load by installing a thrust ball bearing.

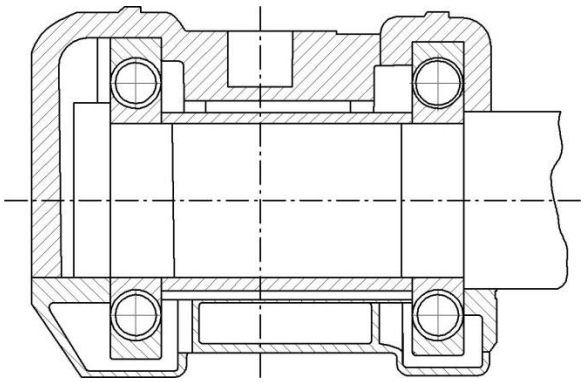

Fig. 1.1.The first design of the axle box with rolling bearings.

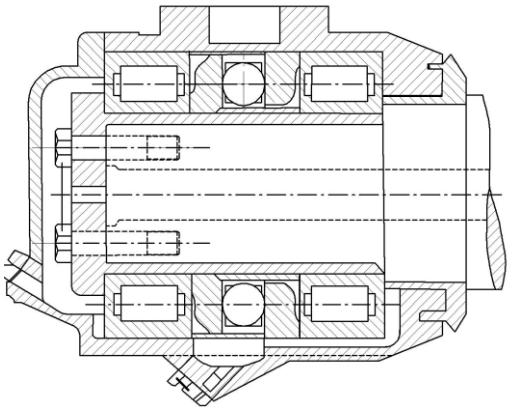

Fig. 1.2. A DVF type axle box

The most important step that accelerated the introduction of roller bearings on rail transport was the invention of spherical roller bearings in Sweden (Fig. 1.3).

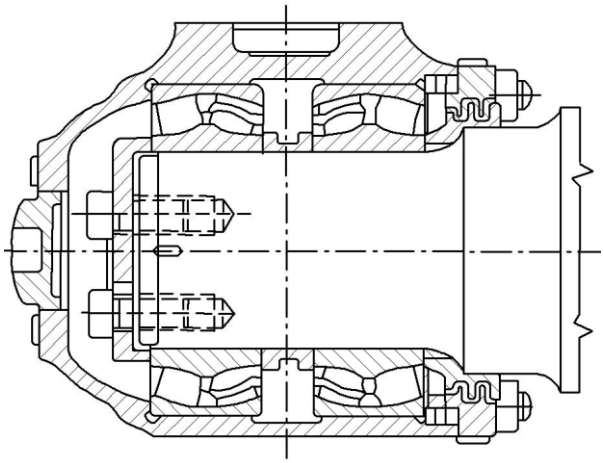

Fig. 1.3. An axle box with two spherical bearings.

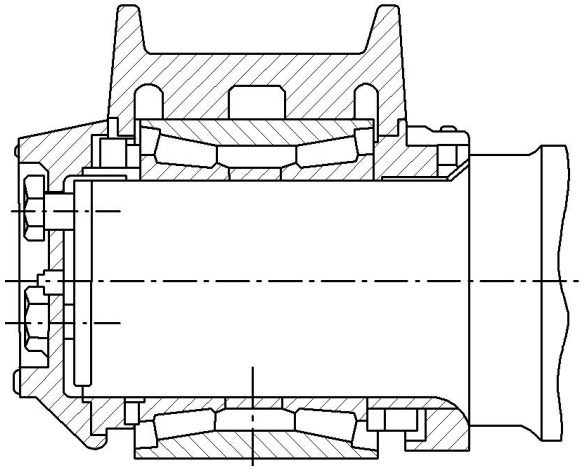

Fig. 1.4. Timken axle box with double row tapered roller bearing.

These bearings inherited a high load capacity from cylindrical roller bearings. The spherical shape of the raceway of the outer ring allowed them to take both radial and axial forces in rolling friction, and also allowed the roller to occupy the optimal position relative to the rings.

Around that time in the USA the designers of the company "Timken" created a double-row tapered roller bearing (Fig. 1.4), which has similar characteristics. In various combinations, the above-mentioned designs are still used in rolling stock in different countries.

1.1. Analysis of the development of domestic designs of axlebox bearing assemblies of railway vehicles

The domestic search for an efficient design of axle box assemblies for the transfer of the railcar fleet to roller bearings began at the turn of the 40s and 50s of the last century. Until now, little experience in the operation of roller bearings in the axle boxes of main passenger cars, axle boxes of suburban electric multiple assemblies and metro cars has been gained [118].

Therefore, when deciding on the choice of the type of roller bearing for main-line railway vehicles, it was necessary to take into account all the accumulated operating experience of roller bearings in the axle boxes of long-distance railway vehicles and electric multiple assemblies.

The research had to find answers to a number of questions:

• how freight cars with roller bearings will behave when rolling down the slopes;

• what effect a unilateral braking on the operation of the roller bearing has;

• how to keep the railway vehicle from unauthorized access to the railway stations tracks located on slopes and und in strong winds.

In addition, many other technical, operational and economic problems had to be solved.

The choice of a standard type of the axle box assembly was preceded by a three -year work to design a reliable and efficient design of a bearing, ensure reliable operation of the wheel axle, develop a rational axle box body, sealing, identifying conditions under which friction losses will be minimal.

At that time, the least suitable for operation were tapered roller bearings, which were very sensitive to skew and required careful adjustment of the gaps [114].

Therefore, at the first stage, three versions of axle box assembly for passenger cars with cylindrical and spherical bearings were designed and tested. Bearings on the bushing fit with dimensions of 130 × 280 × 93 mm were used. Two cylindrical roller bearings or two spherical bearings, or one cylindrical and one spherical bearing were installed in the axle box.

During operation, numerous damages to riveted cages of cylindrical bearings, destruction of thrust bearing rings of cylindrical bearings, shells from fatigue on the raceways of the outer rings of spherical bearings were detected. The fracture of two axle necks was detected in wheel pairs that were in operation less than 45 - 50 thousand km. In a significant number of wheel sets, inspections revealed cracks in the axle necks, which were located near the neck fillets at the end of the mounting bushing. Therefore, they were forced to install bearings of larger dimensions 135 × 300 × 102 mm, which had a greater dynamic capacity. The diameter of the axle neck was increased from 130 to 135 mm to compensate for the increased bending moment.

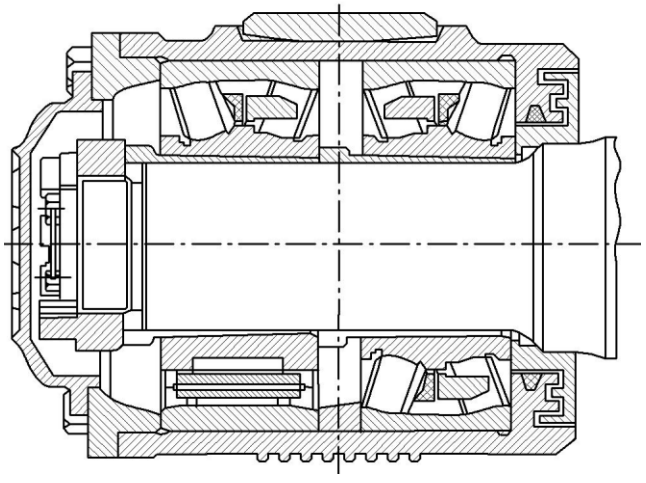

Fig. 1.5. An axle box with spherical and cylindrical bearings produced in 1952-1953.

The option with two cylindrical bearings on the axle neck was excluded due to the impossibility of inspecting the condition of the rear bearing cage. That's why the wagons were equipped with two versions of axle box assemblies. In the first version, two spherical bearings were installed in the box (Fig. 1.5, upper part), in the second - one spherical (rear) and one cylindrical (front) (Fig. 1.5, lower part).

The bearings were end mounted on the axle neck by means of a crown nut, a locking bar and two bolts. The diameter of the axle neck was 135 mm; outer diameter of bearings was 300 mm. The axle boxes had two types of seals: labyrinthine

and felt ring sealing. The weight of the axle box assembly with the neck and abutment was 300 kg in passenger cars and 215 kg in freight cars.

In the batch of freight cars, the load on the axle box was transmitted through a spherical slider (Fig. 1.6). This support provided the possibility of turning the axle box relative to the bogie by increasing the gaps between the guide jaws along the bogie from 7 to 14 mm and across from 10 to 16 mm.

Wagons equipped with such bearings were sent in April-May 1953 for trial operation in freight and passenger cars formation [82].

Operation of passenger cars in winter 1952 - 1953 showed that the new axle box assemblies do not provide normal operating conditions.

By April 1953, at a run of 40-80 thousand km, there had been three cases of axle necks fractures detected.

Inspections of wheel sets revealed multiple cracks in the axle necks.

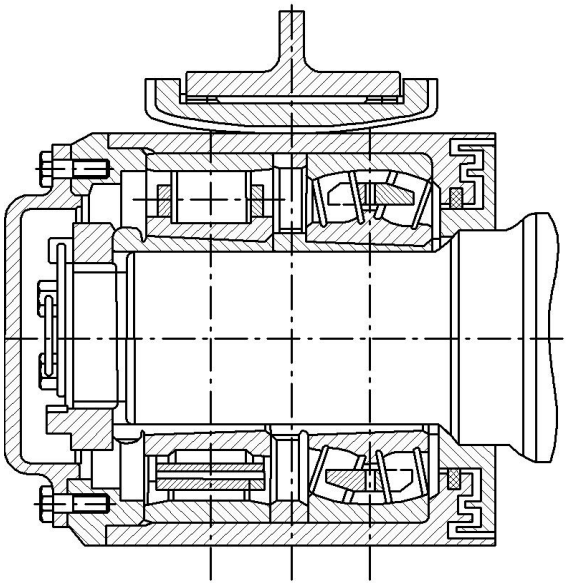

Fig. 1.6. An axle box with a spherical insert.

For some reason, the Moscow-III depot lacked up to 23% of axles in some months. In cylindrical bearings, numerous destruction of brass riveted cages due to the breakage of the rivets occurred.

In spherical bearings, abnormal operation of the inner ring sides, damage caused by fatigue of the inner raceways and especially of the outer rings, ruptures of the inner rings were detected.

Tests to determine the resistance to movement showed that cars equipped with such bearings had even greater resistance to resistance than cars with plain bearings.

Also a disadvantage of such axle boxes was the increased weight of the axle box assemblies (body weight is 140 kg, bearings are 74 kg).

In addition, the operation of freight wagons demonstrated an unsuccessful design solution concerning the support of the bogie frame on the axle box. This triggered the spherical slider, the axle box assembly housing and the side bogie frames. As a result, the radial load was perceived by three rollers, and the central roller received 48% of the total load, which dramatically reduced the durability of the bearings.

Unsatisfactory performance of roller bearings led to the decision to return to the production of passenger cars with plain friction bearings.

In compliance with specially developed specification, taking into account the improvement of the bearings quality, the bearing manufacturing and railcar build-

ing industry agreed to produce a pilot batch of freight and passenger cars with bearings with an outer diameter of 280 mm, a 135 mm inner diameter and a 93 mm width. This made it possible to reduce the weight of one axle assembly of a passenger car by 80 kg compared to bearings with dimensions of 135 × 300 × 102 mm.

For a greater reduction in the size of roller bearings at that time there were no real conditions, although bearings of much smaller size and weight (diameter 250 - 260 mm and weighing about 20 kg instead of 28.5 kg for bearings with a diameter of 280 mm) were abroad used.

In 1954-1955, the industry created a new experimental batch of railway vehicles with roller bearings of the overall dimensions of 135 × 280 × 93 mm [82] for operational tests. This made it possible to reduce the weight of one passenger car by 80 kg.

For comparative testing, shuttle freight cars operating in different climatic conditions were provided.

The axle boxes of the cars of these routes were equipped with:

• two spherical bearings on the bushing fit TsKB-545 with a diameter of 135 × 280 × 93 mm;

• one spherical bearing near the axle neck filler and one cylindrical bearing at the end of the axle neck (both bearings on the bushing fit, size 135 × 300 × 102 mm);

• two cylindrical bearings on hot fitting with bearing dimensions of 135 × 280 × 93 mm (Fig. 1.7);

• one spherical bearing on a bushing fit with 135 × 320 × 128 mm (fig. 1.8) dimensions.

In axle box assemblies of the passenger cars, in addition to the above options, tested axle box assemblies with the installation of bearings on the stepped axle neck, where the cylindrical bearing on hot fit was located near the axle neck, and spherical one on the bushing fit at the end of the neck. The dimensions of the bearings were 135 × 280 × 93 mm.

Cages of cylindrical roller bearings were made of brass, steel, cast iron (the latter were tested only in the axle boxes of freight cars).

Cages of cylindrical roller bearings were made of brass, steel, cast iron (the latter were tested only in the axle boxes of freight wagons).

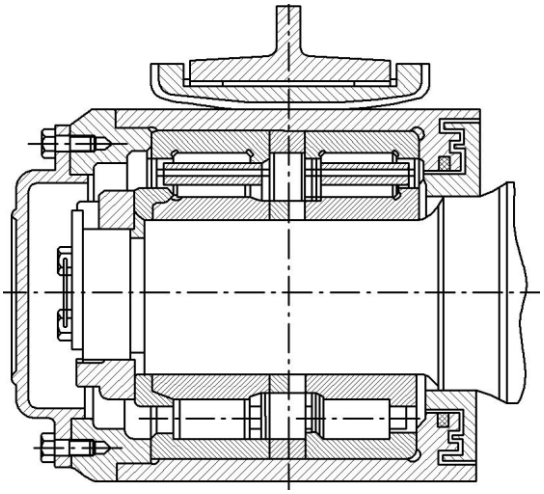

Fig. 1.7. An axle box with two cylindrical bearings

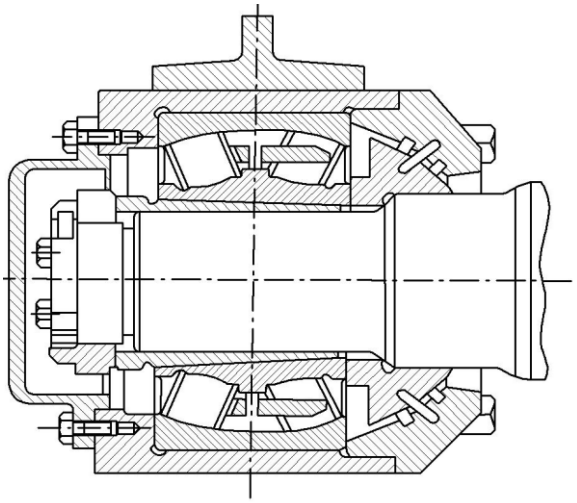

Fig. 1.8. An axle box with one spherical bearing

Tests have shown that the use of a freight car axle box assembly with one spherical bearing in bogies MT-50 or TsNII-X3 (which do not have a cross link between the side frames) for speeds greater than 20.83 m/s (75 km/h) is not possible due to the increased swaying of the car, which causes the danger of derailment.

For non-pedestal bogies of passenger cars, this design was also unpromising. The reasons were frequent failure of the outer bearing rings and unreliable operation of the cages.

The operation of different versions of the experimental axle box assembly showed that the design with two cylindrical bearings on hot fit was rejected in the first winter due to the destruction of the cages, despite the fact that the diameter of the rivet at the cage was increased from 4 to 5 mm. In the axle boxes of freight cars, where the cages functioned more reliably, only a weakening of the rivets, as well as an increase in the diameter of the inner rings and the loss of their tension occurred.

During in-service tests bearing rings of spherical bearings most often failed, but much less frequently than in previous manufacture.

Tests to determine the resistance to movement of passenger and freight cars showed that railway vehicles with roller bearings of a 280 mm diameter in the range of speeds 50 - 70 km/h reduced the movement resistance compared to wagons with sliding bearings by 8 - 10%.

Taking into account the results obtained from the operation of the experimental batch of vehicles, in 1955, roller bearings with overall dimensions of 135×280×93 mm were proposed to be installed: spherical 73727 and cylindrical 72727 ones (Fig. 1.9).

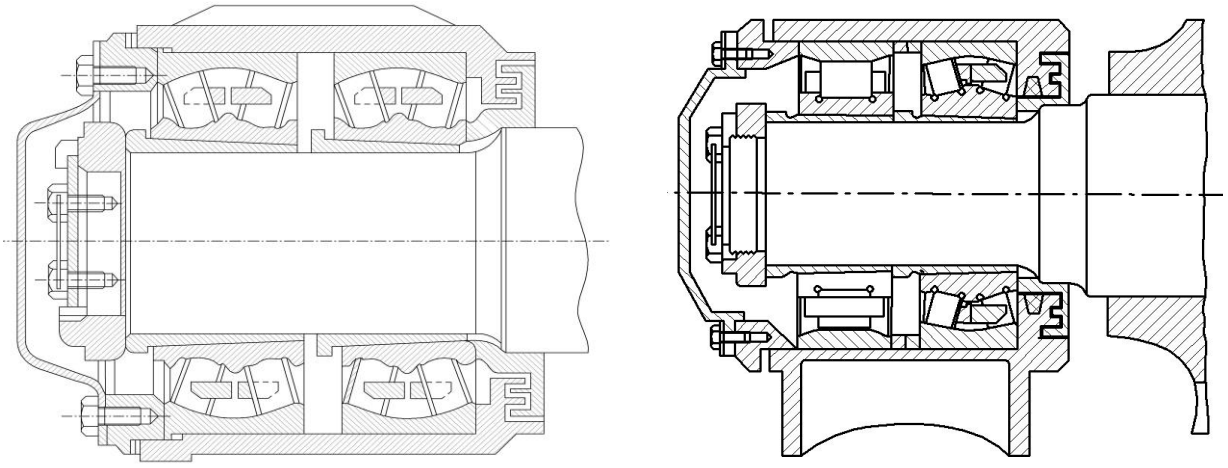

Fig. 1.9. An axle box assembly with bearings on a bushing fit:
a – with two spherical ones; b - spherical and cylindrical

Operational tests made it possible to identify the advantages and disadvantages of spherical roller bearings. The main advantage of the latter is the ability to perceive both axial and radial forces in the rolling friction mode, as well as the possibility of self-installation, as a result of which the selection of paired bearings is simplified due to greater tolerances for the difference in radial clearances. In addition, the bushing fit makes it possible to mount the axle box assembly practically without selecting bearings to the axle neck, and also relieves the end mount due to the transfer of axial forces directly to the mounting surface of the neck.

The disadvantage is the increased labor intensity of assembly and disassembly work, the presence of an additional part (fastening bushing), which requires an exact match of the taper of both the bushing and the holes of the inner rings of the bearings. But the main disadvantage is the lower radial load capacity and, as a result, the relatively low durability of spherical bearings compared to cylindrical bearings of the same dimensions.

The use of rollers in the form of a symmetrical barrel in spherical bearings makes it possible to create a linear contact between the rollers and the outer ring, which increases the load capacity of such bearings. However, at the same time, the internal resistance to the rotation of the bearing increases (3-4 times greater than that of cylindrical bearings). This causes a significant increase in train traction costs.

In addition, the transition to use of roller bearings with a diameter of 280 mm from sliding bearings in freight cars was accompanied by a sharp increase in the weight of the vehicle (145 kg instead of 102 kg). Therefore, the use of such bearings in freight cars could not be considered as a final solution.

At the same time, operational experience showed that cylindrical roller bearings are very resistant to fatigue damage, unlike spherical roller bearings, which were characterized by fatigue damage.

Therefore, work on improving the reliability of cylindrical roller bearings continued. In particular, to improve the performance of riveted cages, a transition from brass to steel cages was made. At the same time, the cross-sectional area of

the bearing cage and the diameter of the rivet increased to 6 mm instead of 5 mm. The operation of passenger cars equipped with such bearings showed that the riveted connection of the cage practically stopped collapsing, but a new type of cage failure appeared, i.e., fatigue fracture along the crack in the corner of the transition from the bridging section to the cage body. The measures taken (rounding the corner, removing chamfers) slowed down the process of destruction of the cages, but did not stop it.

Another significant drawback was found, i.e., an increase in the diameter of the inner rings during hot fitting of the bearings, which leads to a weakening of the fit tension and a decrease in the radial clearance of the bearing.

It was also established that with a decrease in the diameter of the bearings, the cost of equipping wagons with roller bearings significantly decreases. The technical and economic efficiency of the application of roller bearings increased especially when moving to structurally simpler and cheaper cylindrical bearings with a hot fit on the axle neck.

In 1957-1958, cylindrical roller bearings with an outer diameter of 250 mm were used for the first time in a new batch of freight and passenger cars. The transition to such bearings made it possible to reduce, compared to bearings with an outer diameter of 280 mm, the weight of the vehicle on passenger cars by 23 %, and on freight cars by 20 %, and to reduce the diameter of the axle neck from 135 to 130 mm.

In the course of the operational tests, the following types of axle box assemblies were tested:

• equipped with cylindrical bearings on a thermal fit (No. 42726, which were installed near the neck of the axle and No. 232726, which were installed near the end of the axle neck). The dimensions of the bearings were 130×250×80 mm. Bearings of domestic production were equipped with brass cages, and "Steyer" ones with steel cages;

• two spherical bearings of the "C" type (the rollers had the shape of a symmetrical barrel) on a bushing fit with a size of 130×250×88 mm;

• a combination of spherical bearing TsKB-1520 type "C" near the flange of the axle neck and cylindrical one TsKB-1530 near the end of the neck on the bushing. The dimensions of the bearings are 130×250×88 mm;

• one spherical bearing of the "C" type on the TsKB-1523 on thermal fit with dimensions 130×280×93 mm.

The bearings are end mounted on the axle neck in two ways: with the use of an M110 end nut or a disk spring washer and three M20 bolts.

Railway cars with the specified axle box assemblies were subjected to various types of tests: operational in different climatic conditions, special comparative tests on resistance to movement and moving from a place. In addition, the bearings were subjected to bench tests for durability and friction moment. Box bodies were tested on the stand in order to study the rational distribution of the load on bearings and rollers.

Examination of experimental axle box assemblies carried out after the run of 140 – 170 thousand km, revealed the advantages of cylindrical roller bearings No. 42726 and No. 232726 with a rivetless brass cage compared to all other experimental bearings (in particular, manufactured by foreign companies). During inspections in the boxes of passenger cars, bearings with rivetless cages turned out to be the only ones that did not have cage damage.

Comparative tests to determine movement resistance showed that cylindrical bearings provide a reduction in specific movement resistance at speeds from 20 to 90 km/h, respectively, from 25 to 17.5%. This makes it possible to reduce fuel or electricity consumption for train traction by an average of 11%.

Railway cars on "SKF" spherical bearings with dimensions of 130×250×86 mm compared to wagons on cylindrical bearings had 10-15 % more movement resistance.

Thus, in terms of operational reliability and energy gain, hot-fit cylindrical roller bearings No. 42726 and No. 32726 with rivetless bearings cages were the best of all tested.

In the variant adopted for serial introduction, two bearings with cylindrical rollers are installed in the box (Fig. 1.10).

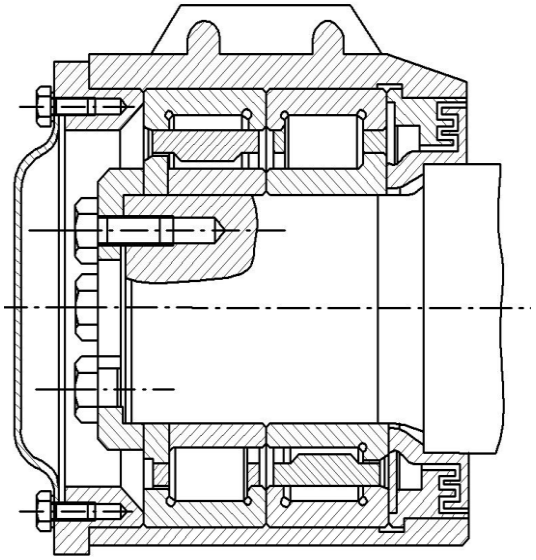

Fig. 1.10. The box assembly of a freight car with cylindrical roller bearings on a thermal fit

The inner rings of the bearings are installed directly on the neck of the axle in a hot state and have a massive rivetless cage.

A design feature of the adopted box assembly option is the installation of bearings close to each other without intermediate distance rings.

The end mounting of the bearings on the neck of the axle was fastened with a hexagonal nut with a diameter of 110 mm.

Since 1971, in addition to fastening with a nut, a fastening made of a disk spring washer, which is attached to the end of the axle with three or four bolts with a diameter of 20 mm has been used in the axles of freight cars.

The bushing seal consists of grooves located in the labyrinth part of the bushing body. The upper part of the axle box body of the passenger cars is made with a variable section, which ensures a rational distribution of the load between the rollers and increases their durability. In order to ensure a better distribution of the load between the rollers and along the generator of the rollers and rings, to increase the durability of the upper part of the body of the box, stiffening ribs are

introduced into the axle box of freight cars, located along the axes of the bearings, and to eliminate overloading of the ends of the rollers and inner rings, the length of the supporting surface of the ribs is limited to 110 mm.

For a more even distribution of the load between the front and rear bearings, the axle box body of the freight cars had a pressed-in labyrinth part. In passenger cars, the axle box has a solid body.

In freight cars with roller bearings, the frame of the car frame rests directly on the box.

Equipping wagons with cylindrical roller bearings makes it possible to significantly reduce the weight of the vehicle and the axle weight of the wheel pair (Table 1.1).

Table 1.1

Comparative characteristics of axle boxes of freight cars

Type of the axle box assembly	Weight, kg			
	bearings	housings	other parts of the axle box assemblies	Total
with spherical bearings No. 73727 and No. 72727	57,0	58,5	29,5	145,0
with cylindrical bearings No. 232726 and No. 42726	38,0	51,5	17,5	107

Installing bearings in a box without spacers makes it possible to shorten the neck of the axle and reduce stress in it and the harmful effect of bending on the redistribution of the load along the generators of rollers and rings. In addition, this installation of bearings is rational for increasing the strength of the axle neck and obtaining a lower mass of the axle box assembly.

Thus, when switching to cylindrical bearings with a diameter of 250 mm, a wheel pair in a composition with roller bearings had a lower mass than a wheel pair with sliding bearings, and the tare weight of the wagon, compared to wagons with roller bearings with a diameter of 280 mm, decreased by 360-370 kg The tare weight of the passenger car decreases by about 400 kg when switching to bearings with a diameter of 250 mm.

An attempt was made by the Ministry of Railways to design an axle box assembly with bearings of a 230 mm diameter. Compared to a 250 mm diameter cylindrical bearing, the 230 mm diameter bearing has a 21.5% reduction in weight and a 3.5% reduction in estimated life. However, due to unsuccessful test results, it was not possible to implement such a design [35].

V. F. Novikov and A. P. Krasiukov [63, 76, 83] proposed to increase the elasticity of the bearing by using hollow rollers (Fig. 1.11).

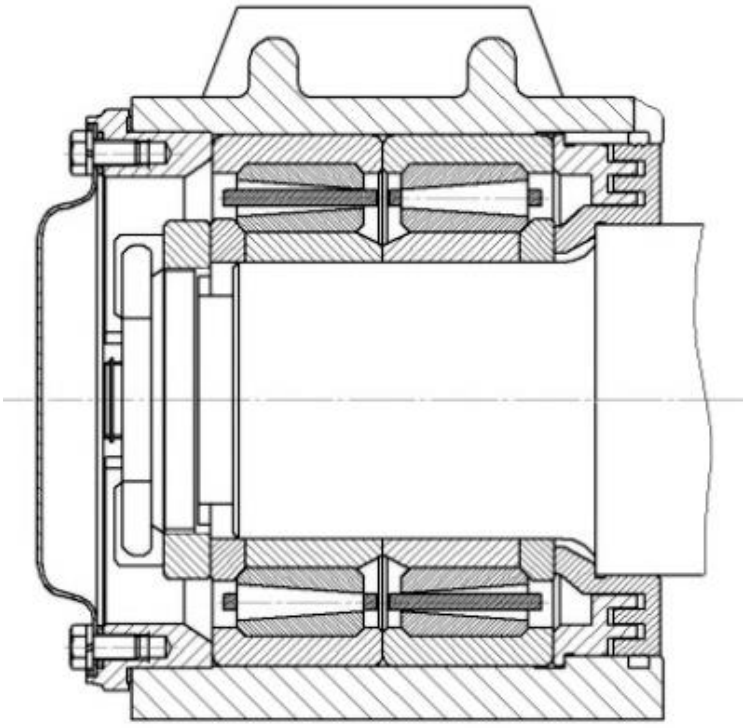

Fig. 1.11. An axle box assembly with bearings equipped with hollow rollers

Previous studies have shown that bearings with such rollers have a high ability to evenly distribute the radial load on the rollers of the load zone. Taking advantage of this, the stress concentration along the contact line of the rolling elements should decrease, and the thermal mode of the bearing should improve [75]. However, the tests showed that hollow rollers have insufficient strength, and their use had to be abandoned.

Great hopes were placed on the use of elastic elements [21] in boxes or changing the stiffness of the elements of the upper part of the axle box by introducing cavities of different configurations into its construction (Fig. 1.12 – 1.13) [20].

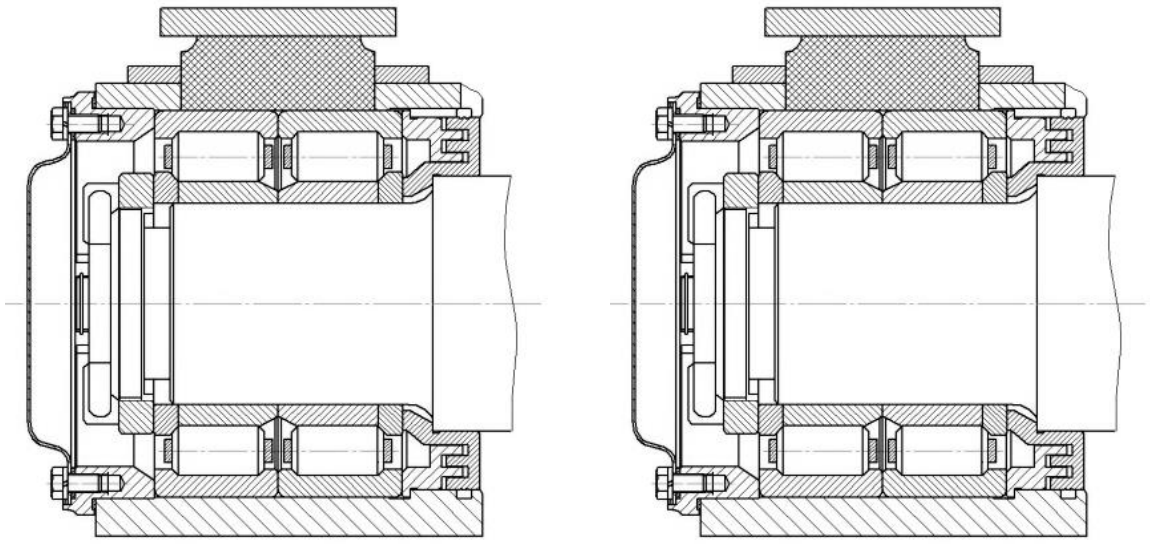

Fig. 1.12. Axle box assembly with a rubber elastic element:
a – without a housing (with adapter)
b –with a housing and a rubber element in the upper part

It was assumed that the use of elastic elements (rubber) would make it possible to more evenly distribute the radial loads on the bearings, reduce the magnitude of the acting axial forces, and reduce the influence of the wagon on the upper structure of the railway track.

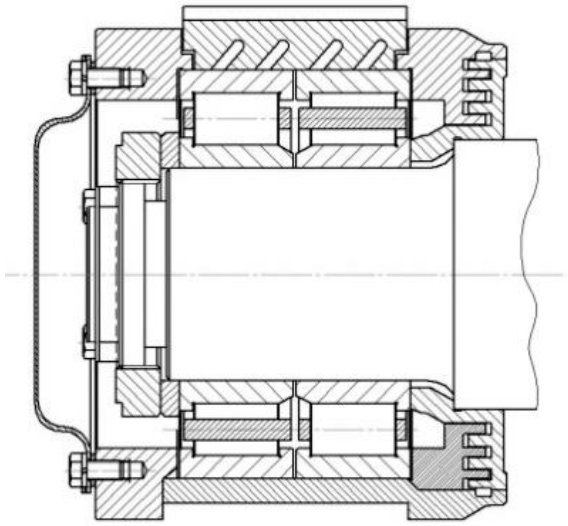

Fig. 1.13. Non-housing axle box assembly with adapter

However, during testing, it was found that the service life of the rubber strips is significantly shorter than the service life of the rest of the axle box elements, and it is technologically impossible to replace the elastic element without carrying out a full revision of the axle box [112].

The use of an adapter with grooves of variable depth turned out to be impossible due to technological difficulties.

Due to the fact that cylindrical roller bearings in typical bushings accept all types of loads (radial and axial), a number of studies are devoted to increasing the bearing capacity of bearings of this type in the axial direction. Thus, the causes of cracks in the sides of the rings and measures to prevent them are proposed by V. M. Tsiurenko in the article [113].

The possibilities of increasing the axial load capacity of cylindrical roller bearings are analyzed in the article [50]. They are divided into two groups: changing the shape of the end of the roller and changing the geometric parameters of the supporting flange in order to ensure the consistency of the oil wedge between the end of the roller and the side.

The assessment of the axial load capacity of locomotive bearings, taking into account the vertical skew and the actual contact area of the roller end, is presented in the article [22].

One of the ways to increase the axial load capacity is to improve the lubricant parameters, in particular, the introduction of anti-seize additives into it [81, 108].

An alternative way is to optimize the contact of the ends of the rollers with the sides of the rings in order to ensure a favorable hydrodynamic mode of lubrication of the rubbing surfaces. To solve this problem, O. M. Filatova, V. S. Martynov and others. [105, 104, 106] suggested using rollers with rounded ends. The authors considered various shapes of the rounded ends of the rollers, determined the radii of their rounding to ensure the best conditions for lubrication and to minimize friction in contact between the roller and the board. However, it should be noted that

the change in the shape of the end of the roller is associated with a significant complication of its manufacturing technology. Taking into account the mass production of rollers, this will inevitably lead to a significant increase in the price of the bearing. In addition, the curvilinear shape of the end reduces the contact area of the roller with the guiding flange of the bearing, contributing to the skewing of the rollers in the cage opening.

A. D. Shavshyshvili [116, 111] proposed to make the working surfaces of the flanges conical in order to create a favorable geometry of the friction bodies (the so-called "flare" of the flanges). This significantly facilitates the modification of the microgeometry of the surfaces in operation and accelerates the transition to the friction mode, when the wear of the surfaces will be minimal. The authors of the article [49] come to the same conclusion.

It has been established that by introducing the "flare" of the sides, the axle roller bearings can perceive axial forces of up to 35 kN [115].

In total, about 50 changes were made to the design of the existing box assembly in order to improve its operation. Thus, high-speed "Aurora" trains were supposed to be equipped with experimental axle boxes with two cylindrical bearings No. 3N32726L and a radial ball bearing No. 3N228L (Fig. 1.14), which accepts axial loads.

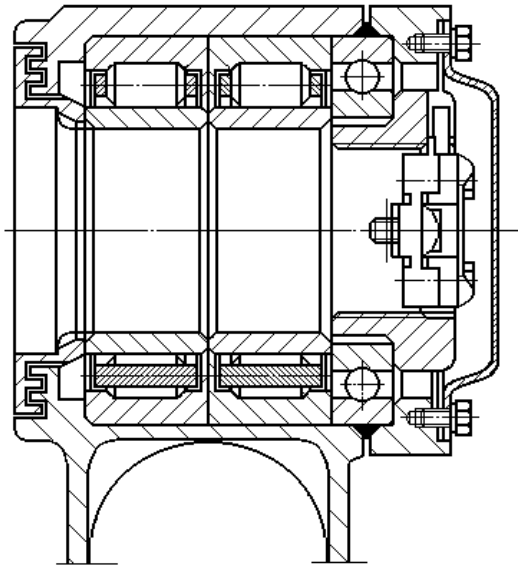

Fig. 1.14. Axle box of high-speed train "Aurora"

In order to ensure interchangeability, a serial housing was used; the axle was mounted on a standard axle. An axial nut of a significantly changed design was used, and the details of its locking and the fastening cover were also changed. The outer ring of the ball bearing was fitted with a sliding fit in the box body and in a special cover that presses the bearing to the outer ring of the cylindrical bearing.

It was assumed that due to the gap between the nut and the inner ring, the ball bearing should not accept radial loads. However, in operation it was not possible to ensure the separation of perception of radial and axial loads. Therefore, the ball bearing accepted both axial and radial loads. As a result, it quickly refused, causing the axle box to heat up.

In 1987 - 1989, tests of the box assembly designed by V. M. Chebanenko were carried out (Fig. 1.15).

A characteristic feature of this design was the installation of a radial thrust ball bearing with removable outer rings between two roller bearings, which had rollers of a shortened length, in the box.

It was assumed that the roller bearings will be completely unloaded from the action of axial forces and will perceive only the radial load.

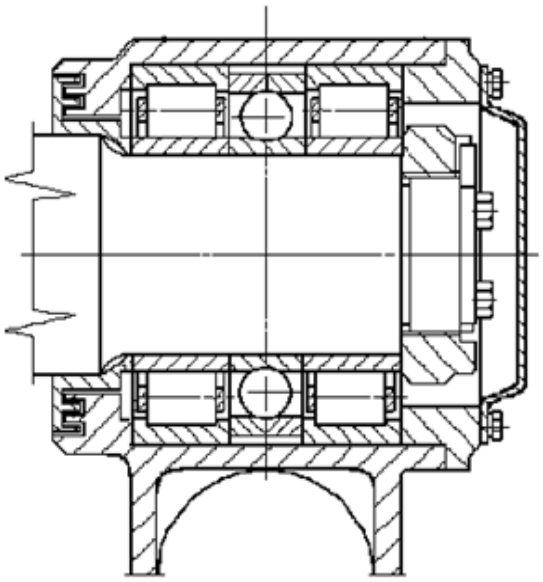

Fig. 1.15. V. M. Chebanenko axle box (Axle box MIIT)"

In the course of operational tests, which took place under freight cars and passenger cars up to a run of 400,000 km, it became clear that this design completely solves the problem of ensuring the reliability of end mounting (for freight cars axle boxes) and cages (for passenger cars axle boxes).

However, Chebanenko's axle box was much more difficult to carry out assembly and disassembly.

Yes, additional adjustment of clearances in the ball bearing was required after mounting the axleboxes, special tools for disassembly, higher qualification of service personnel, rings of ball bearings were not interchangeable. In addition, the fatigue strength of the roller bearings was less than expected. For these reasons, the test was terminated.

1.2. Analysis of the evolution of the designs of axle bearing assemblies of wagons in the countries of the world

Axle boxes, which use bearings with short cylindrical rollers, have become widespread in European countries (Fig. 1.16).

This was facilitated by the combination of high load-bearing capacity in the radial direction with the simplicity of their manufacture and assembly and disassembly. Installation of the inner rings of such bearings is carried out, as a rule, by a thermal method, less often with the help of a press fit. In some designs, the bearings are mounted using mounting bushings (Fig. 1.17). Bearings can have a common outer ring (Fig. 1.18), a common inner ring (Fig. 1.19) or be a double-row bearing with common outer and inner rings.

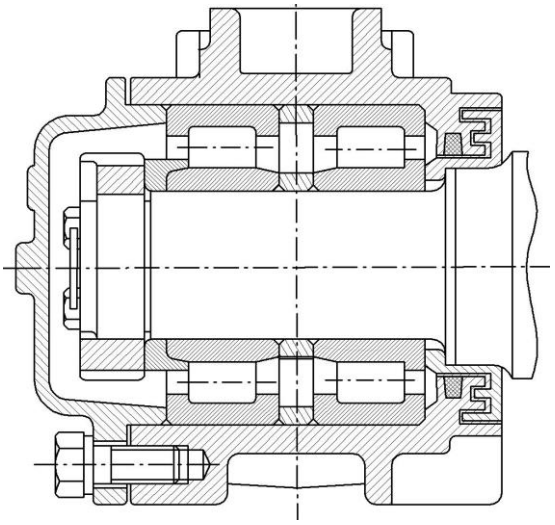

Fig. 1.16. Box with L-shaped thrust ring

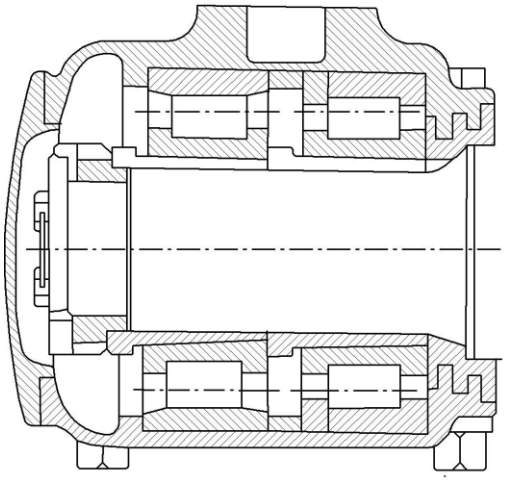

Fig. 1.17. Box with mounting bushings

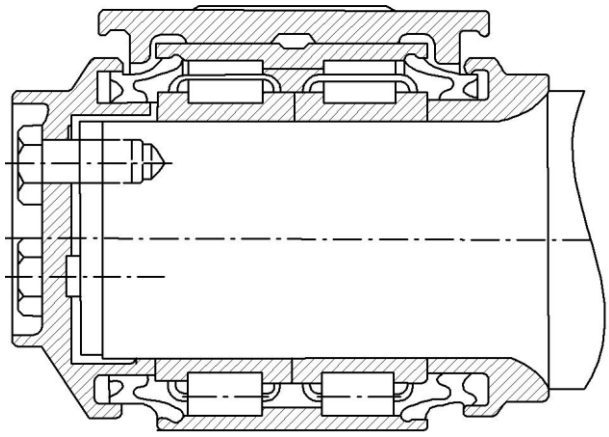

Fig. 1.18. Box with bearings having a single outer ring

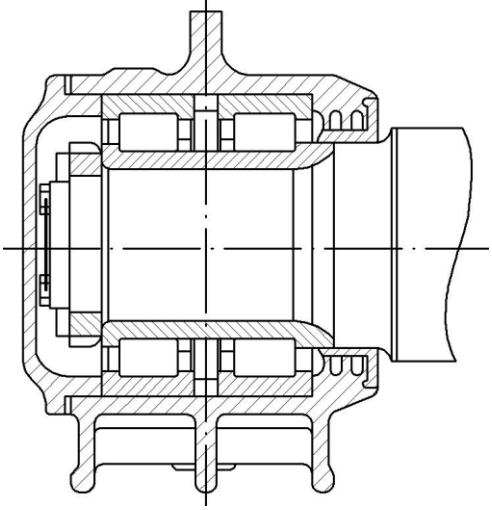

Fig. 1.19. A box with bearings that have a single inner ring

Most of the used box assemblies provide bilateral perception of axial forces. Also, in the practice of world railcar building, there are structures in which the perception of axial forces is carried out only in the direction of the axle fillet. As a rule, there is no end fastening in such boxes, which makes it possible to simplify the technology of manufacturing axle necks and carrying out assembly and disassembly work. However, the use of such structures is possible only in bogies that provide one-way transfer of axial forces to the axles.

In all the axle box assemblies designs discussed above, the axial load is rigidly transmitted by the sides of the bearing rings through the ends of the rollers in the mode of sliding friction. The desire to reduce the level of axial forces led to the creation of structures in which the softening of these forces is carried out by an elastic element mounted in the end mount (Fig. 1.20).

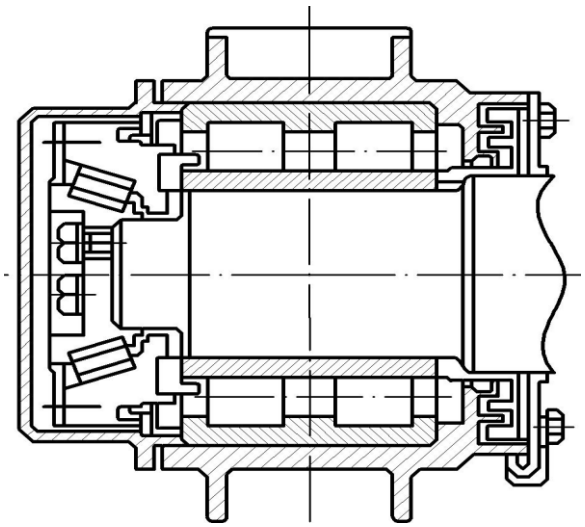

Fig. 1.20. A box with bearings that have a single inner ring

To increase the reliability of the box with cylindrical bearings, technical solutions were developed in which the axial load is transferred to various additional devices. Yes, there were attempts to use axial sliding stops in the axles. But such bushings are used only on locomotives due to the need for constant control of the oil level.

As a device that perceives axial forces, it is possible to use radial-thrust ball bearings in axle boxes of the rolling stock.

For example, in fig. 1.21 shows the design of the axle box assembly (Japan), intended for use in express trains with speeds of up to 66.67 m/s (240 km/h).

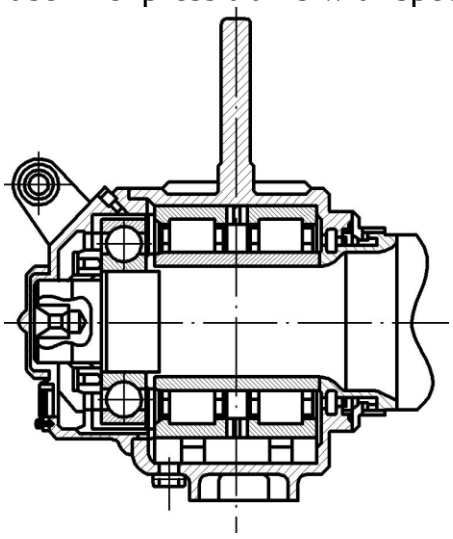

Fig. 1.21. Box of a Japanese high-speed train

These axle boxes have one double-row cylindrical and one radial ball bearing. To prevent the perception of a radial load by a ball bearing, a gap of 0.5 mm is provided between its outer ring and the bushing cover in which it is contained. To soften the blows directed along the axis of the axle, there is an elastic axial stop.

The estimated durability of roller bearings corresponds to a run of 3.8 million km, and ball bearings to 1.2 million km. This design and all similar to it due to the installation of a ball bearing from the end of the axle neck ensure one-sided perception of axial forces. In France, for a high-speed train, the design of the axle box [32] was developed, which provides two-way reception of axial forces by installing a radial thrust ball bearing between two cylindrical roller bearings (Fig. 1.22).

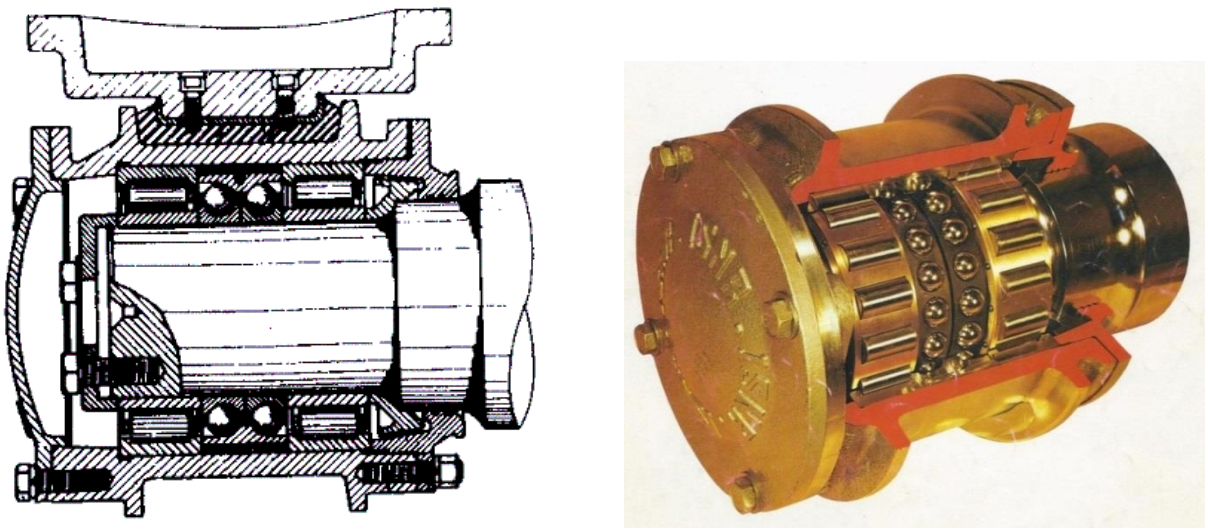

Fig. 1.22. Box of a French high-speed train

However, the assembly and disassembly of such an axle box assembly is extremely difficult, since the ball bearing can be removed only after disassembling the box body and the front bearing with its inner ring.

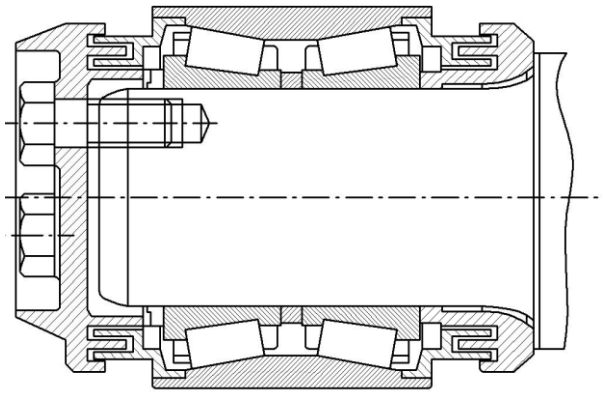

Fig. 1.23. A non-housing axle box without housing with a double-row conical bearing

In the USA and Canada, non-housing assemblies with double-row conical TBU bearings (manufactured by Timken and Brenso) have become widespread on wheel pairs of freight cars. The outer ring of both bearings is common and is simultaneously the body of the bearing assembly (Fig. 1.23).

Table 1.2 contains data on the use of TBU bearings in different countries of the world, from which it follows that such bearings are becoming more and more common in world practice.

Table 1.2

Types of rolling stock where TBU double row tapered roller bearings are used

	High-speed railway vehicles	Locomotives	Passenger cars	Freight cars	Metro cars and trams
TBU 90				Austria, Italy, Germany, Switzerland	Great Britain, Switzerland
TBU 120			Great Britain		Tunisia, France, Belgium
TBU 130×210	Spain		Spain	Italy	Malaysia, Sweden
TBU 130×220	Italy, Sweden, Norway		Switzerland, Germany, Great Britain		Thailand, Switzerland
TBU 130×230	Italy, Germany, France		Austria, Italy, the Netherlands,	Portugal	
TBU 130×240				Belgium, France, Great Britain	
TBU 140		Switzerland			the Netherlands
TBU 150		Austria, India, Great Britain	France, the Netherlands, Portugal		

What is the reason for such interest of specialists? It has been established that, compared to typical cylindrical roller bearings, cassette tapered bearings have the following advantages:

• the use of conical cassette roller bearings significantly facilitates the processes of assembly and disassembly and maintenance. This is due to the fact that the bearing is delivered as part of a ready-made axle box. As a result, costs of material and labor resources for assembly and disassembly work are reduced;

• the bearing assemblies are reliably protected from contamination from the outside by combined seals;

• the use of conical cassette roller bearings makes it possible to fundamentally change the system of repair and maintenance of roller bearings. This is due to increased durability compared to cylindrical bearings.

2. CONDITIONS OF OPERATION AND LOADING APPLICABLE TO AXLEBOX BEARINGS OF RAILCARS

2.1. Operating conditions of cylindrical roller bearings of railcars axle boxes

The operating conditions of roller bearings of railcars axle box are largely determined by the design of the running parts of passenger and freight cars, operational and climatic features [40].

The operating conditions of axle box bearings are very severe. Particularly unfavorable conditions of operation of wheel pairs bearings occur when the railway vehicle moves along a curved section of the track, when passing rail joints and switches, when there are sliders and other defects on the wheels [117]. A specific feature of loading a passenger trolley with a rigid frame is the so-called skew-symmetrical loading. For example, during the movement of a passenger car on curved sections of the track, when significant vertical and horizontal loads occur, their transmission from the body through the frames of two-axle bogies to the bogies is carried out according to the scheme shown in Fig. 2.1.

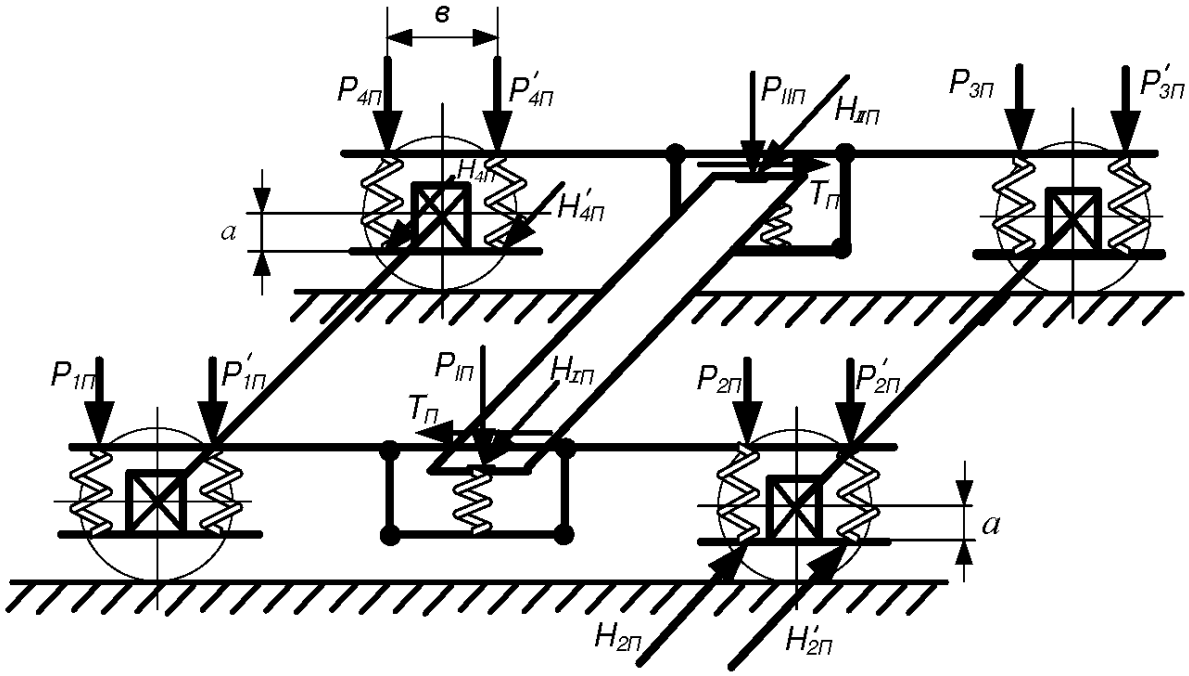

Fig. 2.1. Scheme of load transfer to the axles of a two-axle carriage of a passenger car from the body through the slides

That is, the vertical (radial) static and dynamic forces due to weight are such that $P_{Iп} \neq P_{IIп}$, $P_{Iв} \neq P_{IIв}$, $P_{1п} \neq P'_{1п}$, $P_{2п} \neq P'_{2п}$, $P_{3п} \neq P'3п$, $P_{4п} \neq P_{4п'}$, $P_{1в} \neq P_{2в} \neq P3в \neq P4_{В}$.

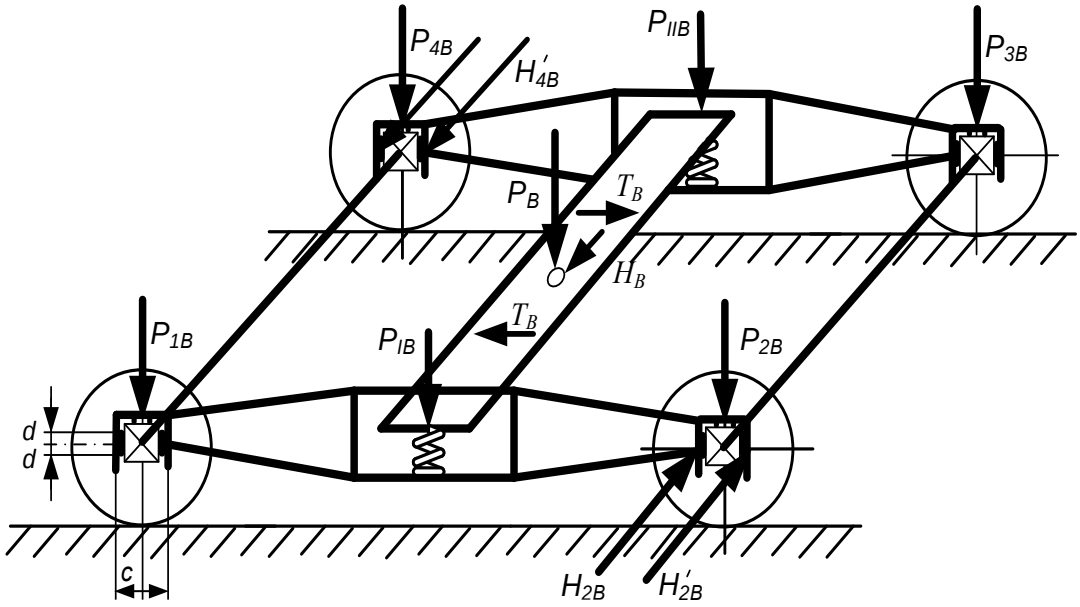

Fig. 2.2. Scheme of load transfer to the axles of a two-axle freight car from the body of the freight car through the bogie center plate.

The inequality of the forces P_{In}, P_{IIn} and $P_{Iв}$, $P_{IIв}$ ($P_{Iв} + P_{IIв} = P_в$) and their components is due to the different amount of deflections of the rails under the wheels, different ultimate stiffness and height of the springs and springs of the box suspension, deviations in the dimensions of wheel pairs, their wear and manufacturing tolerances. Inertia forces during braking and corresponding braking forces cause additional uneven radial loading of box cars. This load is realized in the form of reactions of the connections of the bogie frames with the axle necks acting along the bogie frames are $T_п$,$T_в$. The forces $H_{IIп}$, $H_{IVп}$ and $H_{IIв}$, $H_{IVв}$ are components of the horizontal (axial) load from the body of a passenger and freight car when passing a curved track section. The magnitudes of the component reactions of the connection of the bogie frame with the axle necks from the side of the bogies are such that $H_{2П} \neq H'_{2П}$, $H_{4П} \neq H'_{4П}$,$H_{2в} \neq H'_{2в}$. The inequality of the forces of $H_{IIп}$, $H_{IVп}$ and $H_{IIв}$, $H_{IVв}$ and their components is due to the influence of the rail track corrugation, switches and curved sections of the track, as well as the inaccuracy of the bogie assembly.

Analysis of the schemes in fig. 2.1, 2.2 shows that the transfer of loads from the bodies of the passenger and freight cars through the bogies to the axle boxes occurs unevenly. All bearing assemblies are loaded unequally by both vertical (radial) and horizontal (axial) forces. The nature of the load on the axle bearing assemblies of the wheel pairs of railcars is additionally complicated by the appearance of inertial forces during braking.

The analysis of the designs of the axle assemblies shows that the radial load is unevenly distributed between a pair of bearings in the axle, even after their careful selection, due to the difficulty of taking into account the deformation of the axle neck, the sizes of the radial clearances, and errors in the geometric shape of the bearing parts [90]. Axial forces act on the axles of the pas-

senger car with a fixed eccentricity a (Fig. 2.1), which is determined by the design of the axle wings; axial forces also act on the axle boxes of freight cars with an eccentricity d (Fig. 2.2), but the magnitude is undetermined due to the design of the axle jaws [24].

The change in the vertical (radial) load and the appearance of the horizontal (axial) load on the wagon axle in operation depends on many factors: the distribution of the mass of the wagon, spring suspension parameters, the condition of the running parts of the wagon, unevenness and elastic properties of the track, speed of movement [117, 64, 51 , 65, 107].

The radial static load P on the axle of a freight car can reach 115 kN, a passenger car - 85 kN [60]. The radial dynamic load on the box of the freight car varies within $(0{,}16 - 1{,}7)P$ (with characteristic values $(0{,}83 - 1{,}16)P$, covering up to 95% of the load spectrum. The radial dynamic load on the axle of the passenger car varies within $(0{,}67 - 1{,}7)P$ with characteristic values $(0{,}92 - 1{,}08)P$ covering up to 90% of the load spectrum. The horizontal (axial) load that occurs when the car is braked is short-term and does not exceed $0{,}3P$ for freight cars and $0{,}15P$ for passenger cars. According to the results of train tests of passenger cars, the average values of axial loads increase with increasing speed.

A significant range of values of axial forces acting on the roller bearings of the axle box (2 - 60 kN), as well as significant discrepancies in the data of measurements of axial forces by different authors is explained both by the influence of many random factors that are difficult to predict, and by the complexity of their measurement in operating conditions.

Thus, cylindrical roller bearings of box cars, firstly, perceive the maximum allowable radial and axial forces and, secondly, the forces applied to bearings with eccentricity. These load characteristics of roller bearings can cause misalignment of the rings.

2.2. Analysis of the reliability of axle bearing assemblies of freight cars in operation

The task of ensuring the trouble-free operation of axle boxes of railway vehicles has always been relevant for railway transport specialists, since the safety of train traffic directly depends on it.

This is confirmed by the data of fig. 2.3, which shows the distribution of causes that caused transport events (uncoupling of a car from a train during movement), classified by railway car management, for the period 1995–2019.

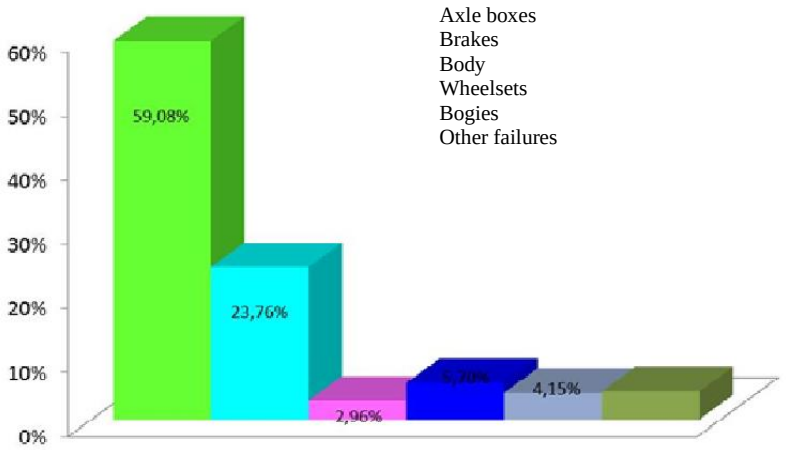

Fig. 2.3. Distribution of the causes that caused transport incidents on the railways of Ukraine for the period 1995–2019 in accordance with the wagon management classification

It is obvious that it was the failures of the axle box assemblies that caused the overwhelming majority of the transport incidents.

According to the data presented by JSC "Ukrzaliznytsia" the number of uncoupling of wagons due to excessive heating of axle box roller bearings, which was detected by remote monitoring devices of PONAB, DISK, ASDK, KTSM, varies widely from 352 cases in 1995 to 27 cases in 2019. But not all cases of heating are detected by technical means of control. The existing system of technical maintenance of wagons provides for its control on the way of the carriage by inspectors of wagons based on external signs. This is carried out during the meeting of cars "on the move" at the stations with subsequent visual control during the train stop Fig. 2.4. In 2016, this number of cases of detection of increased heating of roller bearing assemblies was 1,571 cars, in 2017 – 1,542 cars, in 2018 – 1,164 cars, in 2019 – 1,264 cases, respectively (Fig. 2.4).

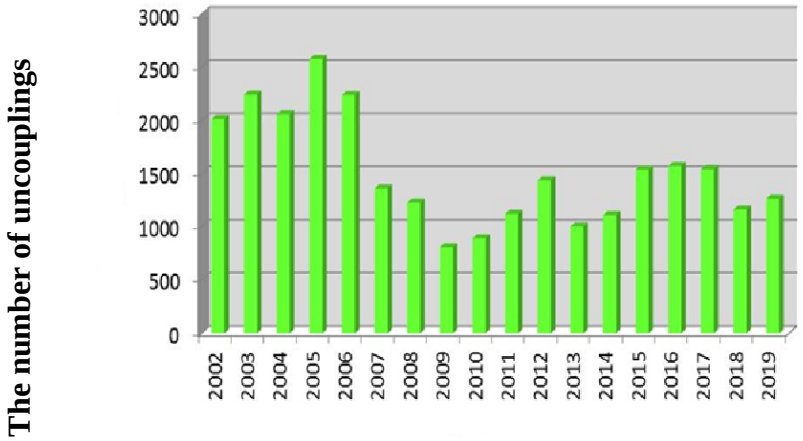

Fig. 2.4. The dependence of changes in the number of uncoupling of wagons due to heating of the boxes, which were detected by automatic control devices and wagon inspectors

The table 2.1 gives the main reasons that caused the heating of the vehicle and the uncoupling of the car from the train for the period 2009-2013.

Table 2.1

The main causes of excessive heating of the axle assemblies, which caused the car to uncouple from the train

Reasons for excessive heating of axle box assemblies	Percentage of the total number of uncouplings
Cage malfunctions	2.68%
Malfunctions of end fasteners	22.22%
Wear out of the treeing type	8.43%
Inner ring rotation	3.83%
Complete destruction of the bearing	3.45%
Contamination or watering of the lubricant	10.34%
Cracks and fractures of bearing rings	4.60%
Sinks on the rolling surface of the rings	2.30%
Other reasons	23.75%
"Human factor"	18.39%

It is obvious that the vast majority of excessive heating of railway vehicles with subsequent uncoupling of wagons on the route is due to insufficient reliability of roller bearings.

As a result, a dependence was obtained that characterizes the change in the number of uncoupling of freight cars for this reason during the period 1995 - 2019 (Fig. 2.5).

Fig. 2.5 Dependence of the change in the number of uncoupling of wagons on the route due to the heating of the axle assemblies

If you start counting from 1995, the resulting dependence will look like this:

$$\Delta t = -0{,}0007t^4 + 0{,}0279t^3 + 0{,}4982t^2 - 34{,}195t + 398{,}6, \quad (2.1)$$

where t are years counted after 1995.

But the resulting dependence gives only a general idea of the nature of changes in the reliability of railways, since it does not take into account those changes that took place in the country's economy, which affected the performance of both railway transport and directly the wagon industry of JSC "Ukrzaliznytsia": a significant decrease in the operating wagons fleet, fluctuations in freight traffic, removal of wagons from inventory, etc.

Fig. 2.6 shows the dependence of the change in the number of uncouplings of freight wagons of the general fleet due to the failure of the axle box assemblies in the calculation per 1000 wagons of the working fleet.

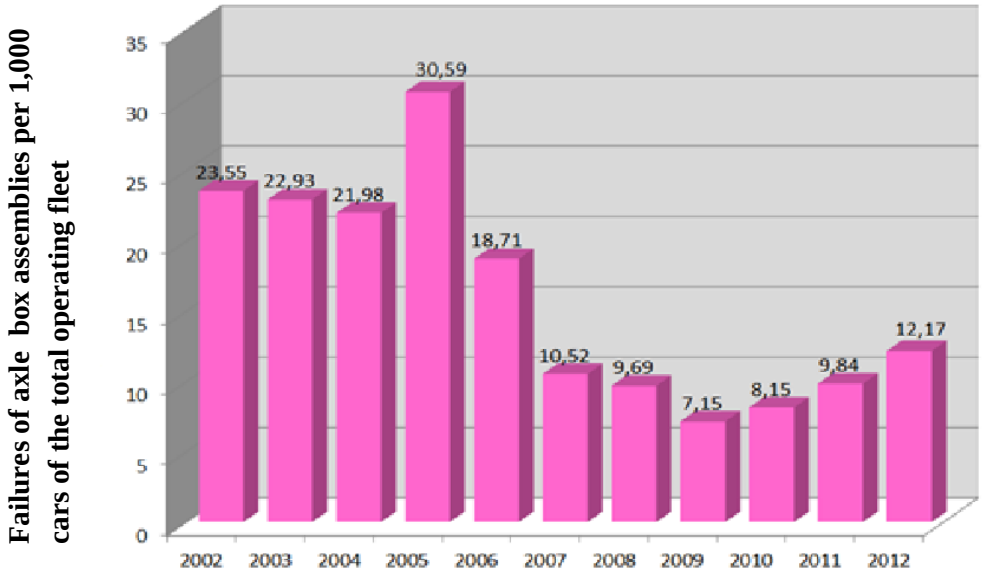

Fig. 2.6. Dependence of the change in the number of uncoupling of freight cars of the general fleet due to the failure of roller boxes per 1000 cars of the operating fleet

Comparing the obtained results with the data given in the article [112], it should be concluded that the reliability of the axle box operation has significantly decreased over the last decades. Yes, if during the period from 1972 to 1979, the parameter of the failure flow $\omega(t)$of freight cars due to the failure of the axle box assembly did not exceed the value of 0.0029 1⁄(weight km), then in the most prosperous year of 2002, the similar indicator was 0.037 1⁄(weight km), that is, almost 13 times more.

To establish the reasons for this, it is necessary to analyze the technical condition of the elements of the axle box assemblies of freight cars wheel pairs,

to develop a mathematical model that will make it possible to determine the reliability indicators of the latter.

2.3. Study of the technical condition of cylindrical roller bearings

It was established that not all damage to the bearings causes the heating of the boxes and, as a result, the uncoupling of the wagons on the route. A significant share of malfunctions is detected during full and intermediate revisions of roller bearings. Thus, according to the work [59] in 10% of box assemblies, the bearings are damaged.

Therefore, in order to ensure the reliable operation of heavy-duty freight cars, it is necessary to study the causes of damage to cylindrical box bearings, to establish various operational factors that affect their operation.

The analysis of the types of damage to parts of cylindrical roller bearings of axles of wheel pairs of wagons was performed in studies [39, 90, 37, 119].

One of the ways to solve the task is the analysis of VU-91 type log book, which are kept in the rolling departments of wagon repair enterprises. In these logs, the designation of the year of production of the bearing, the manufacturing plant and the corresponding malfunctions according to [58] are indicated. But recording in these log books is often carried out very carelessly, the entries made by depot employees do not always correspond to actual data, and therefore the information obtained with their help cannot be considered absolutely reliable.

An even more difficult task is determining the performance indicators of the end mount. This is explained by the fact that, in accordance with the requirements of current regulatory documents [53], the control of tightening of threaded connections is carried out only during intermediate revisions of roller journal box.

If the axle box assembly arrives at the roller department of the wagon repair enterprise for a full inspection, the presence of loosening of the fastening is not controlled, the M110 nut or M20 bolts of the fastening with a washer are unscrewed in any case.

Therefore, in order to obtain accurate information about the damage to the elements of the axlebox assembly, special inspections were carried out in the roller departments of the wagon repair depots. Inspections were carried out at the wagon depots of the regional branches of the "Southern", "Donetsk", "Lviv" and "Odesa" railways.

A specific worksheet was developed for the convenience of carrying out inspections of bearings and facilitating further processing of the received information. In these sheets, all possible malfunctions of the bearings were displayed in accordance with the requirements [58]. In addition, the worksheets contained the datasheet specifications of the wheelset and rolling bearings: their numbers, the year and place of manufacture (formation of the wheelset), the date and place of the last complete inspection of the wheelset.

Inspection of wheel pairs was carried out as follows: when a pair of wheels arrived at the disassembly station, the registration number, date of the last complete inspection and other data of the pair of wheels were recorded. Then, before disassembly, by tapping with a hammer, the condition of the end fasteners was checked (the presence of loosening of the tightening force of the M110 nut, M12 bolts of the locking bar, the condition of the binding wire). In the event that the end fastening was carried out with a washer with M20 bolts, the condition of the tab washer and the weakening of the bolt tightening force were checked. All detected malfunctions were recorded in the inspection card. The condition of the lubricant was also assessed (the presence of extraneous inclusions, water contamination or contamination was monitored).

The inspection of the bearings was characterized by the fact that the main malfunctions of the bearings were fixed in accordance with the requirements [58], and the date of manufacture of the bearings was taken according to the year of manufacture marked on the outer ring of the bearing. This assumption was adopted on the basis of works [112, 87, 110], where it was shown that the outer rings of bearings fail most often. In total, information on almost twenty-three thousand bearings was processed.

The parts of the bearings that were rejected during the inspections and were not subject to repair were divided into several groups:

• defects of fatigue origin (shells, flaking of rings and rollers) (Fig. 2.7–2.8);

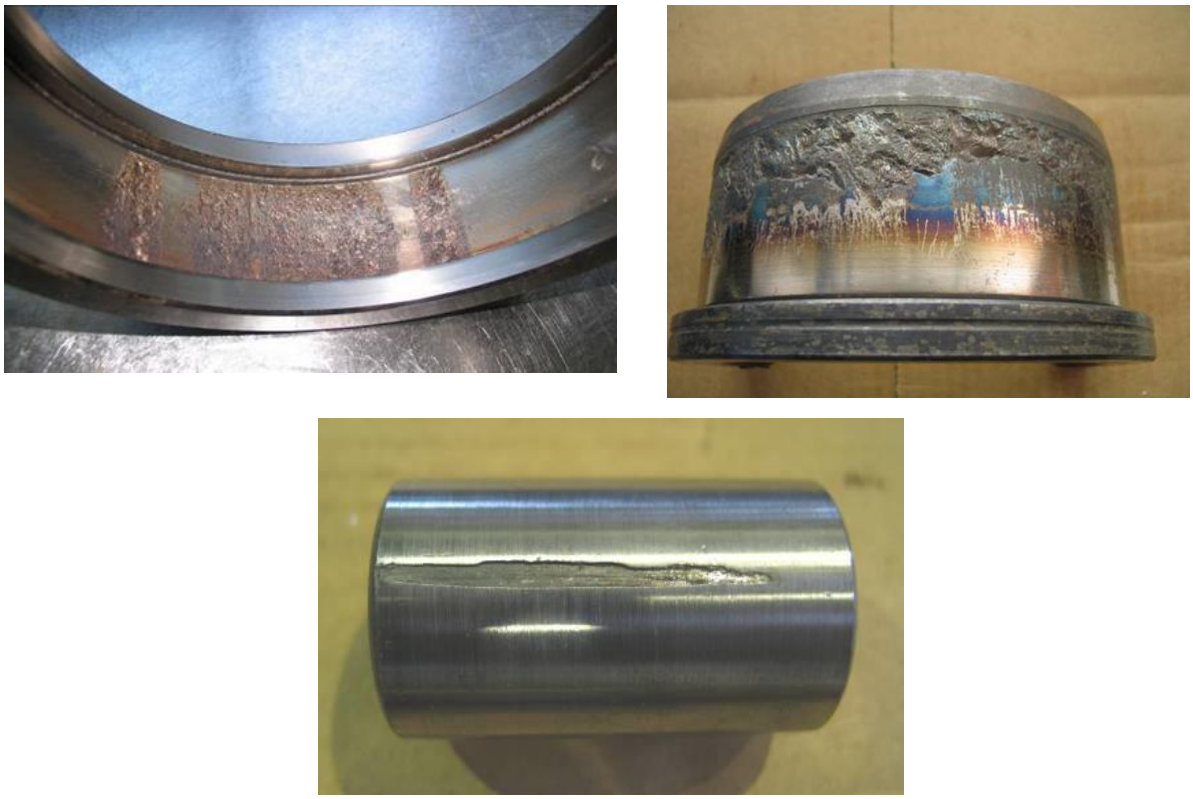

Fig. 2.7. Fatigue sinks on raceways of rings and rollers

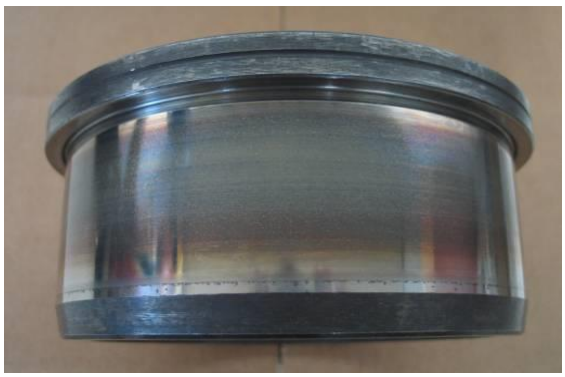
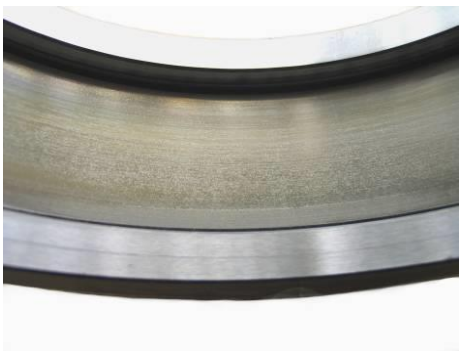

Fig. 2.8. Flaking from fatigue on the raceways of the rings

- defects of sudden origin (breaks, cracks, burrs of bearing rings and rollers, as well as thrust ring) (Fig. 2.9);
- corrosion damage to rings and rollers (Fig. 2.10);
- damage to cages (Fig. 2.11).

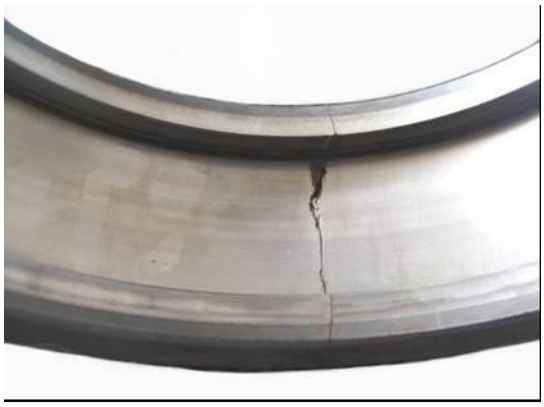


Fig. 2.9. Cracks and breaks in bearing rings and rollers

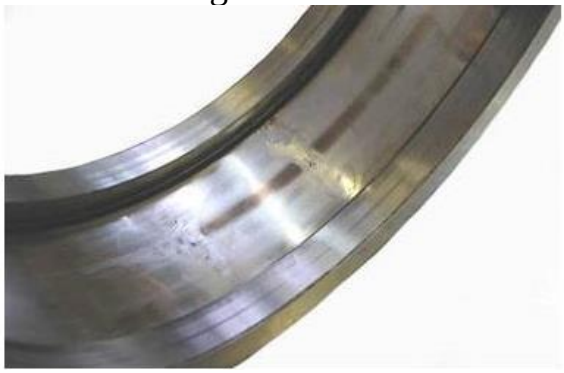


Fig. 2.10. Corrosion shells and pitting on bearing rings and rollers

Fig. 2.11. Destruction and wear of cage rings and bridge sections

The main results of the inspections are presented in table. 2.2.
Table 2.2

Distribution of bearings by types of malfunctions

Types of damage	Percentage of the number of rejected bearings	Percentage of the number of rejected bearings
Shells from fatigue and peeling of the outer ring	9,1	2,82
Shells from fatigue and peeling of the outer ring	0,59	0,18
Shells from fatigue and peeling of the inner ring	7,3	2,26
Cracks and chips of the flanges of the outer ring	0,38	0,12
Roller cracks	0,74	0,23
Corrosive damage to the outer rings	26,56	8,23
Corrosive damage to the inner rings	0,32	0,1
Corrosive damage to rollers	1,28	0,39
Electrical damage	0,22	0,069
Activation of the centering surface of the cage	1,01	0,031
Cage corrosion damage	17,3	5,36
Actuation of the "herringbone" type on the sides of the rings	14,1	4,37
Wear-out of the treeing type on rollers	14,74	4,56
Other damages	6,36	1,97
Total:	100,00	30,69

As a result of processing the received information, it was established that more than 30% of the inspected bearings have damage of varying degrees of severity (Fig. 2.12).

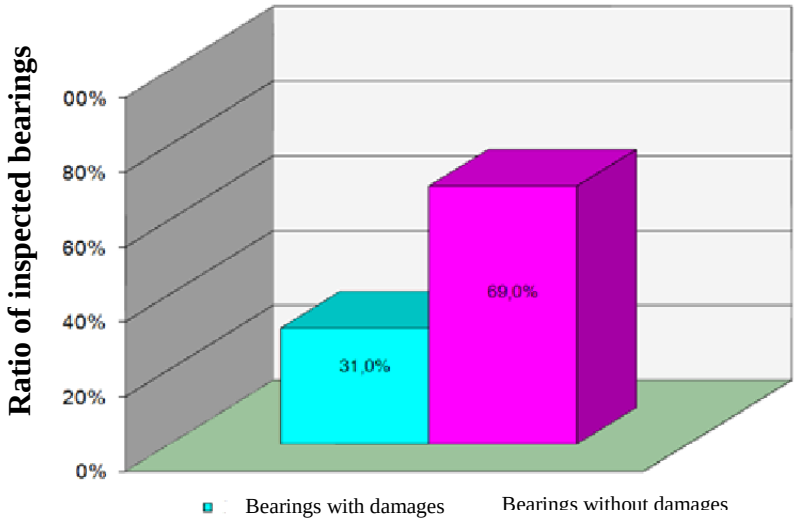

Fig. 2.12. Ratio between rejected and inspected bearings

The analysis of the received data shows that outer rings fail most often - 45.54% of the number of rejected ones. Then there are rollers - 26.42%, inner rings - 8.41%, cage - 19.63% (Fig. 2.13).

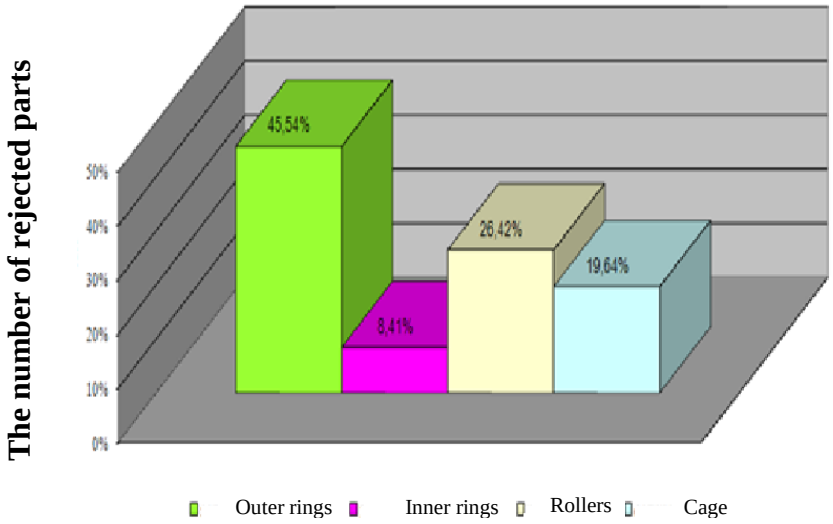

Fig. 2.13. Correlation between damaged bearing parts

8% of the inspected bearings are not suitable for further use. They need to be replaced, and they are missing mainly due to fatigue damage (Fig. 2.14).

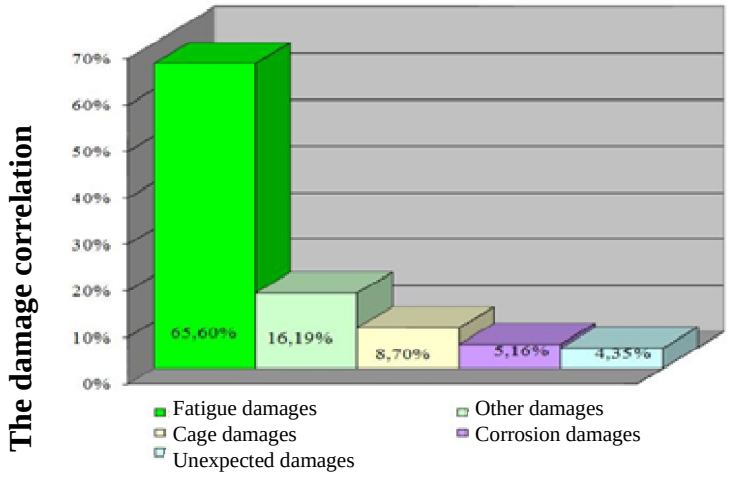

Fig. 2.14. Correlation between the causes of damage to bearing parts

It is interesting to compare the obtained data with the results obtained at the end of the 80-th years. If now 8% of inspected bearings are not suitable for further use and require replacement, then earlier this number was 2.5 times lower.

As before, most often the bearings fail due to fatigue damage.

Although the share of sudden damage in the total amount is small and makes up 4.35% of the number of rejected ones, it has increased by 7 times in comparison 80-90 years of the last century.

There are several reasons for this:

- the aging of rolling stock, a significant decrease in the purchase of new cars in the 90s of the 20th century;
- the physical operation of the elements of the wagons contributes to the growth of the forces of dynamic interaction between the track superstructure and the rolling stock and increases the load of the vehicle.

However, the greatest growth is observed among corrosion damage, especially the inner rings. This is due to the low quality of rubber used for the manufacture of seals by numerous companies that supply it at this time for railway transport.

2.4. Analysis of possible scenarios of the transition of axlebox bearing assemblies to an emergency state

Features of the operation of roller bearings were investigated by V. G. Andrievskii [25, 23], S. V. Batenkov [27, 26], M. Bhardvadzh [33], R. V. Virabov [34], A. V. Haidamaka [39 , 36], M. A. Galakhov [40, 42], O. P. Lelikov [48, 68], V. I. Kvasov [55, 56, 57], L. M. Leikakh [67], A. V. Losev [69, 70], I. E. Martynov [71, 73], V. F. Novikov [77], N. V. Rodzevych [92], A.S. Saverskii [96], N A. Spitsyn [79, 99, 98], V. N. Tsiurenko [110, 111], T. Tellian [100, 101, 102], T. Harris [6], T. Losche [16], K. Kakuta [11], K. T. Kobaiashi [14], R. Kleckner [13], T. Sakaguchi [17], O. Takuya [18].

To establish the reasons for the insufficient reliability of roller axle boxes, it is necessary to analyze the design scheme of a typical axle box assembly, to consider the process of the interaction of elements.

The experience of operating cylindrical roller bearings in various branches of mechanical engineering shows that such bearings work successfully when only radial loads act on them. Let's analyze the load scheme of bushing cylindrical bearings.

Radial P and axial forces Q act on bushing bearings during movement (Fig. 2.15).

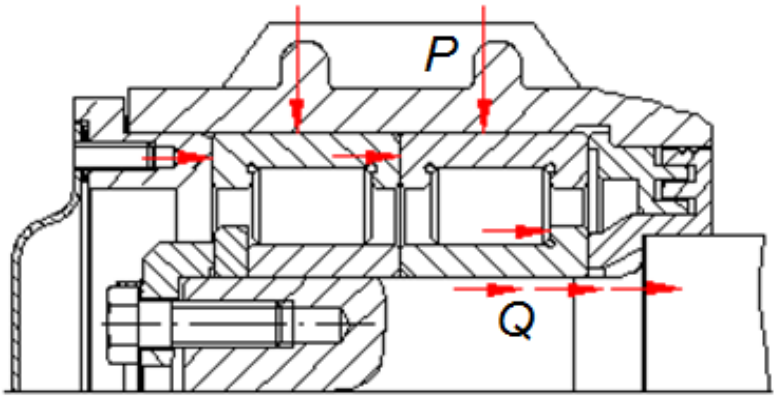

Fig. 2.15. Scheme of load transfer in the axle assembly under the action of axial force in the direction of the flange of the axle neck

It should be noted that the magnitude and nature of the action of radial forces have been studied quite fully. The nature of action of axial forces is much more diverse.

Thus, when the wagon passes through the curved sections of the track, the axial forces are constant.

At the same time, lateral oscillations of the wagon will cause short-term axial loads. And when passing the lateral longitudinal irregularities of the track, the axial forces will have an impact character.

The magnitude of axial forces can reach high values, especially in freight cars. This is confirmed by the results of numerous train tests [52, 91]. The reason is the presence of only a bolster suspension in the design of freight wagons bodies. As a result, the side frame of the bogie, which has a large mass, rests directly on the box body, and the accelerations that occur during the passage of lateral irregularities of the track cause significant axial forces.

Thus, in the course of tests of the axle –box assembly design of the MIIT (MSU PS) in 1987-1989 at the Experimental Ring of the VNIIZHT, the magnitude of the axial forces when passing through the turnout switches reached 130 kN [91].

The axial force can act both in the direction of the fillet (Fig. 2.15) and in the direction of the end of the axle neck (Fig. 2.16).

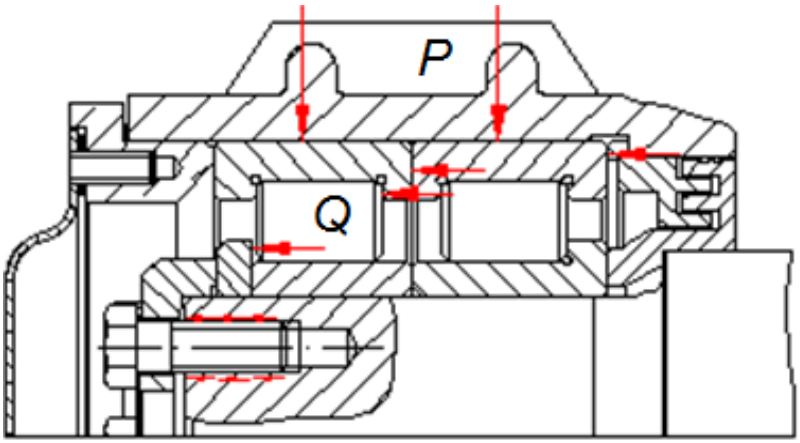

Fig. 2.16. The scheme of load transfer in a bearing axlebox assembly with cylindrical bearings under the action of an axial force in the direction of the end mount

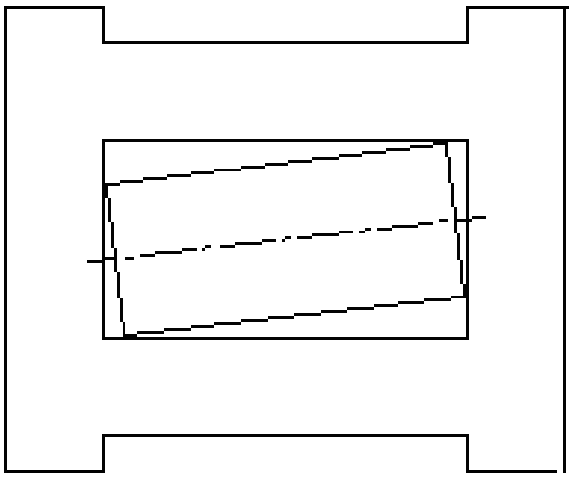

Fig. 2.17. Scheme of force influence on the cage bridge section

Its transmission is carried out through the rollers of only one of the bearings, depending on the direction of action.

The direct transfer of axial force to the end fastener leads to its weakening, and sometimes, under the action of large dynamic forces and the accumulation of defects in the metal, to destruction.

The action of axial forces leads to skewing of the rollers, as a result of which a skew-symmetric load of the cage is generated (Fig. 2.17). In combination with high dynamic forces (especially in winter), this leads to the appearance of fatigue cracks in the corners of the cage opening with their subsequent destruction.

Among the possible types of misalignment of the rings, one should distinguish "free", "limit" and "operational" misalignment angles [29, 6]. The "free" angle of misalignment of the rings occurs in an unloaded bearing when the inner ring is rotated relative to the outer ring by the value allowed by the radial clearance. The "limit" angle of misalignment of the rings occurs in a loaded bearing when the inner ring is rotated relative to the outer ring by an amount permissible radial clearance and contact deformation of the parts. The "operating" angle of misalignment of the rings occurs in a loaded bearing when the inner ring rotates relative to the outer ring by an amount determined by the contact deformation of the parts and part of the radial gap.

The possibility of skewing of the wagon axle relative to the wheel pair both during movement due to non-centrally acting radial and axial forces, and during braking as a result of turning of the wheel pair with unevenly worn brake pads was noted in the works [35, 38].

Instantaneous "operational" distortions of the bearing assembly in the vertical plane may occur due to the dynamic shock nature of their load, when the vertical accelerations of the axles reach 50 g. Thus, in the 1960s and 1970s, railways used passenger cars with a generator gear drive from the end of the axle neck. Such vertical accelerations cause fluctuations in the mass of the reducer with the bushing housing at the end of the axle neck, which leads to the appearance of significant (up to 60 kN) axial forces that destroy the sides of the rings [89]. A significant increase in the axial load (up to 50 kN) on the roller bearing axle boxes, which is caused by the shock interaction of the wheel pair with the rail in the area of the rail bond joints and switches, is also indicated in the paper [89]. It was for this reason that the gear drive of the generator was taken out of operation.

The measurements of the "operational" distortions of the boxes [38] in both the vertical and horizontal planes with the simultaneous registration of axial and radial forces not only confirmed the complex operating conditions of the bearing assemblies of the passenger car, but also made it possible to reasonably perform modeling of the operating conditions on the stand for studying the operation of parts of cylindrical roller bearings of type 2726.

Skews of the roller bearing rings contribute to the rotation of the rollers, which significantly change the kinematics and interaction forces of the parts. In fig. 2.18 shows the possible positions of the cylindrical rollers after their turns in the bearing.

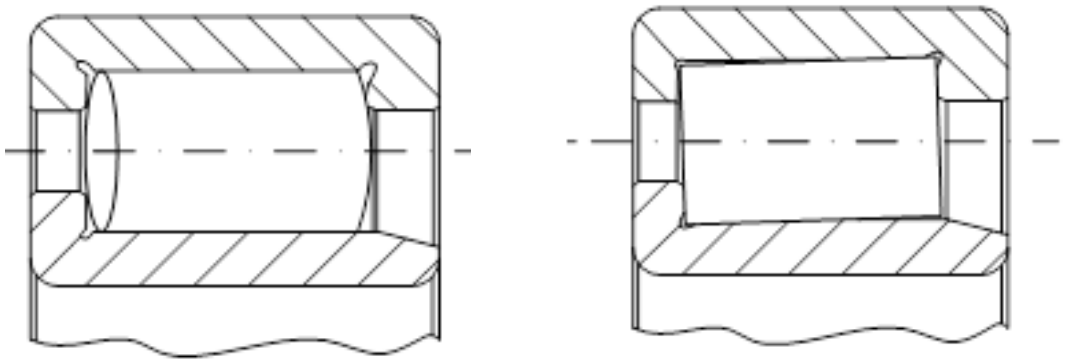

Fig. 2.18. Schemes of contact of the rotated roller with the sides of the rings: a - in the horizontal plane;
b - in the vertical plane

It was established experimentally in train conditions [109] that the rollers of cylindrical bearings of type 2726, which are in the load zone and perceive radial and axial loads, turn in the tangential (horizontal) plane at a small angle (up to 0.5°) relative to the axis of the bearing (Fig. 2.18, a). At the same time,

the ends of the cylindrical roller are in contact with the sides of the rings not over the entire plane, but are located in relation to them at some acute angle. As a result, when the car moves, the axial forces are transmitted by the ends of the rollers in the mode of sliding "steel on steel" on the guide sides of the rings (Fig. 2.19).

Under the action of axial forces, high specific loads occur at the point of contact, since the interaction area is minimal (point contact). As a result of this mode of friction between the flanges and ends of the rollers, intense heat is released and the oil film is torn between the rubbing surfaces in the heating zone. This case of contact is similar to the cutting scheme, where the role of a cutter with an acute cutting angle is performed by the guide board in the absence of its flare. The combination of high pressures with high speeds of relative movement of the surfaces of rings and rollers made of the same metal inevitably creates conditions for sticking and seizure of the working surfaces.

As a result of the dry friction mode, the initial strength of the metal of the sides is significantly reduced. This leads to microseizure of the metal in the contact zone and causes a "treeing" type of wear-out on the rollers and rings flanges.

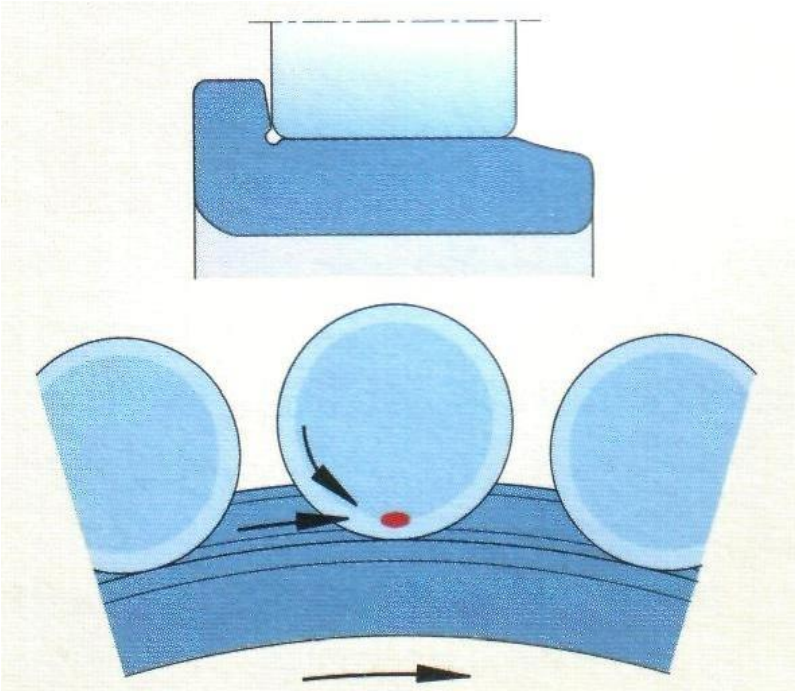

Fig. 2.19. Scheme of the end-flange interaction of the roller

The layer of lubricant ceases to separate the sliding surfaces, and the final results of these processes can be different, that is, in the best case burrs appear, in the worst case - cracks in the flanges, which in the future can lead to the appearance of metal chips, their entry between the rolling bodies and the destruction of the entire bearing. In the future, the presence of such a trigger contributes to the appearance of cracks, shears or even complete destruction of the flanges.

In addition, there is an increased resistance of the bearings to rotation, which is accompanied by local heating in the contact zone. This accelerates the aging process of the lubricant and leads to its contamination with wear products.

The skew of the rollers creates an additional stress concentration in the contact zone of the roller with the raceways of the rings, which leads to the intensive formation of shells caused by fatigue.

It is obvious that a significant part of malfunctions detected during scheduled inspections, as well as the majority of emergency failures, are the result of an insufficiently substantiated design scheme of the axle box assemblies, where the axial load is transmitted through the rollers ends in the sliding friction mode.

2.5. Morphological analysis of the existing designs of rolling stock axlebox assemblies with rolling bearings

In engineering practice, there are usually no methods that allow immediately choosing the optimal structure of the device, provided there is a technical specification. As a result, the development process is interactive. Usually, the developer determines to which class of device the designed model can belong, and then tries to narrow this class through tests to several technical solutions that belong to this class and choose the most optimal one.

The essence of the morphological method is to find the shortest way to solve a technical problem or object by choosing the preferable construction options.

Morphological analysis and synthesis of technical solutions, based on a heuristic approach, were used in the work. With the help of this method, it becomes possible to examine the object from a systemic point of view and carry out a targeted selection of possible solution options, as well as reject deliberately unnecessary objects and reduce to a minimum the number of options that can be subjected to technical and economic comparison.

The axle box assembly is a technical object, for the optimization of which it is necessary to implement the technical and operational criteria for evaluating the variants of the axle box assembly design.

The optimization was carried out in the following sequence: first, according to the indicated criterion, several basic options were selected from technically justified structures, then, with the help of a technical and economic comparison, the most rational variant of the structures of the axle assembly was chosen, which could fully connect between with a bogie frame and a pair of wheels, and also to ensure the reliability of freight cars operation.

At the stage of analytical data processing with the help of a morphological table (table 2.3), arithmetic calculations were carried out, including comparative and factor analysis, at the stage of presenting the results of the analysis of various constructions of axle box assemblies, a summary of these indicators (table 2.4) obtained as a result of this analysis is presented .

Table 2.3

Comparative and factorial analysis of the constructions of axle box assemblies

Bearing type	Design features	Bearing fit on the axis	End mounting	Advantages	Disadvantages
1	2	3	4	5	6
ball	–	–	–	–	low durability
spherical	riveted cage	bushing	crown nut M110	- radial and axial forces acting on the bearing are perceived in the mode of rolling friction; - the selection of paired bearings is simplified due to greater tolerances for the difference in radial clearances; - fit allows you to mount the axle box assembly without selecting the bearings to the axle neck	- not high enough durability due to damage to the raceways of the rings due to fatigue; - mass failures of riveted cages due to broken rivets; - a significant increase in the weight of the axle assembly; - increased labor intensity of assembly and disassembly works
spherical	rivetless cage				the same, except for the cage
cylindrical	brass cage	thermal	crown nut M110 or a washer with four	- reduction of the specific resistance of movement at speeds from 29 to 90 km/h respectively from 25 to 17.5; - reduction of the mass of the axle box assemblies; - the need to carry out intermediate and full revisions	- the need to correctly select the radial and axial clearances; - radial forces are perceived in the mode of friction of the rollers rolling along the raceways of the rings, and axial forces are perceived in the mode of friction of the rollers ends sliding against the guide flanges of the rings; - fatigue cracks in the corners of the cage opening

The end of Table 2.3

1	2	3	4	5	6
cylindri-cal	polyamide cage	thermal		- increased reliability; - elimination of non-ferrous metal costs	- the need for the correct selection of radial and axial clearances; - radial forces are perceived in the mode of friction of the rollers rolling along the raceways of the rings, and axial forces are perceived in the mode of friction of the ends of the rollers sliding against the sides of the rings; - uncertainty with the actual resource of the cage
two cylindrical and one ball bearing	- a ball bearing located between the roller bearings; - reduced length of rollers,	thermal	thermal crown nut	- increased reliability due to full absorption of axial loads by the ball bearing and release of rollers from the perception of axial forces	- complicated design; - increased labor intensity of assembly and disassembly works;
two cylindrical and one ball bearing	- a ball bearing located on the end of the axle neck			- increased reliability due to the partial release of rollers from the perception of axial forces	- complicated design; - increased labor intensity of assembly and disassembly works - perception of axial forces only in one direction
double-row conical	non-cassette type press	press fit		- perception of radial and axial forces by rolling friction	- the need for periodic clearance adjustment
double-row conical	cassette-type	press fit	washer	absorption of radial and axial forces by rolling friction; • liquidation of intermediate revisions of books; • increased reliability, increased resource	high cost of the bearing assembly

When using the morphological table, it was ensured that the amount of raw data of the analytical record was reduced, systematization and detection of regularities, as well as the obvious full illustrativeness of the research. The set of analyzed values was arranged according to the principle from the best option to the worst. The best value was assigned the first place, the next - the second, and so on. The places obtained were summed up, and the best one was the version of the axle box assembly design that gained the smallest value.

Table 2.4

Compilation of indicators for assessing the qualities of the axle box assemblies designs

Bearing type	Quality assessment			Final coefficient
	Features of the design	Bearing fit on the axis	End mounting	
balls	9	3	1	13
spherical	8	3	1	12
spherical	7	3	1	11
cylindrical	6	2	1	9
cylindrical	5	2	1	8
two cylindrical and one spherical	4	2	1	7
two cylindrical and one spherical	3	2	1	6
double row conical	2	1	1	4
double row conical	1	1	1	3

As a result of the morphological analysis, it can be concluded that in the totality of all the values of the designs of axle box assemblies, the lowest points were obtained by the design scheme of the block assembly with double-row conical bearings. Such a design has fundamental advantages especially in axle box assemblies of freight cars. Axle box assemblies with double-row conical bearings of the cassette type perceive the axial forces by the end parts of the rollers with rolling friction.

3. RESEARCH OF THE STRESSED AND DEFORMED STATE OF AXLEBOX ASSEMBLIES OF FREIGHT CARS

The bearings used in the axle boxes are complex mechanical systems. The actual loads acting on the axle bearings depend on many factors and often differ significantly from the initial loads.

Previously, the basis for a reliable calculation of bearings was an experiment. However, the experimental way of improving bearing assemblies is far from always possible. The reason is the duration and high cost of carrying out such experimental studies.

Therefore, today, a promising tool for calculating and improving bushing bearings is the construction and research of a mathematical model based on some basic experiments.

The issue of studying the stress-deformed state of railway bearings under the action of various forces was considered in a number of works [28, 30, 31, 41, 43, 62, 66, 85, 93, 94, 95, 97, 106, 1, 3, 4, 5, 7, 10, 9, 12].

However, these works were mainly devoted to the problems of increasing the durability of cylindrical roller bearings. The issue of improving the design of tapered roller bearings remained outside the attention of researchers.

Therefore, it is necessary to build a mathematical model of the box bearing assembly of a freight car with a double-row conical bearing and to evaluate the stress-strain state of its elements, and first of all, a double-row conical bearing.

3.1. Study of the distribution of loads between the rolling elements of a double-row tapered roller bearing

The operational characteristics of the bearing assembly include the load and pressure in the contacts; axial, radial and angular stiffness; the thickness of the lubricating film in the contacts; kinematics of rolling elements and cages; moment of resistance to rotation; vibration level and spectrum; loads acting on the cage from the side of the rolling elements; type of movement of the cage; durability. To calculate the listed characteristics, it is necessary to develop a mathematical model of the axle box assembly, which includes all significant factors at the selected level.

All loads perceived by roller bearings are transmitted through the rollers from one bearing ring to another. The load perceived by an individual roller depends on the design of the inner part of the bearing and the nature of the applied load.

Considering the tapered roller bearing as a system of material bodies, we refer to the external loads: the forces of the housing and the shaft, respectively, on the outer and inner bearing surfaces, the weight of the bearing parts. The same forces can include dynamic loads acting on the rollers.

The most important requirements for bearings are limitations regarding durability and the magnitude of maximum contact loads. According to this, the formulation of the task of choosing a bearing for box freight cars will look like this:

$$\begin{cases} \sigma_{max}(D_{зов}; d_{вн}; l; n) \le [\sigma], \\ L_{10}(D_{зов}; d_{вн}; l; n) \ge L_{10}^{min}, \end{cases} \tag{3.1}$$

where $[\sigma]$ is an allowable contact stresses; L_{10}^{min} 90-percent lifetime, $D_{зов}$ is an outer diameter of the bearing, m, $d_{вн}$is an inner diameter of the bearing, m; l is a bearing length, m; n is a number of rollers in the bearing.

At the same time, the following restrictions were introduced: $[\sigma]$ does not exceed 3,500 MPa, and a 90 - percent resource is at least 800,000 km.

To determine the loads acting on the bearing rollers and further study their stress-strain state, consider a tapered roller bearing (Fig. 3.1).

Let's introduce the XYZ coordinate system with the Z axis, which is located along the axis of the bearing, and the X axis, which is directed vertically upwards.

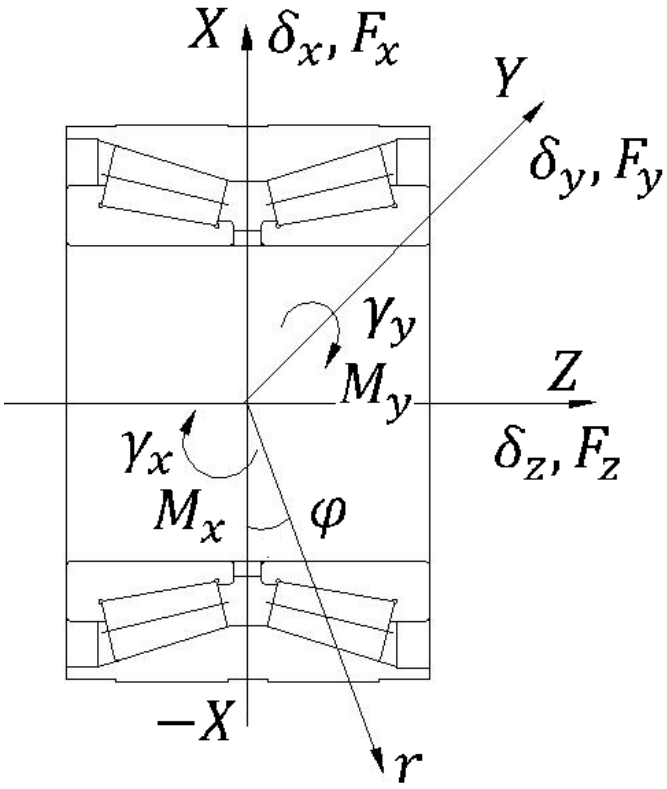

Fig. 3.1. Coordinate systems and bearing load scheme

The *XOY* plane passes through the middle section of the bearing. The coordinate system is fixed relative to the inner ring of the bearing. We will also introduce a cylindrical coordinate system r, φ, z with the same starting point and z axis, where the angle φ is the angle between the r axis and the negative direction of the x axis (Fig. 3.2).

The axis of each roller makes a certain angle k with the axis of the bearing, so it is advisable to introduce the corresponding inclined coordinate system ξ, η, ζ (Fig. 3.3). The axis ξ makes an angle k with the direction r.

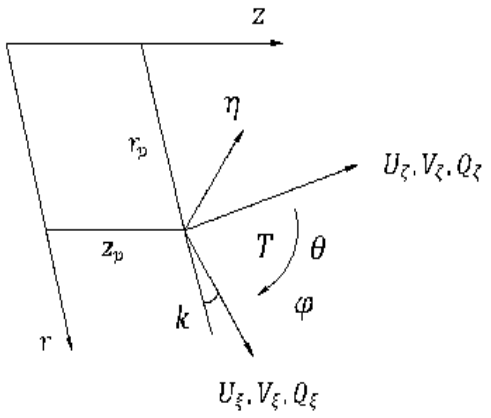

Fig. 3.2. Coordinate systems of a separate roller of a conical bearing

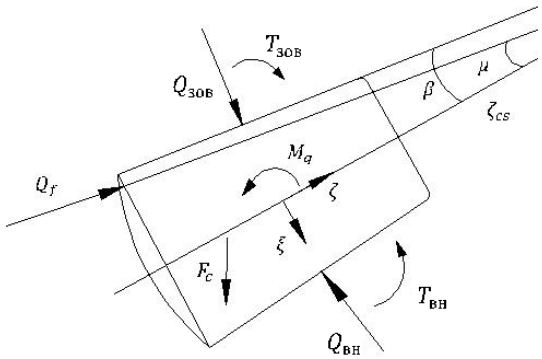

Fig. 3.3. Roller loading scheme

External loads act on the bearing, which are the vector {F}:

$$\{P\}^T = \left(F_x, F_y, F_z, M_x, M_y\right). \quad (3.2)$$

The action of these loads will cause corresponding movements

$$\{\delta\}^{\mathrm{T}} = \left(\delta_{\mathrm{x}}, \delta_{\mathrm{y}}, \delta_{\mathrm{z}}, \gamma_{\mathrm{x}}, \gamma_{\mathrm{y}}\right). \quad (3.3)$$

The inner ring is loaded with a system of forces determined by the vector {Q} at the point with coordinates (r_p,z_p):

$$\{\mathrm{Q}\}^{\mathrm{T}} = (\mathrm{Q_r}, \mathrm{Q_z}, \mathrm{T}). \quad (3.4)$$

Corresponding movement vectors:

$$\{\mathrm{u}\}^{\mathrm{T}} = (\mathrm{u_r}, \mathrm{u_z}, \theta)\ ,\ . \quad (3.5)$$

$$\{\mathrm{v}\}^{\mathrm{T}} = (\mathrm{v_r}, \mathrm{v_z}, \varphi). \quad (3.6)$$

The vectors $\{u\}$, $\{v\}$, $\{Q\}$ are determined in the oblique coordinate system by the index k using the transformation matrix:

$$\{\mathrm{u}\}^{\mathrm{T}} = \left(\mathrm{u_\xi}, \mathrm{u_\zeta}, \theta\right), \quad (3.7)$$

$$\{\mathrm{v}\}^{\mathrm{T}} = \left(\mathrm{v_\xi}, \mathrm{v_\zeta}, \psi\right), \quad (3.8)$$

$$\{\mathrm{Q}\}^{\mathrm{T}} = \left(\mathrm{Q_\xi}, \mathrm{Q_\zeta}, \mathrm{T}\right), \quad (3.9)$$

$$\{Q\}=[K]^{\wedge}T\cdot\{u\}, \tag{3.10}$$

$$\{u\_k\}=[K]\cdot\{u\}, \tag{3.11}$$

$$\{v\_k\}=[K]\cdot\{v\}. \tag{3.12}$$

$$[K]=\begin{bmatrix} cosk & sink & 0 \\ -sink & cosk & 0 \\ 0 & 0 & 1 \end{bmatrix}. \tag{3.13}$$

The load vector $\{Q\}$, which is applied to a separate roller, is transformed into an equivalent force vector $\{f\}$, which is applied to the ring:

$$\{f\} = [R]^T \times \{Q\}, \tag{3.14}$$

where the transposed matrix$\{R\}^T$ is the transformation matrix.

The equivalent forces acting from the rollers on the rings can now be added to obtain the general equilibrium equation of the bearing

$$\{F\} + \sum_{j=1}^{n} \{f\}_j = \{0\}.$$

Substituting expression (3.14) into (3.15), we get:

$$\{F\} + \sum_{j=1}^{n} [R]^T \cdot \{Q\}_j = \{0\}. \tag{3.16}$$

Finally, the system of equations takes the following form:

$$\begin{Bmatrix} F_\xi \\ F_\zeta \\ M_\eta \end{Bmatrix} + \begin{Bmatrix} Q_{зов}cos\beta & -Q_{вн}cos\beta & Q_f sin\mu & F_c cosk \\ -Q_{зов}sin\beta & -Q_{вн}cos\beta & Q_f cos\mu & -F_c sink \\ T_{зов} & -T_{вн} & Q_f \zeta_{cs} sin\mu & F_c \cdot \zeta_{cs} \cdot cosk \end{Bmatrix} = \begin{Bmatrix} 0 \\ 0 \\ 0 \end{Bmatrix} \tag{3.17}$$

where β is half of the roller taper angle (Fig. 3.3);

$F_c$is a centrifugal force;

$Q_f$is a force of interaction of the end of the roller with the support board;

$Q_{зов}$, $Q_{вн}$ are the force of interaction of the roller with the outer and inner ring, respectively;

$T_{зов}$, $T_{вн}$ are the moment in the contact zone with the outer and inner ring, respectively; μ is the contact angle of the roller end.

Regarding railway conical bearings, which have relatively large dimensions, it should be noted that they are used at low rotation frequencies.

Therefore, the effect of centrifugal forces can be neglected. Then the system of equations for determining efforts takes the following form:

$$\begin{Bmatrix} F_\xi \\ F_\zeta \\ M_\eta \end{Bmatrix} + \begin{Bmatrix} Q_{\text{зов}}cos\beta & -Q_{\text{вн}}cos\beta & Q_f sin\mu \\ -Q_{\text{зов}}sin\beta & -Q_{\text{вн}}cos\beta & Q_f cos\mu \\ T_{\text{зов}} & -T_{\text{вн}} & Q_f\zeta_{cs}sin\mu \end{Bmatrix} = \begin{Bmatrix} 0 \\ 0 \\ 0 \end{Bmatrix}. \quad (3.18)$$

This system was solved numerically by the Newton-Raphson method. After solving it, we get the loads acting on each of the rollers. But the proposed model for determining the loads on the rollers of the axle bearing in the upper zone does not take into account the flexibility of the axle box body, the presence of which significantly affects the distribution of loads between the rollers.

To determine the stress-strain state of the roller at any point, we use the Businesk solution [2], according to which the elastic deformation at point A, located at a distance r from the point of application of force P, is equal to

$$U = \frac{P(1-\nu^2)}{\pi E r}. \quad (3.19)$$

Having considered the point of the roller $P(x, y, z)$, which is located at a distance r from the element of the pressure field $p(x', z')$ acting on the site $dy'dz'$ (Fig. 3.4), taking into account (3.19), we can write

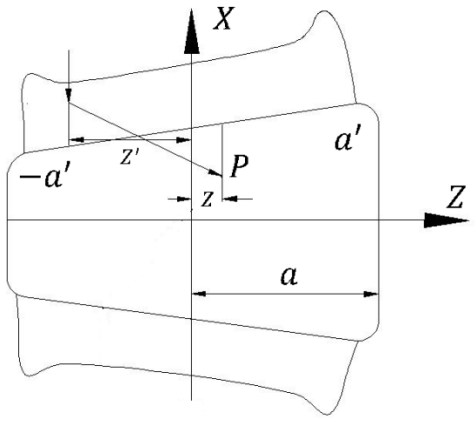

Fig. 3.4. Roller loading scheme

$$d\sigma_R = \frac{p(y', z') \cdot dx'dz'}{2\pi}\left\{(1-2\nu)\left(-\frac{1}{R^2} + \frac{x}{R^2 r}\right) - \frac{3R^2 x}{r^5}\right\}, \quad (3.20)$$

$$d\sigma_\Theta = \frac{p(y\prime, z\prime)\cdot dy'dz\prime}{2\pi}\left\{(1-2\nu)\left(-\frac{1}{R^2} + \frac{x}{R^2 r}\right) + \frac{x}{r^3}\right\}, \quad (3.21)$$

Where

$$R^2 = (y'-y)^2 - (z'-z)^2, \quad (3.22)$$

$$R^2 = (y'-y)^2 - (z'-z)^2, \quad (3.22)$$

$$r^2 = (y' - y)^2 + (x' - x)^2 + (z' - z)^2. \quad (3.24)$$

Then the complete stress state of the roller in the contact zone with the outer ring, caused by the distribution of contact stresses on the rectangular area, is determined by the following dependencies:

$$\sigma_x = -\frac{3}{2\pi} \int_{-a'}^{a} \int_{-b}^{b} p(y', z') \cdot \frac{(c + x)^3}{r^5} dy' dz', \quad (3.25)$$

$$\sigma_y = \frac{1 - 2\nu}{2\pi} \int_{-a'}^{a} \int_{-b}^{b} p(y', z') \left\{ \left(1 - \frac{(c + x)}{r} \right) \cdot \frac{(y' - y)^2 - (z' - z)^2}{R^4} + \right. \left. + \frac{(c + x) \cdot (z' - z)^2}{R^2 \cdot r^3} \right\} dx' dz' - \quad (3.26)$$
$$- \frac{3}{2\pi} \int_{-a'}^{a} \int_{-b}^{b} p(y', z') \cdot \frac{(y' - y) \cdot (c + x)}{r^5} dy' dz',$$

$$\sigma_z = \frac{1 - 2\nu}{2\pi} \int_{-a'}^{a} \int_{-b}^{b} p(y', z') \left\{ \left(1 - \frac{(c + x)}{r} \right) \frac{(z' - z)^2 - (y' - y)^2}{R^4} + \right. \left. + \frac{(c + x) \cdot (y' - y)^2}{R^2 \cdot r^3} \right\} dy' dz' - \quad (3.27)$$
$$- \frac{3}{2\pi} \int_{-a'}^{a} \int_{-b}^{b} p(y', z') \cdot \frac{(c + x) \cdot (z' - z)^2}{r^5} dy' dz',$$

$$\tau_{xy} = -\frac{3}{2\pi} \int_{-a'}^{a} \int_{-b}^{b} p(y', z') \cdot \frac{(c + x)^2 \cdot (y' - y)}{r^5} dy' dz', \quad (3.28)$$

$$\tau_{xz} = -\frac{3}{2\pi} \int_{-a'}^{a} \int_{-b}^{b} p(y', z') \cdot \frac{(c + x)^2 \cdot (z' - z)}{r^5} dy' dy', \quad (3.29)$$

$$\tau_{yz} = \frac{1-2\nu}{2\pi} \int_{-a'}^{a} \int_{-b}^{b} p(y', z') \left\{ \left(1 - \frac{(c+x)}{r} \right) \cdot \frac{2}{R^4} - \frac{c+x}{R^2 \cdot r^3} \right\} \times$$
$$y \times (y - y')(z' - z) dy' dz' - \frac{3}{2\pi} \int_{-a'}^{a} \int_{-b}^{b} p(y', z') \cdot (c + x) \times \quad (3.30)$$
$$y \times \frac{(y-y') \cdot (z'-z) dy' dz}{r^5} dy' dz,$$

where c is the roller radius at the stress determination point;

x, y, z are the coordinates of the point where the pressure is applied;

x', y', z' *are the* coordinates of the point where stresses are calculated;

ν is Poisson's ratio;

a is the length of the contact area;

b is the half-width of the contact area.

Accordingly, the stresses in the contact zone of the roller with the inner ring of the bearing are calculated as follows:

$$\sigma_x = -\frac{3}{2\pi}\int_{-a'}^{a}\int_{-b}^{b} p(y', z') \cdot \frac{(c-x)^3}{r^5}\, dy x' dz', \tag{3.31}$$

$$\sigma_y = \frac{1-2\nu}{2\pi}\int_{-a'}^{a}\int_{-b}^{b} p(y', z') \left\{ \left(1 - \frac{(c-x)}{r}\right)\frac{(y'-y)^2 - (z'-z)^2}{R^4} + \right. \left. + \frac{(c+x)\cdot(z'-z)^2}{R^2 \cdot r^3} \right\} a \tag{3.32}$$

$$- \frac{3}{2\pi}\int_{-a'}^{a}\int_{-b}^{b} p(y', z') \cdot \frac{(y'-y)\cdot(c-x)}{r^5}\, dy' dz',$$

$$\sigma_z = \frac{1-2\nu}{2\pi}\int_{-a'}^{a}\int_{-b}^{b} p(y', z') \left\{ \left(1 - \frac{(c-x)}{r}\right)\frac{(z'-z)^2 - (y'-y)^2}{R^4} + \right. \left. + \frac{(c+x)\cdot(y'-y)^2}{R^2 \cdot r^3} \right\} a \tag{3.33}$$

$$- \frac{3}{2\pi}\int_{-a'}^{a}\int_{-b}^{b} p(y', z') \cdot \frac{(c-x)\cdot(z'-z)^2}{r^5}\, dx y' dz',$$

$$\tau_{xy} = \frac{3}{2\pi}\int_{-a'}^{a}\int_{-b}^{b} p(y', z') \cdot \frac{(c-x)^2 \cdot (y'-y)}{r^5}\, dy' dz', \tag{3.34}$$

$$\tau_{xz} = \frac{3}{2\pi} \int_{-a'}^{a} \int_{-b}^{b} p(y', z') \cdot \frac{(c - x)^2 \cdot (z' - z)}{r^5} dy'dz', \tag{3.35}$$

$$\begin{aligned} \tau_{yz} = {} & \frac{1 - 2\nu}{2\pi} \int_{-a'}^{a} \int_{-b}^{b} p(y', z') \left\{ \left(1 - \frac{(c - x)}{r} \right) \cdot \frac{2}{R^4} - \frac{c - x}{R^2 \cdot r^3} \right\} \times \\ & \times (y - y')(z' - z) dy x' dz' - \frac{3}{2\pi} \int_{-a'}^{a} \int_{-b}^{b} p(y', z') \cdot (c - x) \times \\ & \times \frac{(y - y') \cdot (z' - z) dy'dz}{r^5} dy'dz', \end{aligned} \tag{3.36}$$

The stresses determined by formulas (3.25 – 3.36) will differ from zero at the edges of the roller.

The calculation results for the central roller indicate that it is in a safe state. The voltage is significantly lower than those allowed. Thus, σ_x did not exceed 225 MPa, similarly $\sigma_y$varied within the range of up to 627 MPa, that is, the strength of the rolling elements will be ensured.

But it should be noted that from the point of view of ensuring the reliability of the bearing assembly as a whole, the value of the contact stresses arising in the contact zone is of considerable interest.

3.2. Study of contact stresses arising along the generating element of rollers

3.2.1. Mathematical model of solving the contact problem

To determine the durability of bearings, the most important thing is not the strain-stress state of the rolling elements and bearing rings, but the distribution of contact loads along the generator of the rollers.

It is known: the load applied to the bearing is perceived by the very small areas of contact between the rolling elements and the raceways, therefore the stresses at the contact points are very significant even with relatively moderate loads. The normal stresses allowed in rolling bearings in the places of point and linear contact are equal to [σ]=5000 MPa and [σ]=3500 MPa, respectively.

However, the effective area of the load-bearing roller increases sharply as it moves away from the surface. As a result, high compressive stresses are concentrated only in the contact zone, not spreading over the entire mass of the rolling body. Therefore, the strength of rolling bearings depends mainly on the stresses that occur on the contact surface, more precisely, at some depth near the

surface layer. At the same time, the deformations in the contact of the rolling surfaces, taking into account their high hardness, are very small.

H. Hertz in his work [8] proposed a solution to the problem, which has become a classic, for determining local stresses and deformations of two elastic bodies with point contact. It follows that in the zone with point or linear contact when a load is applied, a small contact area is formed, and the distribution of the load on the surface of this area is subject to regularity, which makes it possible to determine the surface tension. At the same time, the following assumptions are accepted:

1. The stresses in the material of the touching bodies do not exceed the limits of proportionality, that is, all deformations occur in the elastic zone, and there are no plastic deformations;

2. The applied load is perpendicular to the contact area (that is, the influence of surface tangential stresses can be neglected). In real operating conditions of the bearing, during its rotation under load on the contact surfaces of bodies and raceways, in addition to normal stresses, significant tangential stresses occur, which significantly affects the first initiation of fatigue damages of these surfaces;

3. The dimensions of the contact area are significantly smaller than the radii of curvature of the bodies in contact, and the radii of curvature of the contact areas are much larger than the dimensions of these areas. Compliance with this condition depends on the type of contact of the rolling surfaces: in bearings with a high degree of contact, that is, in most ball and roller spherical bearings, the contact areas formed under high loads have a large curvature and contact area dimensions of are very significant compared to the radii of curvature;

4. The stuff of mutually contacting bodies must be homogeneous and isotropic. This condition is limited for metallic bodies having a crystalline structure. The modulus of elasticity of metals, which is considered as a constant value, is actually the average value obtained for individual crystals with an arbitrary arrangement of axes;

5. During mutual movement of bodies, the contact can be considered static if the relative speed is small compared to the speed of propagation of small disturbances in the bodies.

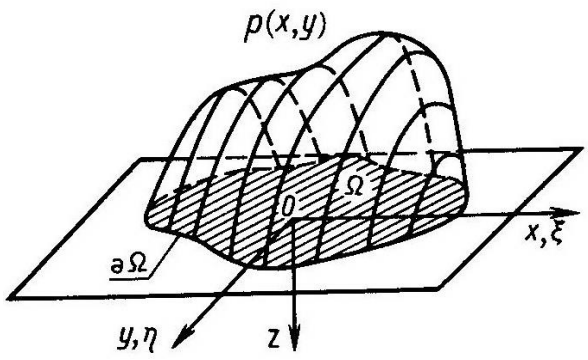

Fig. 3.5. Scheme of contact of two surfaces

In determining the displacement of the surface points, the body can be considered half a space.

From the theory of elasticity, it is known that normal movement ω under the action of pressure distributed in some area ω (Fig. 3.5) is calculated by the formula

$$\omega(x,y) = \frac{1}{\pi E'} \int\limits_{\Omega} \frac{p(\xi,\eta)d\xi d\eta}{\sqrt{(\xi - x)^2 + (\eta - y)^2}}, \tag{3.37}$$

where $E' = \frac{E}{1-\nu^2}$.

After passing to the polar coordinates $r_0(\varphi)$with the pole at the point $r'(\varphi)$, the expression (3.37) takes the form

$$\omega\omega(x,y) = \frac{1}{\pi E'} \int\limits_{\varphi_1}^{\varphi_2} d\varphi \int\limits_{r_0(\varphi)}^{r'(\varphi)} \rho(\rho,\varphi)d\rho\,, \tag{3.38}$$

where $\varphi = const$ are the coordinates of the intersection points of the beam

φ=const with the boundary $d\Omega$ of the region Ω (if the point with coordinates (x,y) lies outside Ω;

$\varphi_1$and $\varphi_2$are the limit values of φ at which the ray $\varphi = const$ crosses the region Ω. If the point (x,y) belongs to Ω , then φ_1=0, φ_2=2π, $r_0(\varphi)\equiv 0$.

In this case, if in (6.38) we take the integral over ρ from 0 to $r'(\varphi)$ at $\varphi = const$, and then from 0 to $r(\varphi + \pi)$ along the ray $\varphi + \pi$, then the sum of the intervals will be the area $S(\varphi)$ of the intersection of the area under the graph $p(x,y)$ with the plane passing through the line $\varphi = const$. Next, this area must be integrated over φ from 0 to π.

This technique simplifies the calculation of displacements according to formula (3.39). If the boundary of the area Ω is an ellipse, then its equation will be as follows

$$\frac{\xi^2}{a^2} + \frac{\eta^2}{b^2} = 1, \tag{3.39}$$

where a, b are its major and minor semi-axes. Then the pressure $p(\xi,\eta)$ will be distributed according to the semi-ellipsoidal law

$$p(\xi,\eta) = p_0 \sqrt{1 - \left(\frac{\xi}{a}\right)^2 - \left(\frac{\eta}{b}\right)^2}. \tag{3.40}$$

The equation of the limit $r = r'(\varphi)$, when the beginning of the polar coordinate system is located at the point with coordinates (x,y), is obtained if we substitute $\xi = x + r \cdot cos\varphi, \eta = y + r \cdot sin\varphi$.. In the intersection of the semi-ellipsoid, the plane passing through the line $\varphi = const$ will be a semi-ellipsoid with a horizontal semi-axis $(r_1 + r_2)/2$, where $r_1 = r'(\varphi), r_2 = r'(\varphi + \pi)$.

When the pressure is distributed according to the law (6.40), the movement of the points of the surface of the half-space located in the load area is determined by the following formula

$$\omega = \frac{1-\mu^2}{E}\frac{p_0}{a}\left[ab \cdot K(e) - \frac{b}{a}M(e) \cdot x_1 - \frac{a}{b}(K(e) - M(e)\right. \quad (3.41)$$

where μ is Poisson's ratio;

E is modulus of elasticity;

$K(e) = \int_0^{\pi/2} \frac{d\varphi}{\sqrt{1-e^2 \cdot sin^2\varphi}}$ is a complete elliptic integral of the first kind;

$e = \sqrt{1-(b/a)^2}$ is a relative eccentricity of the ellipse;

$L(e) = \int_0^{\pi/2} \sqrt{1-e^2 \cdot sin^2\varphi}d\varphi$ is a complete elliptic integral of the second kind;

$M(e) = \frac{1}{e^2}[K(e) - L(e)]$.

In the case of mutual contact of two cylinders after applying the load, the contact line turns into a rectangular area (Fig. 3.6) with the axes l (in the direction perpendicular to rolling) and 2b (in the direction of rolling).

The width of the site is determined by the following formula:

$$2b = 6{,}68 \cdot 10^{-3}\left(\frac{Q}{\sum \rho l}\right)^{1/2}, \quad (3.42)$$

where Q is the applied load;

$\sum \rho l$ is the sum of the curvatures of the cylinders.

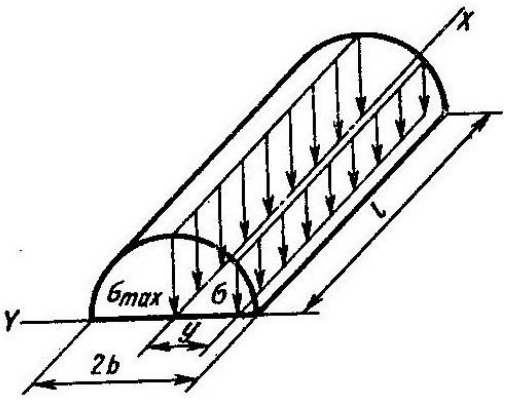

Fig. 6.6. Stress distribution in linear contact

Known solutions of the contact problem, given in the works of S.V. Pinegin [84], K.V. Johnson [46], belong to the cases of contact of bodies with surfaces of constant curvature, when the contact area has the shape of a strip or an ellipse. The problem of the contact of two cylinder-trees of infinite length was theoretically solved in the fundamental work of L.A. Halin [44].

However, in real machine-building structures, cylinders always have a finite length. In addition, when touching two rollers, if the generator of at least one of them has a variable curvature, the pad has a different shape, and, given the great mathematical difficulties, there is no exact solution for such cases. This largely hinders work on optimizing the forms of bearing surfaces in order to increase the durability of such important assemblies as rolling stock rolling bearings, since it is impossible to determine the magnitude and distribution of pressure during compression of bodies of complex shape based on known dependencies.

In addition, the surfaces of the parts operating under contact load conditions at the maximum pressure p_0 >300 MPa already at the start of operation

undergo significant changes in shape caused by the remaining deformations. In a number of cases, this circumstance is aggravated by the uneven operation of the working surfaces, which leads to additional changes in their shape. Therefore, practically during the entire period of operation of this pair, the value and distribution of the contact pressure differ significantly from the initial ones and are not amenable to engineering calculation. Therefore, it is of interest to obtain an approximate solution that, with a degree of accuracy acceptable for practical purposes, would make it possible to judge the magnitude and nature of the pressure distribution on non-elliptical contact surfaces.

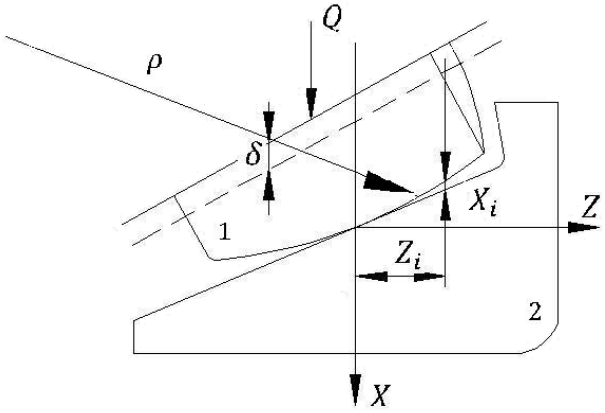

Fig. 3.7. Scheme of contact of the conical roller with the inner ring

The rolling bodies in contact will be presented in the form of two cones: truncated cone 1, imitating a roller and having a ball of radius ρ, and truncated cone 2, imitating the inner ring of a bearing (Fig. 3.7).

Before applying the load, the contact between the bodies occurs at a point. The $X0Z$ coordinate system will be located at the same point.

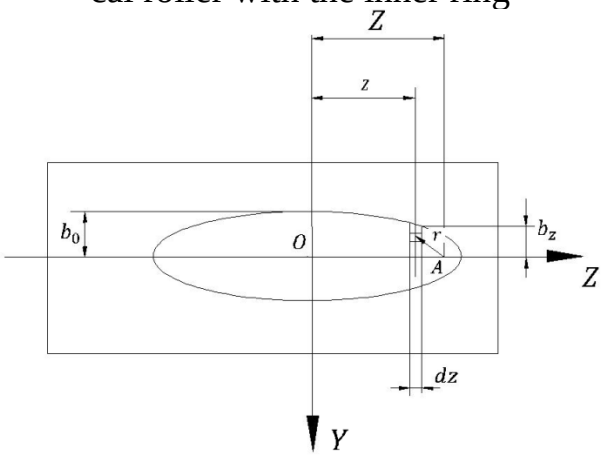

Fig. 3.8. Scheme of the contact area

The clearances between the rolling elements at the distance Z_i are equal toX_i. If we determine through δ the general approximation of rolling bodies (Fig. 3.8), we can write that after applying the load, the deformations within the contact area are determined as follows

$$U_{z_i} = \delta - x_{z_i}, \quad (3.43)$$

where U_{z_i} is the elastic deformation of the rolling elements in the i-th intersection in the direction of the X axis;

$x_{z_i}$is the gap between the bodies in the xoz plane at the z_i intersection.

Outside the contact boundary, this equation is invalid because the contour of the deformed surface in the $X0Y$ plane is no longer a straight line. We assume that each of the strips of length b_z and width dz represents an element of the contact area of two cones under a running load q_z.

According to [80], the maximum pressure in the section z

$$p(z,0) = C_0 \cdot b_z, \tag{3.44}$$

Where

$$C_0 = \frac{0{,}5}{\eta \cdot R}. \tag{3.45}$$

ording to Businеski's solution [2], the elastic deformation at
ıt A, located at a distance r from the point of application of
e P, is equal to

$$U = \frac{P(1-\nu^2)}{\pi E r}. \tag{3.46}$$

Since the total compliance of both bodies is taken into account when calculating convergence, then

$$U = \frac{P}{\pi r}\left(\frac{1-\nu_1^2}{E_1} + \frac{1-\nu_2^2}{E_2}\right). \tag{3.47}$$

Cut the contacting rolling bodies into planes parallel to the $X0Y$ plane and separated from each other by the same distance $l = b_0$ ($b_0 = b_{max}$for this contact area) (Fig. 3.9). Accordingly, the contact area will be divided into n strips of width l, parallel to the $0Y$ axis.

The zero band, on which $b_i = b_{max}$, is located symmetrically about this axis. Numbers on the right have a positive sign, on the left - negative.

We take the number of strips n such that the value nl is much larger than the length $2a$ of the contact area.

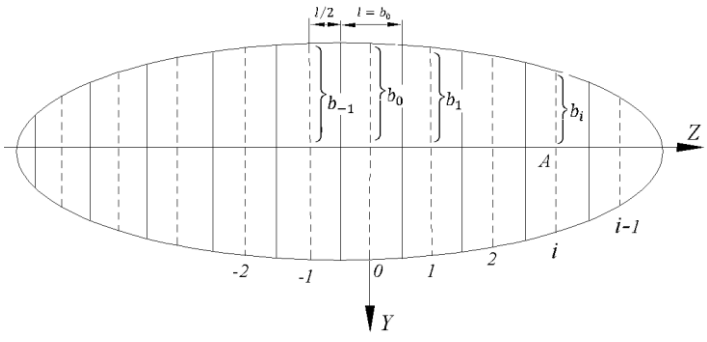

Fig. 3.9. Layout of the contact area

Let's find the deformation i U_{ij}n the middle of the i -th strip (at point A), which is caused by the influence of the load distributed on the strip j, the middle of which is distant from point O by a distance z (we assume $b_z = b_i$).

The distance between the strips is equal to $-z = (j-i)l$, where Z is the abscissa of the middle of the j-th strip, so

$$r = \sqrt{(Z - z)^2 + y^2}. \tag{3.48}$$

With an elliptical law of load distribution in the direction of the y axis

$$p(z, y) = C_0 \sqrt{{b_z}^2 - y^2}. \tag{3.49}$$

Then

$$U_{ij} = 2 \int_0^{b_l} \frac{K' \cdot p_{z,y} \cdot l}{r} dy = 2K' \cdot C_0 \cdot l \int_0^{b_l} \frac{\sqrt{{b_j}^2 - y^2}}{\sqrt{(i - j)^2 \cdot l^2 + y^2}} dy. \tag{3.50}$$

By similarly finding U_{ii}, it is possible to compose a system of n equations as follows

$$\sum_{j=1}^{n-1} U_{ij} + U_{ii} = \delta - x_{z_i}. \tag{3.51}$$

Each of these equations determines the elastic strain on some strip i. The system contains n + 1 unknowns: n values of b_i i and δ. The missing equation can be obtained from the condition of equality of the load applied to the bodies distributed over all bands.

However, solving the system and obtaining specific values poses significant mathematical difficulties. Therefore, from a practical point of view, it is more appropriate to use finite element method.

Finite element method is currently a fundamental method for solving solid body mechanics problems using numerical algorithms. The basis of the method is the discretization of the object for the purpose of solving the equations of the mechanics of a solid medium under the assumption that these relations are fulfilled within each of the elementary areas. These areas are called finite elements. They can correspond to a real part of space or be a mathematical abstraction, like elements of rods, beams, plates and shells. Within the limits of the finite element, the properties of the area of the object bounded by it are assigned (for example, the stiffness and strength characteristics of the material, density, etc.) and the fields of values are described (regarding the mechanics of solid bodies, these are displacements, deformations, stresses, etc.). The parameters from the second group are assigned at the nodes of the element, and then interpolating functions are introduced, with the help of which the corresponding values can be calculated at any point inside the element or on its boundary. The task of mathematical description is reduced to linking the factors operating in the nodes. In the mechanics of a continuous medium, it is, as a rule, displacement and effort.

The task of determining the field of displacements in the axle box assembly structure can be reduced to the task of minimizing the total potential energy by nodal displacements.

In the theory of elasticity, the relationship between stresses and deformations is defined as follows:

$$\{\sigma\} = [D] \cdot \{\varepsilon\}, \tag{3.52}$$

where $\{\sigma\} = \left|\sigma_x, \sigma_y, \sigma_z, \sigma_{yz}, \sigma_{xz}, \right|^T$ is the stress vector;

[D] is an elasticity matrix;

$\{\varepsilon\} = \left|\varepsilon_x, \varepsilon_y, \varepsilon_z, \varepsilon_{yz}, \varepsilon_{xz}, \right|^T$ is the vector of total (total) deformation.

The components of the stress vector are shown in Fig. 3.10.

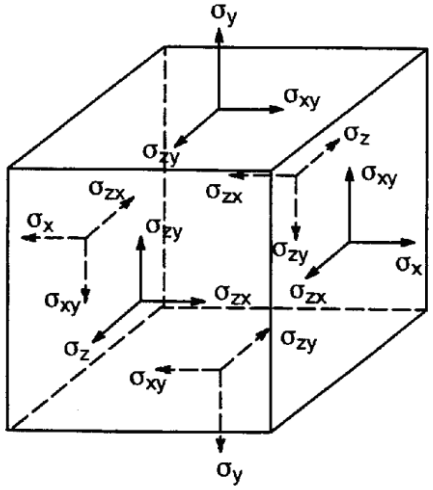

Fig. 3.10. Components of the stress vector

Equation (3.52) can be transformed as follows:

$$\{\varepsilon\} = [\mathrm{D}]^{-1} \cdot \{\sigma\}. \tag{3.53}$$

The matrix $[D]^{-1}$ has the form

$$[D]^{-1} = \begin{vmatrix} 1/E_x & -\nu_{xy}/E_y & -\nu_{xz}/E_z & 0 & 0 & 0 \\ -\nu_{yx}/E_x & 1/E_y & -\nu_{yz}/E_z & 0 & 0 & 0 \\ -\nu_{zx}/E_x & -\nu_{zx}/E_y & 1/E_z & 0 & 0 & 0 \\ 0 & 0 & 0 & 1/G_x & 0 & 0 \\ 0 & 0 & 0 & 0 & 1/G_x & 0 \\ 0 & 0 & 0 & 0 & 0 & 1/G_x \end{vmatrix}. \tag{3.54}$$

The potential energy of deformations is determined by the formula

$$V = \iiint \{(\sigma_x^2 + \sigma_y^2 + \sigma_z^2) - 2\nu(\sigma_x\sigma_y + \sigma_x\sigma_y + \sigma_z\sigma_y) + \\ +2(1+\nu)(\tau_{xy}^2 + \tau_{yz}^2 + \tau_{zx}^2)\}dxdydz. \quad (3.55)$$

The stresses in the direction x $(\sigma_x, \tau_{xy}, \tau_{zx})$ are negligible compared to the stresses in the y and z directions. Accordingly, instead of three stress functions, we introduce only one function φ, which satisfies the biharmonic equation $\nabla^4\varphi = 0$ under the given boundary conditions and provides a minimum for the strain energy. Then the expression (3.55) takes the following form

$$V = \iiint \{(\sigma_x^2 + \varphi_{yy}^2 + \varphi_{zz}^2) - 2\nu(\sigma_x\varphi_{yy} + \varphi_{yy}\varphi_{zz} + \varphi_{zz}\sigma_x) + \\ +2(1+\nu)(\tau_{xy}^2 + \varphi_{yz}^2 + \tau_{zx}^2)\}dxdydz \quad (3.56)$$

Solving this problem is equivalent to finding the function φ, the minimum for equation (3.56) for strain energy.

It is recommended [19] to search for this function in the form of a series

$$\varphi = \varphi_0 + \alpha_1\varphi_1 + \alpha_2\varphi_2 + \cdots \ \alpha_i\varphi_i\,, \quad (3.57)$$

where φ_0 satisfies the boundary conditions for φ, and zero stresses on the boundaries correspond to the functions φ_i.

Expression (3.57) corresponds to the following expressions for the normal stresses in the y and z directions and for the tangential stress

$$\frac{\partial^2\varphi}{\partial z^2} = \varphi_{zz} = \sum_{n=1}^{\infty} \alpha_n \cdot \varphi_{nzz} + \varphi_{0zz} = \sigma_y, \\ \frac{\partial^2\varphi}{\partial y^2} = \varphi_{zz} = \sum_{n=1}^{\infty} \alpha_n \cdot \varphi_{nyy} + \varphi_{0yy} = \sigma_z\,, \quad (3.58) \\ -\frac{\partial}{\partial y}\left(\frac{\partial\varphi}{\partial z}\right) = -\varphi_{yz} = -\varphi_{0yz} - \sum_{n=1}^{\infty} \alpha_n \cdot \varphi_{nyy} + \varphi_{nyz} = \tau_{yz}.$$

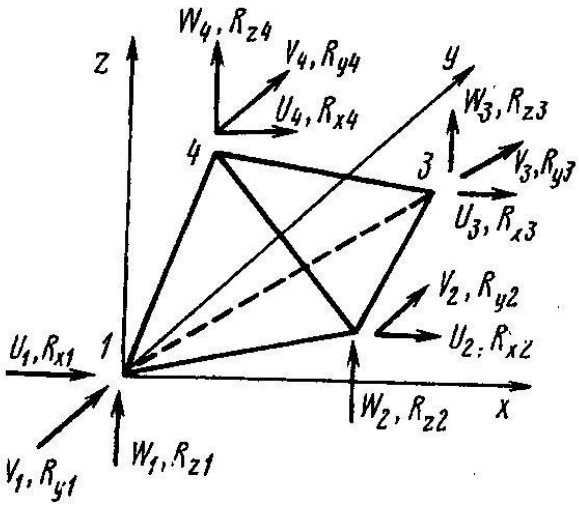

Fig. 3.11. Tetrahedral finite element

To solve three-dimensional stress state problems, finite elements in the form of a tetrahedron (Fig. 3.11) are most often used, having three degrees of freedom at the node and a polylinear approximation of u_x, u_y, u_z movements.

When calculating massive bodies using the finite element method, dependencies for a three-dimensional stress state are used.

These dependencies are the most general, since they are free from various hypotheses and prerequisites characteristic of some individual tasks (hypotheses of plane sections for a rod, straight normals for bending plates, about zero stresses, orthogonal planes of the system, for a plane stress state, etc. n.).

3.2.2. Schematization of the form of calculation objects

Any task about the stress-strain state (SSS) of a structural element is reduced to finding the fields of displacements, deformations, stresses or other functions through which they can be expressed, satisfying a given set of equations in some region and a given set of boundary conditions on the boundary of the specified area. The mentioned area is some schematization of the real space area occupied by the part being calculated.

Thus, the task of schematizing the shape of the object when constructing a calculation scheme is reduced to the description of the area, which is called the geometric model of the object. In the process of solving this problem, a decision is made explicitly or implicitly, to which typical object - plate, shell, rod - should be assigned the part being calculated. Then the specific parameters of the part are described in the terms accepted for this type of objects. The task of classification is solved on the basis of accepted hypotheses about the nature of the work of the part, taking into account what loads it perceives and how it transmits them, whether some dimensions of the part prevail over others, etc.

A simple class of geometric models are rod models. Rods are used to describe objects, one of whose dimensions (length) significantly, by 5-10 times, prevails over the other two (thickness and width). Thus, from the point of view of geometric modeling, a rod is a special case of a kinematically specified object, that is, an object formed by the movement of an object of smaller size, describing one of its intersections, along a straight or curved trajectory. The geo-

metric model of the rod includes a description of its cross-section and the shape of the axis, that is, the geometric location of the points of various cross-sections, which are the centers of gravity.

In addition, in the tasks of mechanics, it is customary to call objects rods, the nature of the distribution of efforts in which makes it possible to use a number of characteristic assumptions in the calculation of SSS. So, it is assumed that the rods perceive mainly axial forces, bending and torsional moments. A number of static and kinematic hypotheses are introduced regarding the law of stress and strain distribution in the cross section. As a result, the task of calculating SSS is reduced to a one-dimensional function, i.e., a calculated function (deflection, moment, etc.), which depends only on the coordinate directed along the axis of the rod. The shape of the cross-section is reflected in the statement of the task of calculating the strain-stress state of the rod not directly, but only through parameters that reflect some integral characteristics of the cross-section (moment of inertia, moment of resistance, etc.).

The next class of geometric models used in solid mechanics are models of shells and plates. These models apply to objects whose size in one direction, such as thickness, is many times smaller than the other two dimensions. Objects of this kind are usually described by specifying the shape of the contour of the middle surface (for plates - in the middle of the plane) and thickness. In some cases, the shell can be multi-layered or have regular reinforcement, which is not displayed explicitly in the geometric model, but by entering given characteristics (thickness, stiffness, etc.).

Thus, the basis of the geometric model used in the calculation scheme of the shell is a description of the middle surface of the object with additional parameters and attributes set on it.

Geometric models of a bending plate and a body in a plane stress state include the description of a flat figure (the middle plane of the object) and additional attributes (thickness, reduced stiffness), given functions of the coordinates of the middle plane. Geometric models of long prismatic bodies under conditions of plane deformation and axially symmetric bodies of rotation are also reduced to the description of a flat contour representing an arbitrary cross-section of a body.

The listed objects basically represent the class of details for the calculation of which one- and two-dimensional geometric models can be used. At the same time, it should be borne in mind that for submitting the task of calculating the strain-stress state in a one- or two-dimensional formulation, the above-mentioned geometrical restrictions relating to the shape of the details are necessary, but not sufficient. The nature of stress distribution and, in particular, the validity of the hypothesis about their independence from one or two coordinates also depend on the type of applied loads. In particular, in an asymmetrically loaded body of rotation, despite its axisymmetric shape, a substantially three-dimensional strain-stress state is realized.

The most general class of geometric models of the mechanics of a deforming body include models of three-dimensional bodies, for which the computational domain Ω is a region in three-dimensional space. The same class includes models of combined structures that include, together with massive three-dimensional parts, thin-walled (lamella, shell, rod) elements.

The main problems of building geometric models of constructions and their elements are reduced to the tasks of analytical or numerical description of three-dimensional bodies, surfaces and curves. These tasks can be solved without the use of computers only in relatively simple cases. They are of particular interest in the creation of CAD, where the geometric model of the product is used not only in the process of calculating strength, but also at almost all stages of design. The use of computers for the formation, storage and use of geometric models allows you to automate time-consuming calculations related to the determination of coefficients of surfaces and lines passing through given points, the calculation of differential characteristics of surfaces, the transformation of coordinates, etc.

It is equally important to automate the process of forming and processing logical connections and relationships between geometric objects. The specified relations determine such group properties of objects as contiguity, that is, the presence of common elements of a lower level, and incidence - the occurrence of an object in one or more objects of a higher hierarchical level. Speaking about the hierarchical level of a geometric object, they mean that any three-dimensional body as an object of the highest level is limited by some surfaces, objects of a lower level. The latter, in turn, are placed inside certain contours consisting of lines. Finally, lines are bounded by endpoints lowest-level objects.

Thus, surfaces and lines can be not only geometric models of shells and rods, but also constituent parts of geometric models of three-dimensional bodies.

Previously, practically the only type of geometric models used in the mechanics of a deforming body were models of canonical objects, i.e. simple two- and three-dimensional figures, which are completely described with the help of many parameters. Examples of canonical objects can be a solid and hollow cylinder, a half-plane, a rectangular and triangular prism, a cone, a torus, a rectangle, a strip, etc. Exact and approximate analytical methods of calculation, as a rule, could be applied only to this kind of objects of simple form. The bulk of the solutions of two- and three-dimensional problems obtained in a closed circuit refer to objects on the surfaces of which one of the coordinates of the coordinate system used is constant. These are, for example, a strip, a half-plane and a cube in the Cartesian coordinate system, a cylinder in a cylindrical one and a hemisphere in a spherical one, etc.

A generalization of models of canonical objects are models obtained by joining canonical objects on common surfaces. Such models can be parameterized. This means that with a fixed structure (topology) of the part, its real dimensions can be represented by dependencies on some set of parameters. Add-

ing values to these parameters allows you to get a whole family of parts based on one model.

Further generalization leads to models built using object modelling technique (OMT) over basic objects.

Canonical objects can act as base objects, and both unlimited (half-plane, infinite cylinder, half-space cone) and limited (rectangle, parallelepiped, cylinder, prism, cone truncated on two sides, etc.), and as well as more important objects obtained from some of the modeling methods described below. Thus, geometric models of OMT are among the most general.

Models based on the representation of bodies using boundaries (boundary models - BM) can also be considered the most general.

In BM models, the topology of a three-dimensional body is represented by a list of its flat or non-flat faces, which in turn are represented by bounded edges. Finally, the edges are bounded by vertices. This topological description of the object is supplemented by a description of its geometry, which allows you to determine the coordinates of vertices, the equation of lines and surfaces on which edges and faces are located. The distinction between the terms "line" and "edge", as well as "surface" and "edge" in the description of the MM model is due to the fact that the lines of the surface are, as it were, the carriers of the geometric shape, and the edges and lines are introduced for highlighting on these carriers of parts related to this object.

Thus, the most general description of the edge includes: the alignment of the line in which the edge is located; reference to two vertices (points) located in the mentioned line and corresponding to the beginning and end of the edge. It is obvious that an edge is a segment of a straight line, the coordinates of two vertices are enough to restore the line. For some other types of lines, instead of the coefficients, it is also convenient to store the coordinates of the edge points, by which this equation can be reconstructed. Thus, the description of a face includes the equation of the surface on which the face is located, a list of edges that create the external and possibly internal contours of the face.

For flat faces, it is not necessary to specify the coefficients of the equation of the plane carrying the given face, since it can be easily calculated from the coordinates of the vertices that limit any two edges of the contour of the face that do not lie on the same straight line.

As indicated above, the boundary representation of a three-dimensional body is defined by a list of its faces. If you impose additional restrictions on the topology of the modeled object, for example, require that it be a convex polyhedron, then to describe it, it is enough to list all its edges. Since each edge is included in the description of two faces, the total amount of information entered will be reduced.

Even simpler objects, for example, hexahedra, tetrahedra, can be described not only by any of the above methods, but also simply by an ordered list of vertices. Models based on the representation of more complex bodies by a set of such elementary objects can be distinguished as a separate set of geometric

models, although they can be considered as a special case of OMT models with the only permissible operation of joining along a common line or along its time mud The specificity of these models, which consists in the simplicity of the basic objects and operations on them, led to their fairly wide application for generating grids in the finite element method. At the same time, new objects can be considered as macroelements, each of which, if necessary, is divided into a given number of ordinary finite elements similar to the initial macroelement. In the extreme case, instead of macroelements, it was possible to directly divide the body into finite elements.

3.2.3. Construction of a geometric model of an axle box bearing assembly with a double-row tapered roller bearing

A finite-element model was developed to study the stress-strain state of a bearing assembly with cassette tapered bearings.

At the first stage, a three-dimensional geometric model of the axle box assembly was created using the ANSYS automated three-dimensional solid body design program (Fig. 3.12).

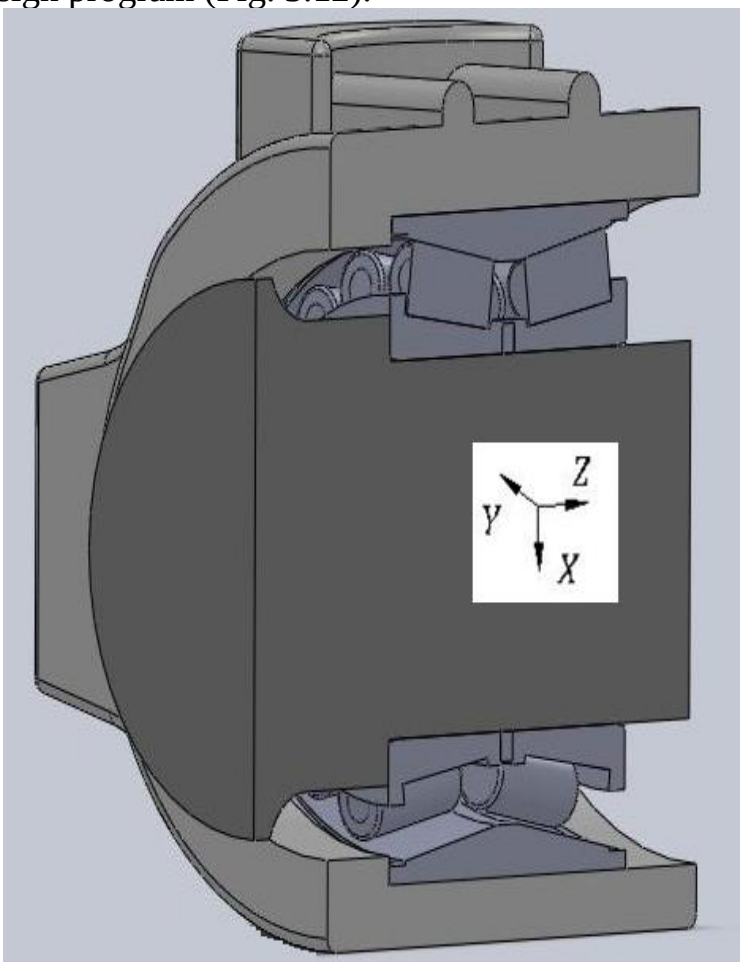

The axle box assembly consists of an axle housing, in which a double-row conical bearing is placed. The latter, in turn, consists of outer and inner rings, between which in each of the rows there is a set of 21 rollers.

Since the bearing is axisymmetric and the applied loads are also symmetrical, half of the model was considered to reduce the complexity of the calculations.

Fig. 3.12. Geometrical model of an axle box bearing assembly with a double-row conical bearing

The presence of a cage does not affect the distribution of contact loads of rollers and rings, so it was excluded from the model. Instead, special connections were introduced to keep the rollers at a certain distance from each other.

For the same reasons, elements of sealing and end fastening were excluded from consideration.

The source data file provides information about the coordinates of nodes, a description of the finite elements used, geometric characteristics of the structure, properties of the material structure, fastening and loading of the model.

The next stage of the work was the transformation of the geometric model of the axle box assembly with a double-row conical bearing into a finite-element model. This work was carried out taking into account the availability of a large library of finite elements in the ANSYS package, which allows modeling a wide range of tasks.

Finite elements of the SOLID 92 type were used to model volumes. These elements are quadratic elements, suitable for modeling irregular grids obtained when importing models from various CAD complexes. The element is determined by ten nodes that have three degrees of freedom in each node: movement in the direction of the X, Y, Z axes in the node coordinate system (Fig. 3.13).

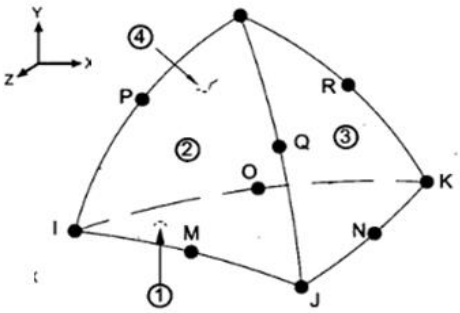

Fig. 3.13. The geometry of the SOLID92 element

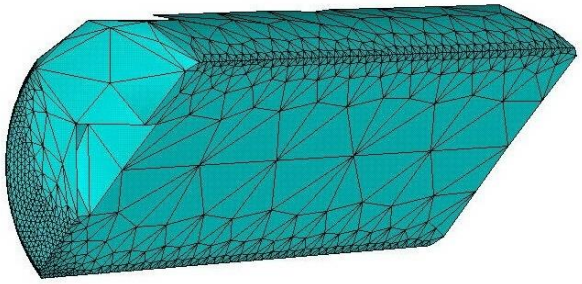

Fig. 3.14. Generation of a finite-element mesh on a roller

ANSYS has special contact elements for modeling contact interaction. In our case, CONTA174 type contact elements were used (Fig. 3.14).

They are used to model the contact interaction between three-dimensional surfaces and the deformable surface defined by this element. The element has the same geometric dimensions as the volume elements associated with it. Contact occurs when the contact node is inserted into the TARGE170 surface element. These contact elements have a common set of geometric characteristics.

The developed model consisted of 4100 volume finite elements of SOLID92, which had the form of a tetrahedron, and 120964 nodes (Fig. 3.15).

Fig. 6.15. Finite element model of a bearing assembly with a double-row conical bearing

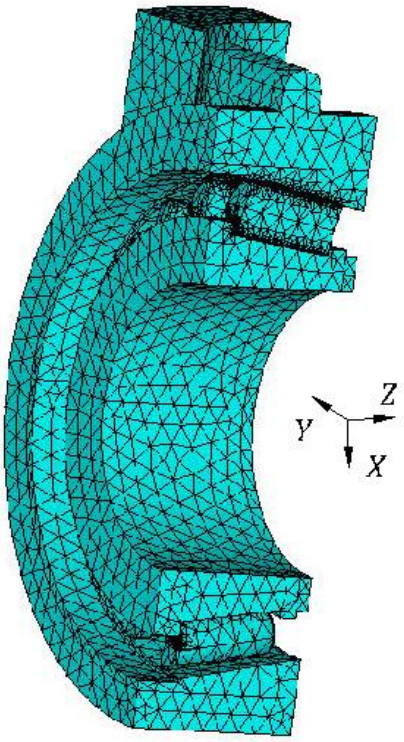

Fig. 6.16. The final finite element model of a bushing bearing assembly with a tapered roller bearing

During the creation of the model, the following assumptions were made, which correspond to the main provisions of Hertz's theory:

• the load to the contacting surfaces is applied perpendicular to the contact area;

• the contact area is small compared to the radii of curvature of the contacting bodies;

• the materials of the contacting bodies are homogeneous, isotropic and perfectly elastic;

• the impact of technological deviations during the assembly of elements of the running parts on the load of the bearing elements, as well as their possible activation in operation, is not taken into account;

• the effect of lubricant on the contact strength of bearing parts is not taken into account.

In order to reduce the amount of computational work, and taking into account the symmetry of the design, the fourth part of the bearing assembly was further considered (Fig. 3.16).

3.3. Study of the stress-strain state of elements of a double-row tapered roller bearing

The loading of the model was carried out in the planes of the global coordinate system (XYZ). The seat surface of the inner ring was fixed completely (movements along all three degrees of freedom were equal to 0). The movement of the bearing rings along the axis neck (along the Z axis) was also limited.

The proposed model allows you to simulate various loading options with an assessment of the stress-strain state of both the bearing itself and the bushing assembly as a whole.

With the help of the developed model, calculations were carried out in two stages:

1) study of the stress-strain state of the elements of the bearing assembly under the action of radial load with an increasing load step;

2) study of the stress-strain state of the elements of the bearing assembly under combined loading, taking into account the action of axial forces.

The dependence of stresses in the contact zone of the central (upper) roller on the value of the radial load is shown in Fig. 6.17.

It is obvious that the obtained stress values are significantly lower than those allowed (3500 MPa). It was established that this value of stress is reached with a radial load of 1500 kN, which is 5 times higher than the actual loads acting on the axle box bearings in operation. Thus, it can be concluded that the contact strength of the rolling elements in the static mode will be ensured.

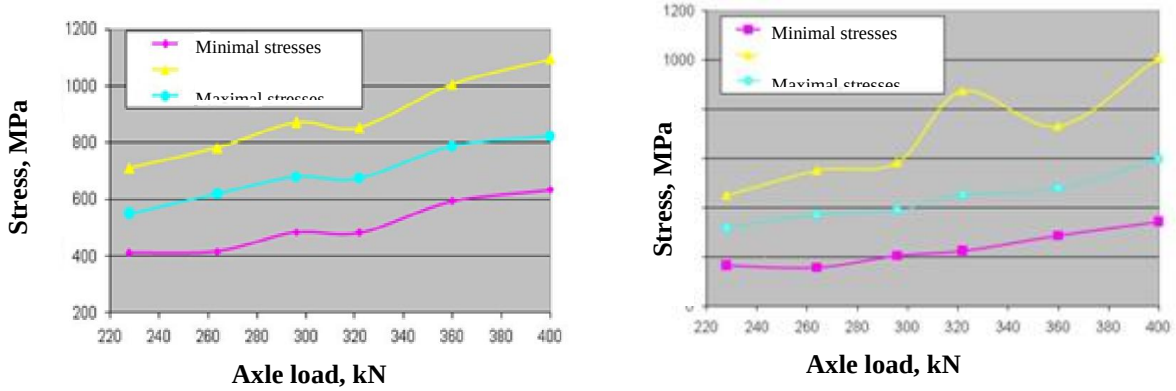

a b

Fig. 3.17. Dependence of changes in contact stresses and a in the contact zone with the outer ring; b in the contact zone with the inner ring

The influence of the combined action of radial and axial loads on the stress state of the rollers is shown in fig. 3.18-3.19. The value of the radial load varied from 228 to 360 kN per axle, and the axial load - from 7.5 to 45 kN.

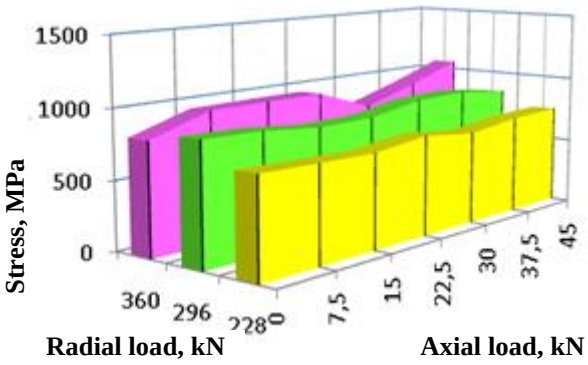

Fig. 3.18. Dependence of changes in contact stresses under the action of axial load in the contact zone of the roller with the outer ring

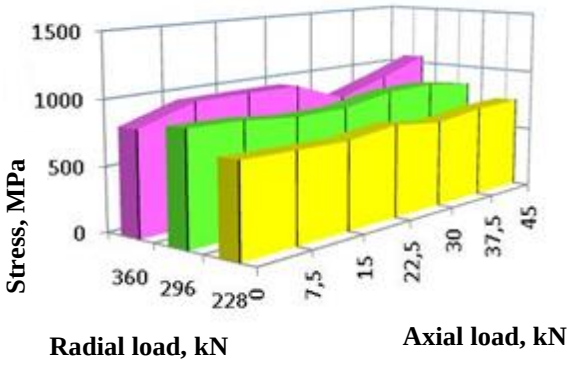

Fig. 3.19. Dependence of changes in contact stresses under the action of axial load in the contact zone of the roller with the inner ring

It is obvious that the appearance of axial forces does not significantly affect the magnitude and character of stress distribution.

The stress distribution along the generating roller is shown in Fig. 3.20. The corresponding dependencies are shown in fig. 3.21 - 3.22.

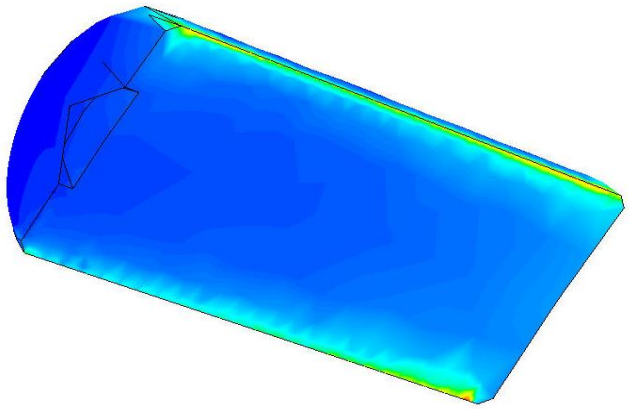

Under the action of a radial load of 360 kN, the nature of the stress distribution is approximately the same for both the inner and outer rings: the maximum values near the edges of the roller and a gradual decrease in the middle of the roller.

Fig. 3.20. Stress distribution along the generating element of the roller

The highest stresses occur at the ends of the second (1198 MPa) and third rollers (1111 MPa).

The appearance of axial forces causes a redistribution of stresses in the bearing (Fig. 3.23-3.24). With the combined effect of a radial load of 360 kN and an axial load of 45 kN in the contact zone with the outer ring, the distribution of stresses both between the rollers and along the bearing becomes more uniform.

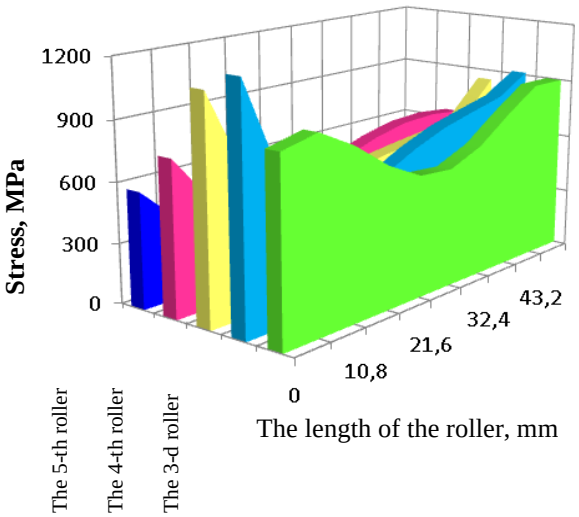

Fig. 3.21. Distribution of stresses along the generating line of the rollers under the action of radial load in the contact zone of the rollers with the outer ring

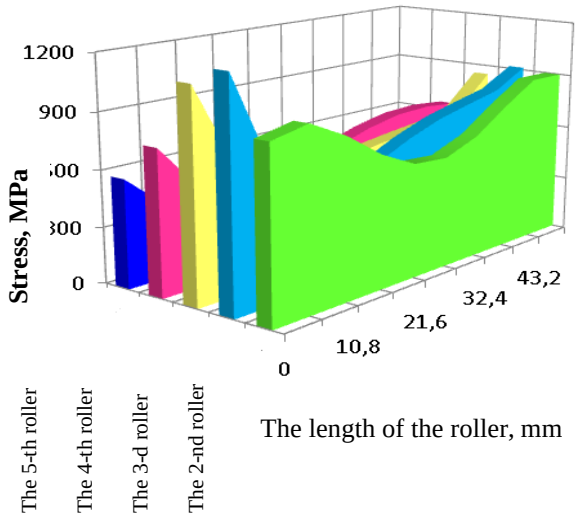

Fig. 3.22. Distribution of stresses along the generating rollers under the action of radial load in the contact zone of the rollers with the inner ring

In the area of contact between the rolling elements and the outer ring, the greatest stresses occur in the area of the central (first) roller. At the same time, in the contact zone of the rolling elements with the inner ring, the maximum stresses are reached in the zone of the next (second) roller.

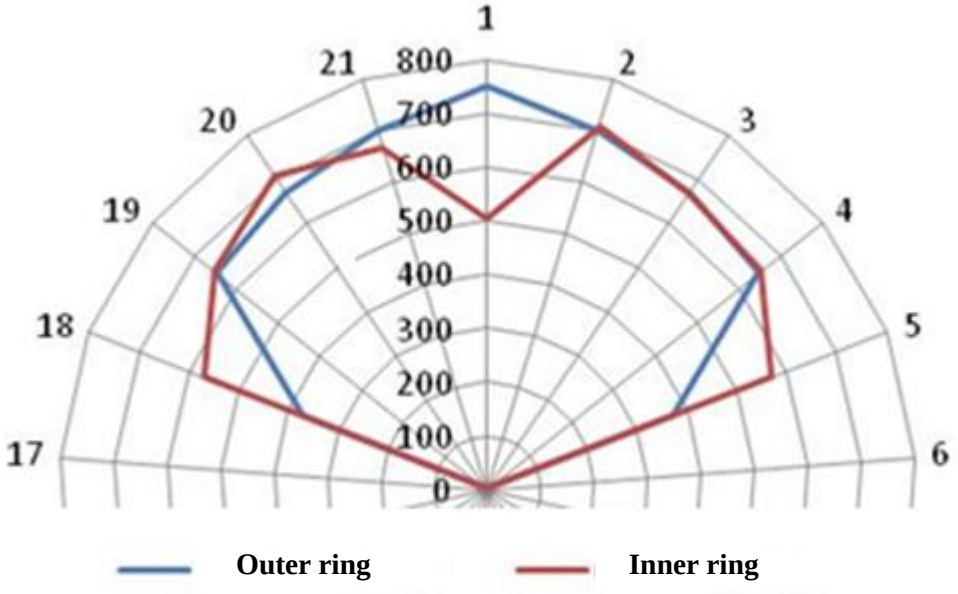

Fig. 3.25. Distribution of maximum contact stresses between rollers (load 230 kN)

A similar pattern remains unchanged when the radial load increases (Fig. 3.26).

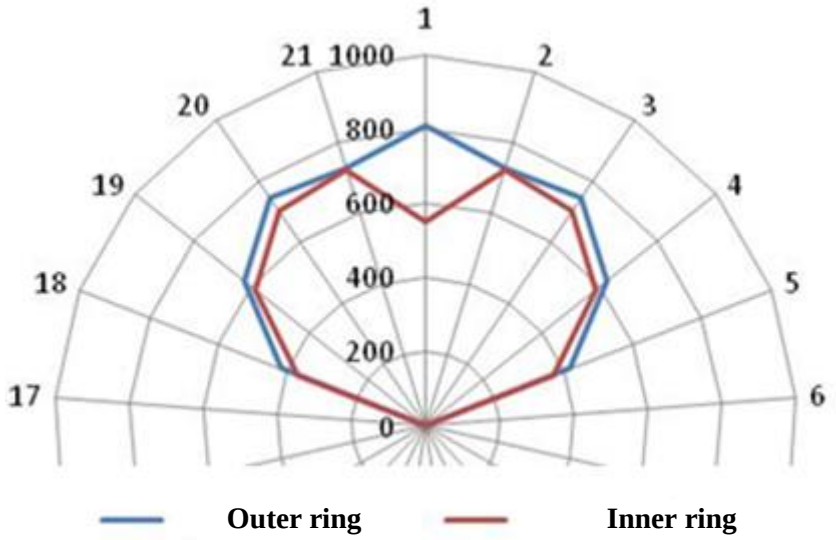

Fig. 3.26. Distribution of maximum contact stresses between rollers (360 kN load)

The appearance of axial forces does not fundamentally change the nature of the distribution of contact stresses (Fig. 3.27).

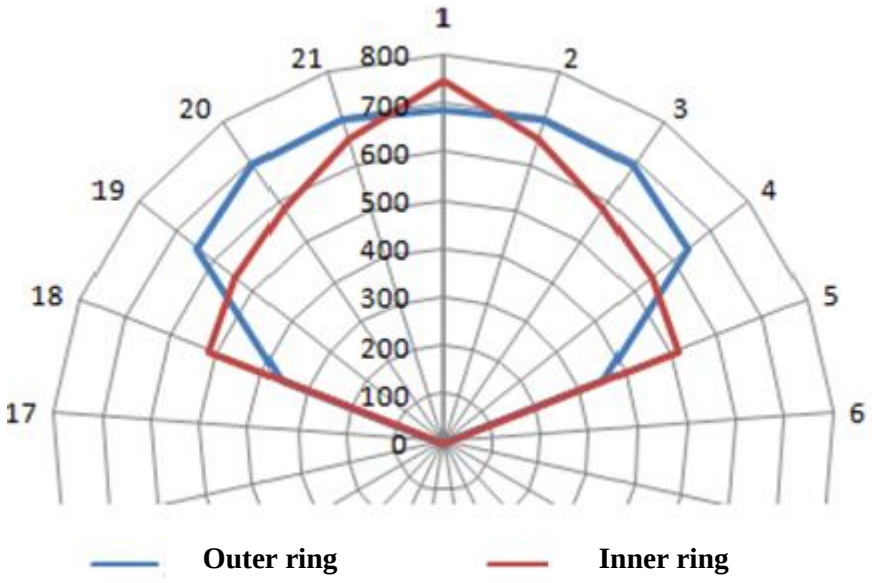

Fig. 3.27. Distribution of maximum contact stresses between rollers (radial load 230 kN, axial load 15 kN)

Fig. 3.28 shows the distribution of contact stresses along the forming line for the upper and second rollers.

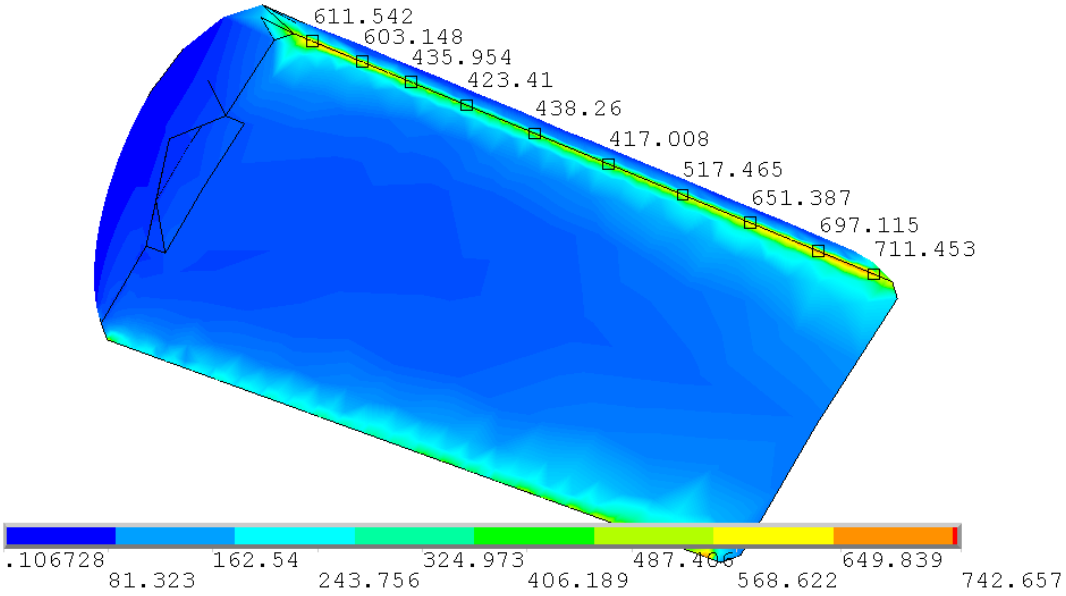

a) distribution of contact stresses

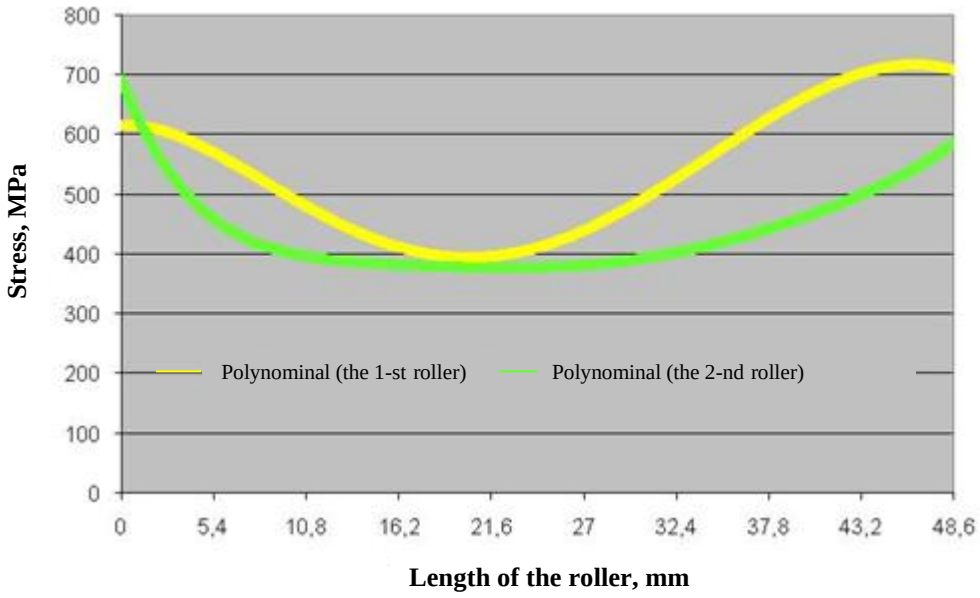

b) approximating dependencies

Fig. 3.28. Distribution of maximum contact stresses along the forming roller (radial load 230 kN)

It is obvious that the amount of stress is minimal in the middle of the roller and increases to maximum values in the zone of transition from the forming roller to its end (that is, the so-called "edge" effect takes place).

The dependences of the change in the maximum stresses in the contact zone of the upper roller with the outer ring are shown in Fig. 3.29. The corre-

sponding dependences of the maximum stresses in the contact zone of the next (second) roller with the inner ring are shown in Fig. 3.30.

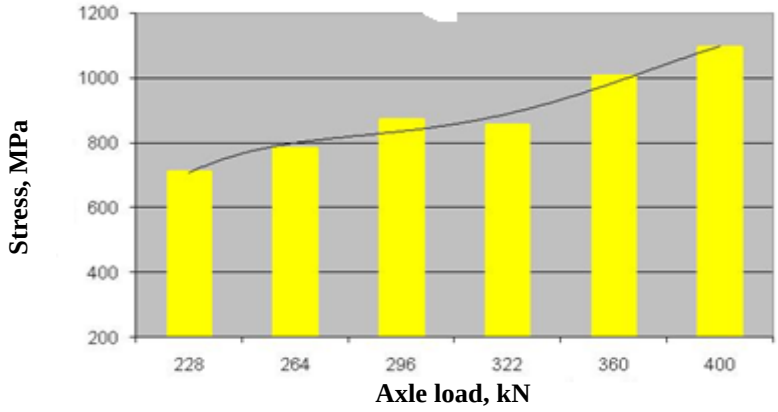

Fig. 3.29. Dependence of the change in maximum contact stresses in the contact zone of the upper roller with the outer ring

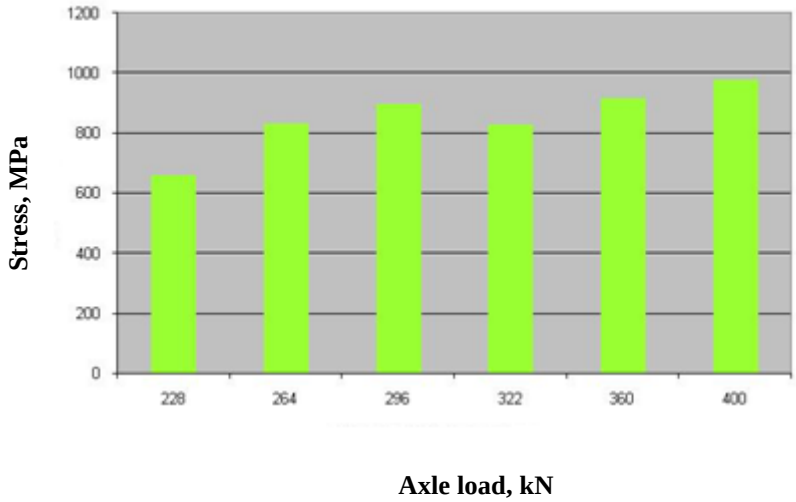

Fig. 3.30. Dependence of the change in the maximum contact stresses in the contact zone of the second roller with the inner ring

As a result, the dependences of the maximum contact stresses on the value of the radial load in the contact zone of the rolling elements with the outer ring were obtained.

$$\sigma_{max}^{\text{зов}} = -2{,}084(Q^{\text{в}})^4 + 33{,}22(Q^{\text{в}})^3 - 175{,}5(Q^{\text{в}})^2 + 417{,}7Q^{\text{в}} + 434 \quad (3.59)$$

A similar dependence for the contact zone of the rolling elements with the inner ring

$$\sigma_{max} = -3{,}375P^4 + 58{,}91P^3 - 356{,}1P^2 + 898{,}3P + 58 \quad (3.60)$$

3.4 Study of the strength of the half-bush (adapter) design

When calculating the half-bush (adapter), the following assumptions were made:

• the material of the half bushing (adapter) works in the elastic stage of deformation and has constant characteristics - modulus of elasticity E = 2.1×105 MPa and Poisson's ratio μ = 0.3;

• the abutment of the adapter on the bearing in the calculation scheme was simulated by introducing kinematic fastening in the nodes corresponding to the inner part of the half-bush.

The vertical load was modeled by applying a force acting normal to the upper tides of the adapter (Fig. 3.31-3.32).

The longitudinal load was applied normal to the side guides of the adapter and was calculated based on the maximum possible load on the axis. In the calculations, the most unfavorable loading option was taken into account (taking into account the coefficient of vertical dynamics according to [78].

It was established that the greatest stresses do not exceed 80 MPa, which is significantly less than the strength limit (Fig. 3.33).

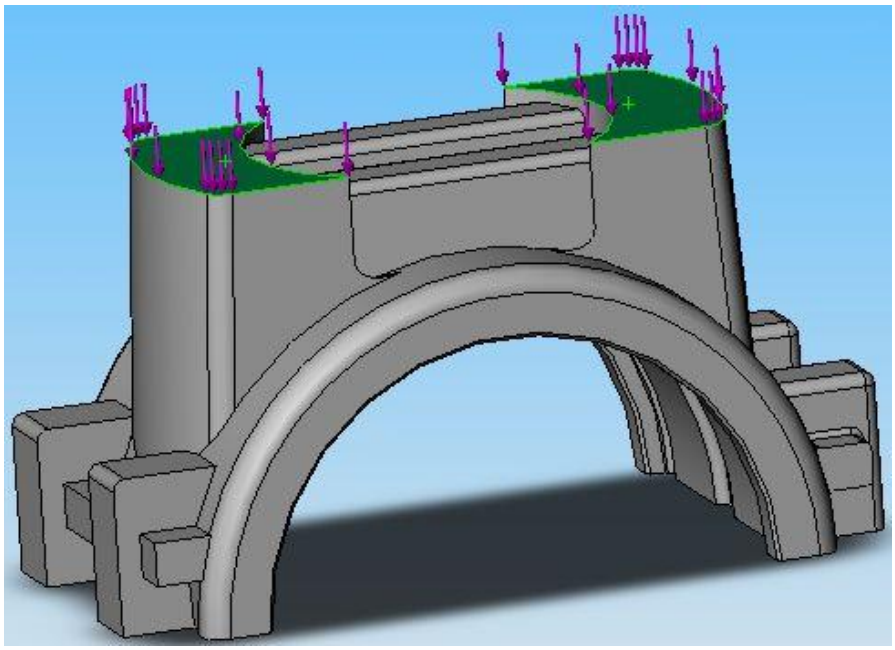

Fig. 3.31. Scheme of application of vertical load

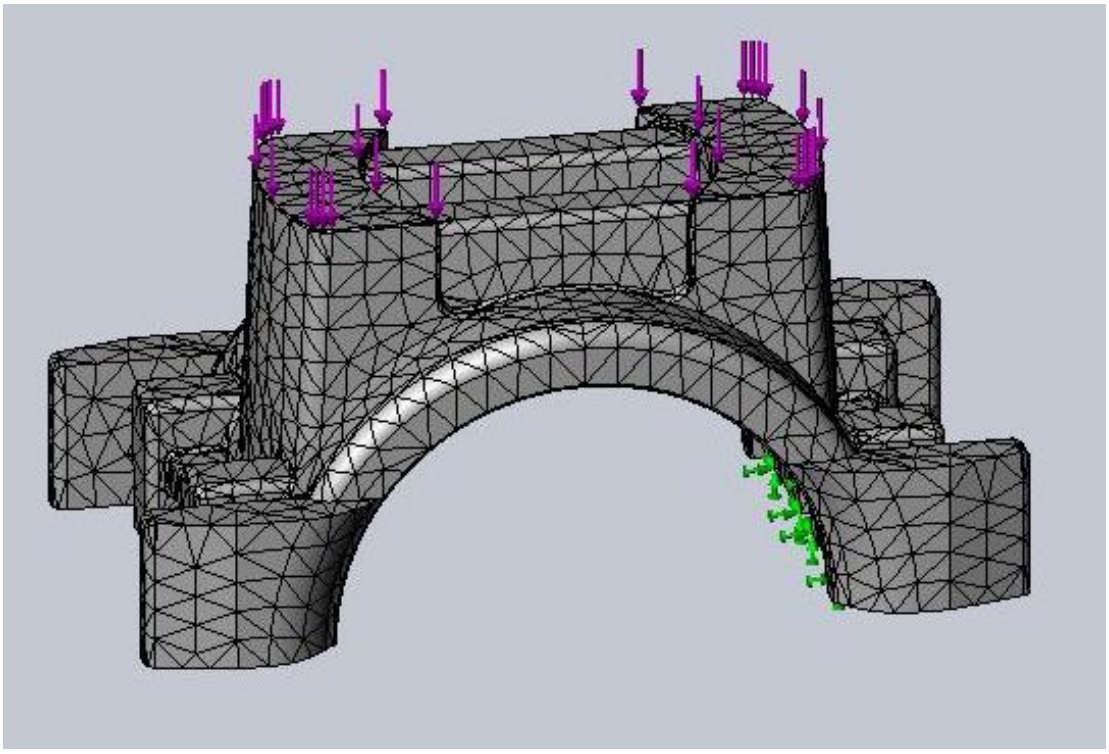

Fig. 3.32. Finite-element grid and scheme of applying loads on the adapter

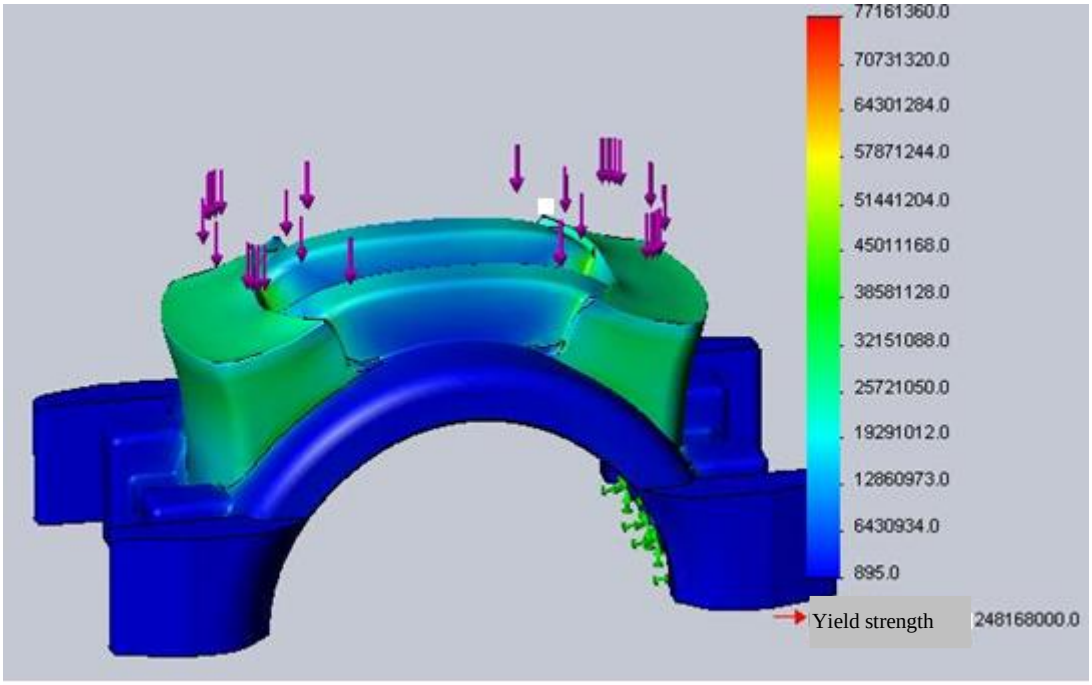

Fig. 3.33. Stress distribution in the adapter

The largest movements of the adapter elements take place in the areas of contact of the supporting surfaces of the adapter with the side frame of the bogie (Fig. 3.34).

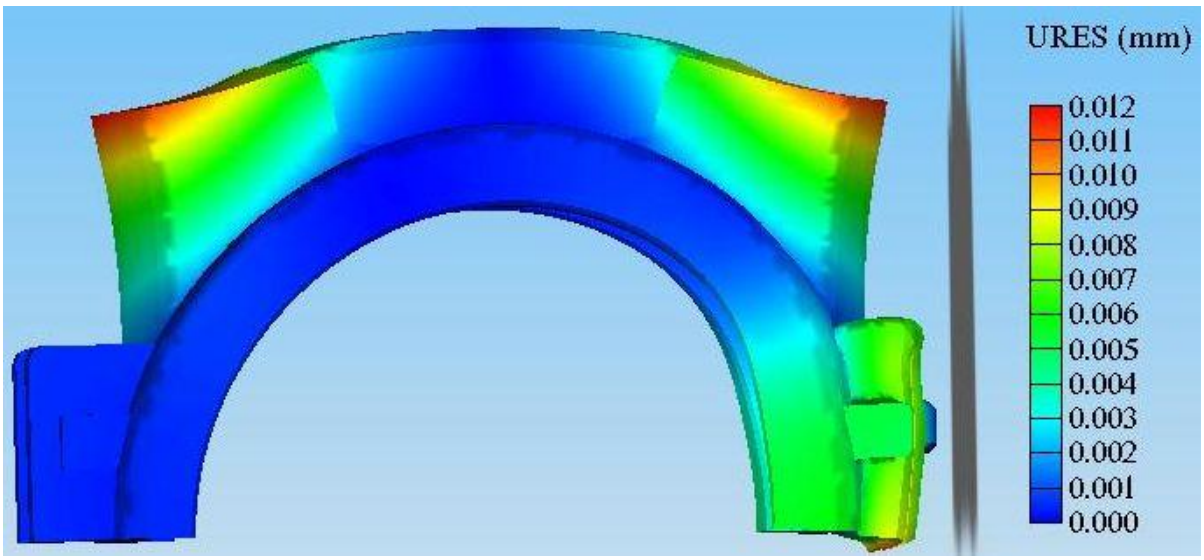

Fig. 3.34. Distribution of movements in the adapter

The safety factor in the upper part of the adapter is at least 3.22 (Fig. 3.35). This ensures the necessary conditions for the safe operation of rolling stock.

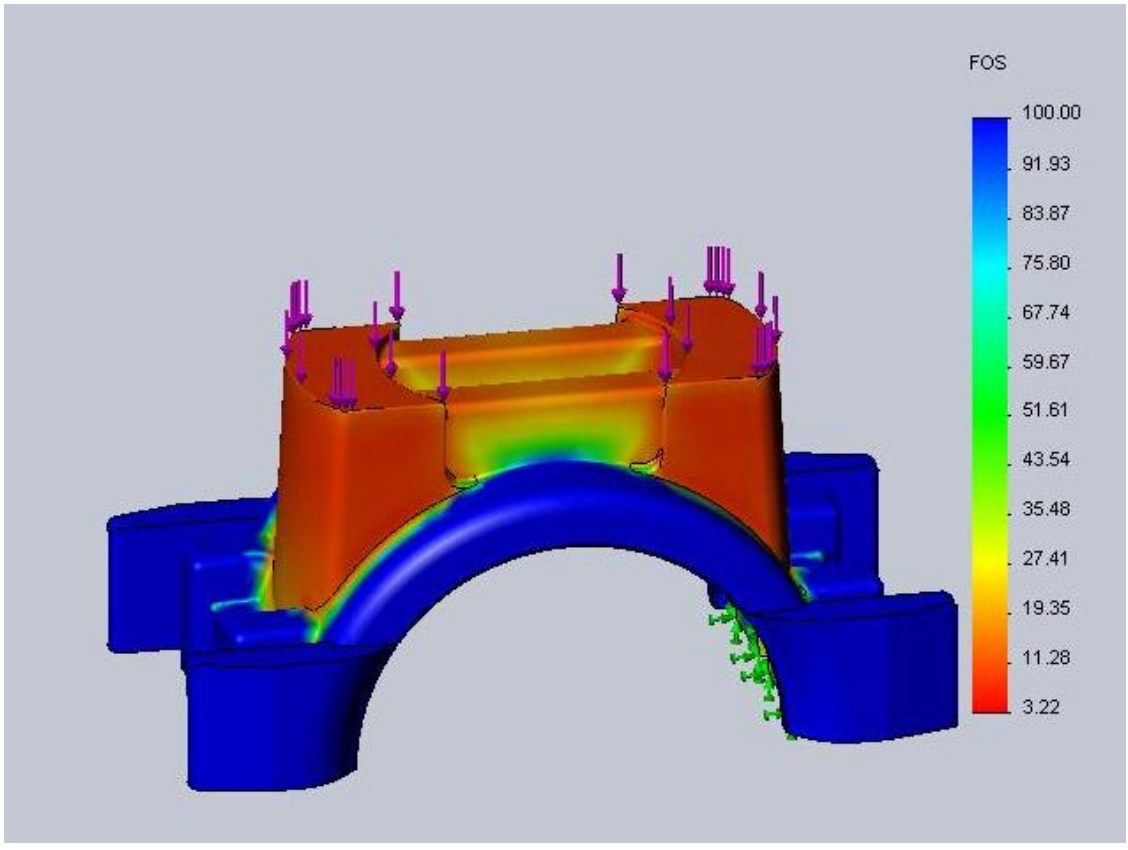

Fig. 3.35. Distribution of the safety factor in the adapter

3.5 Features of the model of the axlebox bearing assembly with a double cylindrical bearing

A finite-element model was developed to study the stress-strain state of the bearing assembly of freight cars with double cylindrical bearings.

At the first stage, a three-dimensional geometric model of the BW was created using the ANSYS program for automated three-dimensional design of solid bodies.

The axle assembly consists of an axle housing in which a double cylindrical bearing is placed (Fig. 3.36-3.37).

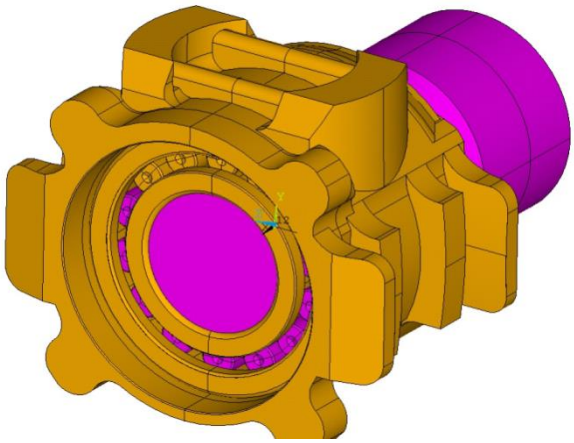

Fig. 3.36. Geometrical model of an axlebox bearing assembly with a double cylindrical bearing

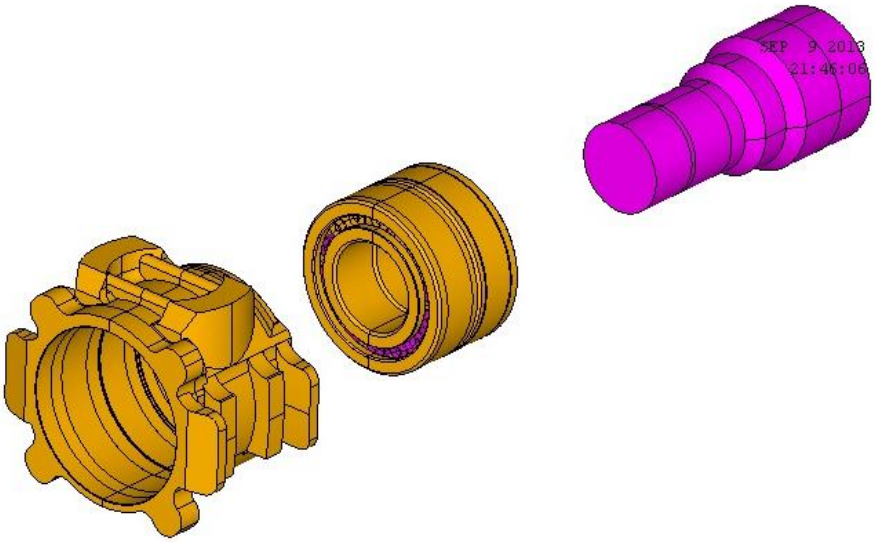

Fig. 3.37. Elements of a geometric model of an axlebox bearing assembly with a double cylindrical bearing

When constructing the geometric model, the main features of the construction of real axlebox bodies were taken into account, namely:

• the presence of dents in the middle part and at the edges (places where there are no rollers in the bearing);

• the presence of the lug in the upper part of the body, designed to absorb the vertical load and ensure its distribution between the rollers;

• the presence of ribs in the side part of the axlebox body, designed for its fixation between the pedestal jaws of the side frame, and ensuring the perception of horizontal loads.

When constructing a geometric model of a double cylindrical bearing, the diameter of the inner ring was 130 mm, and the diameter of the outer ring was 250 mm, between which in each row there is a set of 14 rollers.

Since the bearing is axisymmetric and the applied loads are also symmetrical, half of the model was considered to reduce the complexity of the calculations.

The cage in any bearing is designed to keep the rolling elements at a given distance from each other, so it does not affect the distribution of the contact loads of the rollers and rings. Accordingly, it can be excluded from the geometric model. Instead, special connections were introduced to keep the rollers at a certain distance from each other. For the same reasons, elements of sealing and end fastening were excluded from consideration.

The next stage of the work was the transformation of the geometric model of the axlebox assembly into a finite element model. This work was carried out taking into account the presence of a large library of finite elements in the ANSYS package, which allows modeling a wide range of tasks.

Curvilinear tetrahedral elements suitable for modeling irregular grids were used to model volumes. The element is defined by ten nodes that have three degrees of freedom in each node: movement in the direction of the X, Y, Z axes in the node coordinate system.

The developed model consisted of 4100 volumetric finite elements and 120964 nodes (Fig. 3.38).

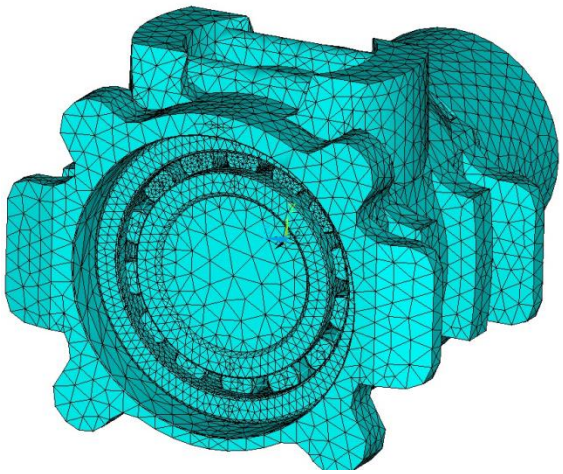

Fig. 3.38. Finite element model of an axle box bearing assembly with a double cylindrical bearing

A feature of roller modeling was the use of significantly smaller finite elements in the contact area between the rolling elements and the raceways (Fig. 3.39). The aim was to provide more accurate results of calculations in the contact zone.

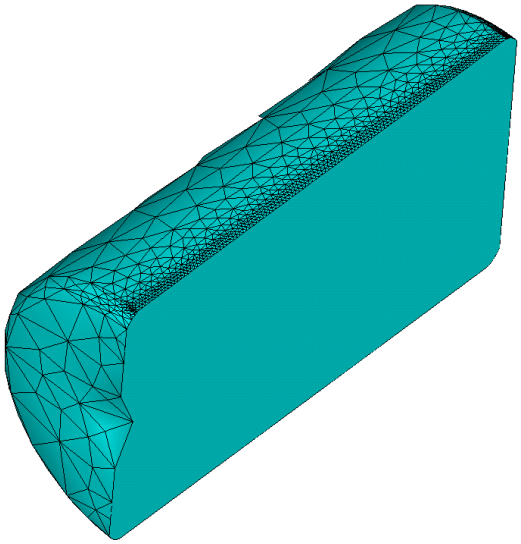

Fig. 3.39. Generation of a finite-element mesh on a roller

During the creation of the model, the impact of technological deviations on the load of the bearing elements, as well as their possible activation during operation, was not taken into account. The effect of lubricant on the contact strength of the bearing parts was also not considered.

3.6 Study of the stress-strain state of elements of a double cylindrical roller bearing

The loading of the model was carried out in the global coordinate system (XYZ) (Fig. 3.40).

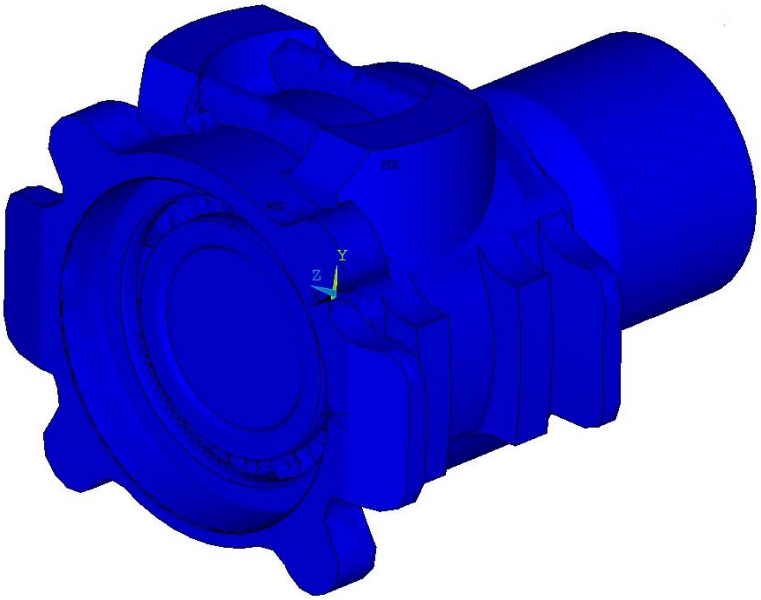

Fig. 3.40. General view of an axle box bearing assembly with a double cylindrical bearing

The seat surface of the inner ring was fixed completely (movements along all three degrees of freedom were equal to 0). The movement of the bearing rings along the axis neck (along the Z axis) was also limited.

With the help of the developed model, the study of the stress-strain state of the elements of the bearing assembly under the action of exclusively radial load with its different magnitudes, as well as the study of the stress-strain state under combined loading taking into account the action of axial forces, was carried out. In order to reduce the amount of computational work and, taking into account the symmetry of the structure and the applied load, in the future, half of the bearing assembly was considered.

In the course of calculations, it was established that 9 rollers are included in the load zone of the bearing (Fig. 3.41).

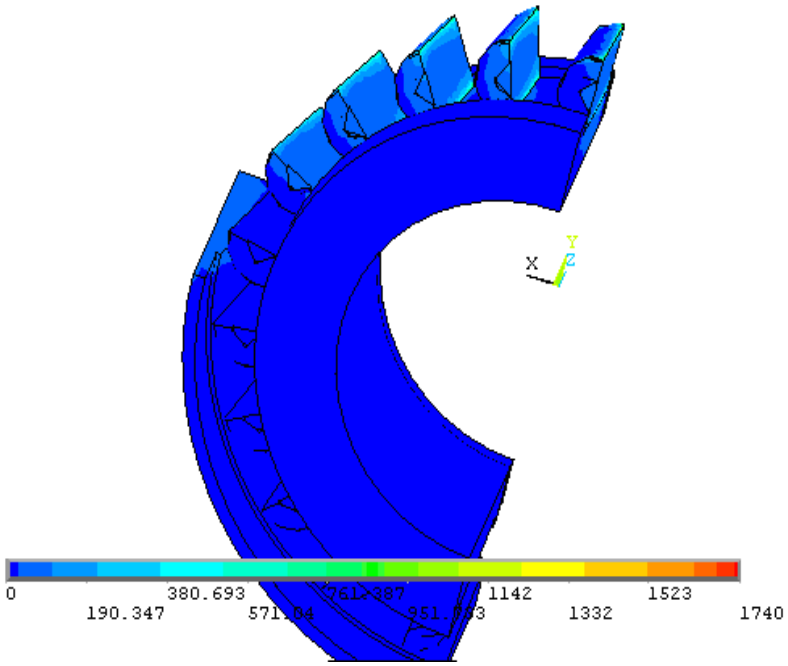

Fig. 3.41. Load zone in a double cylindrical bearing

The distribution of contact loads between rollers and raceways is shown in Fig. 3.42- 3.43.

It is obvious that the rear bearing is loaded more than the front. Moreover, the maximum stresses occur in the contact zone of the roller of the rear bearing with the inner ring, and this does not depend on which roller is considered: the upper one or the one following it.

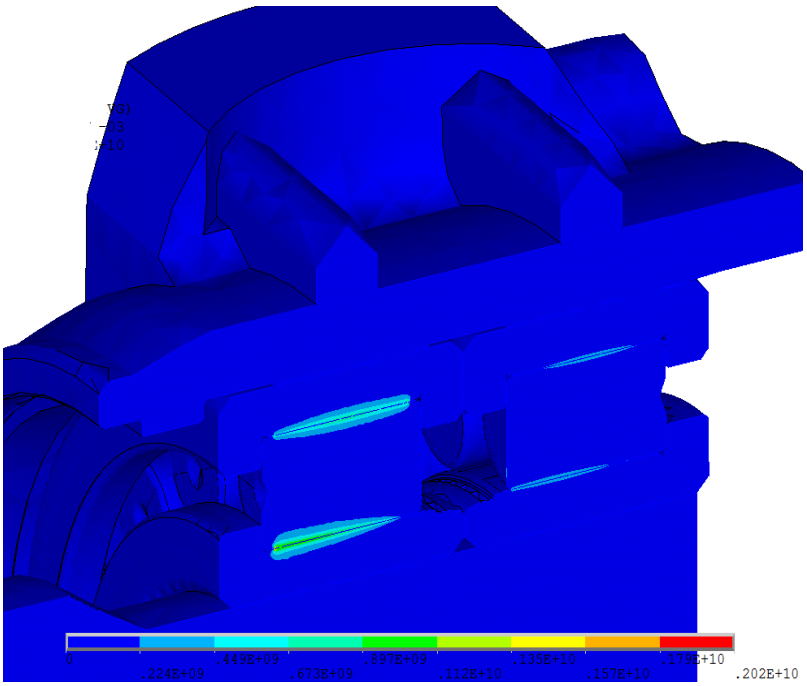

Fig. 3.42. Distribution of contact stresses along the forming rollers in a double cylindrical bearing

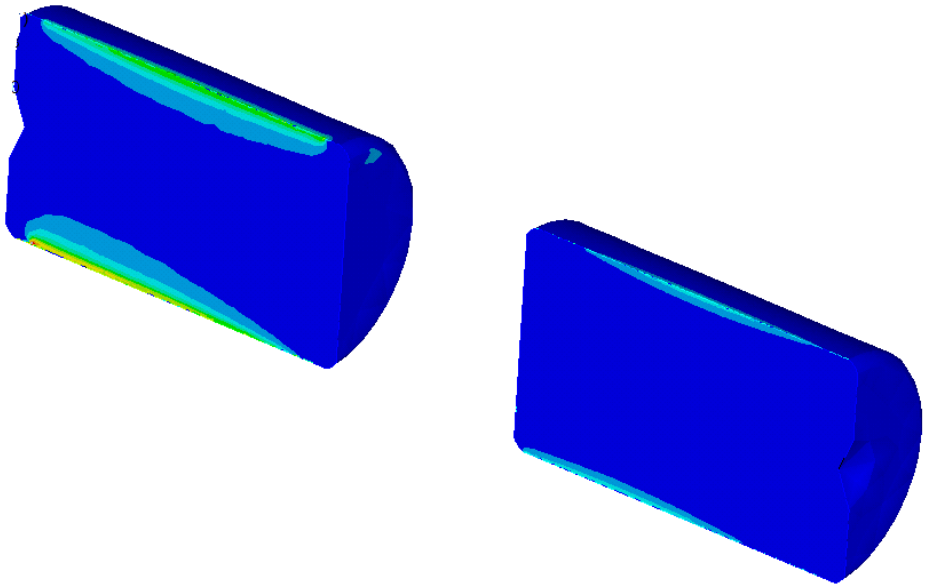

Fig. 3.43. Distribution of contact stresses along the forming central rollers of a double cylindrical bearing

Obviously, it is the deflection of the axle neck under load that contributes to the uneven distribution of contact stresses.

The dependences of the change in the maximum stresses in the contact zone of the upper roller with the inner (outer) ring for the front and rear bearing at a minimum axle load of 230 kN are shown in Fig. 3.44 - 3.45.

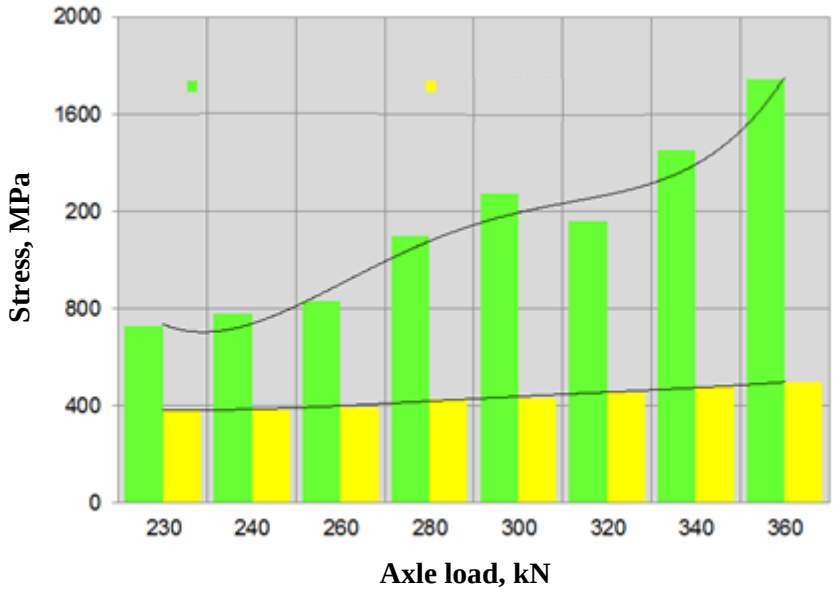

Fig. 3.44. The dependence of the change in the maximum contact stresses in the contact zone of the upper roller with the inner ring for the front and rear bearings

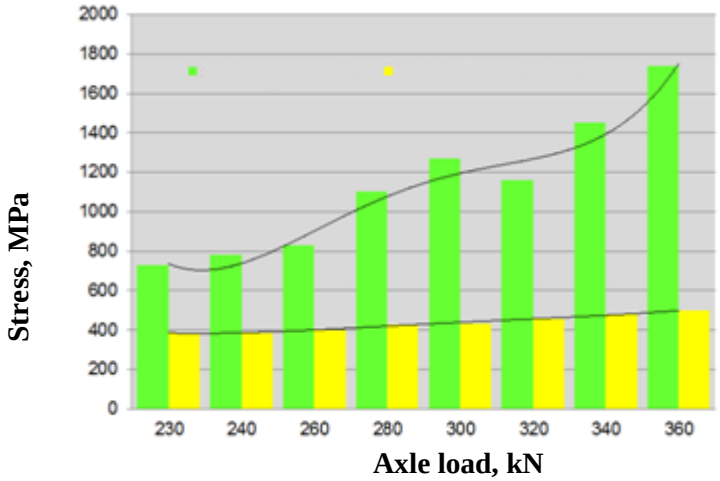

Fig. 3.45. The dependence of the change in the maximum contact stresses in the contact zone of the upper roller with the outer ring for the front and rear bearings

The corresponding analytical dependences of changes in the maximum contact stresses in the contact zone of the upper roller with the inner ring have the following form for a rear bearing

$$\sigma_{\max}^{вн}(з) = 1{,}24\left(P^{в}\right)^4 - 29{,}9{,}24\left(P^{в}\right)^3 + 212{,}3\left(P^{в}\right)^2{}_2 - 360{,}24P^{в} + 152{,}1 \quad (3.61)$$

For a front bearing

$$\sigma_{\max}^{вн}(п) = 0{,}99\left(P^{в}\right)^4 - 28{,}06\left(P^{в}\right)^3 + 229{,}4\left(P^{в}\right)^2{}_2 - 568{,}8P^{в} + 856{,}5 \quad (3.62)$$

where $P^{в}$ is a vertical load acting on the axle box bearing.

The corresponding analytical dependences of the change in the maximum contact stresses in the contact zone of the upper roller with the outer ring have the following form:

For a rear bearing

$$\sigma_{\max}^{зов}(з) = 3{,}45\left(P^{в}\right)^4 - 59.7\left(P^{в}\right)^3 + 353{,}2\left(P^{в}\right)^2{}_2 - 691{,}6P^{в} + 1130 \qquad (3.63)$$

For a front bearing

$$\sigma_{\max}^{зов}(п) = 0{,}13\left(P^{в}\right)^4 - 2.65\left(P^{в}\right)^3 + 18{,}9\left(P^{в}\right)^2{}_2 - 38{,}8P^{в} + 407{,}5 \qquad (3.64)$$

The dependences of the change in the maximum stresses in the contact zone of the second roller (next to the upper one) with the inner ring for the front and rear bearings are shown in Fig. 3.46.

The corresponding dependences of the maximum stresses in the contact zone of the upper roller with the outer ring for the front and rear bearings are shown in Fig. 3.47.

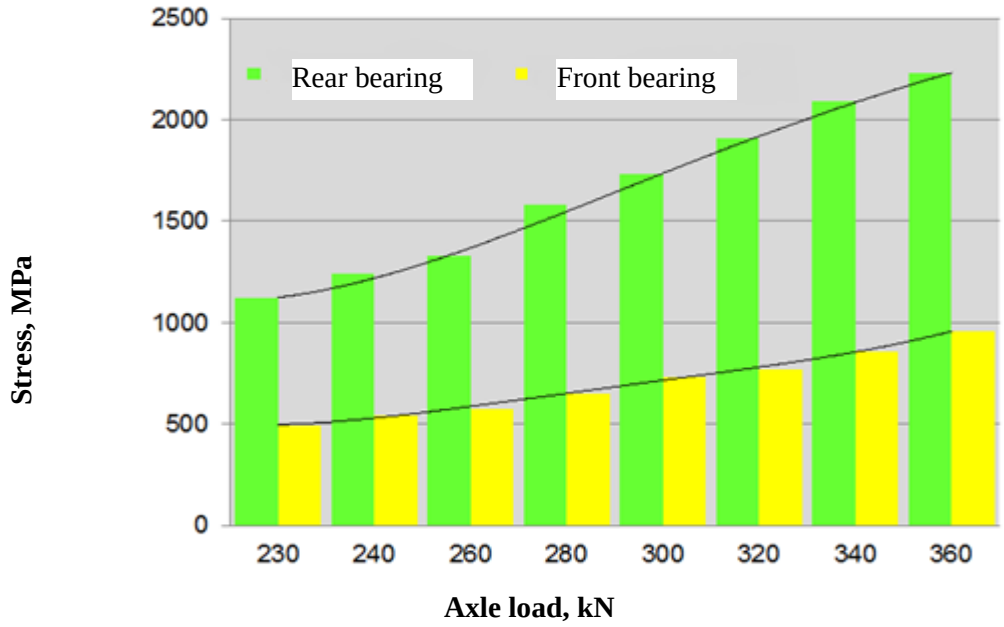

Fig. 3.46. The dependence of the change in the maximum contact stresses in the contact zone of the second roller with the inner ring for the front and rear bearings

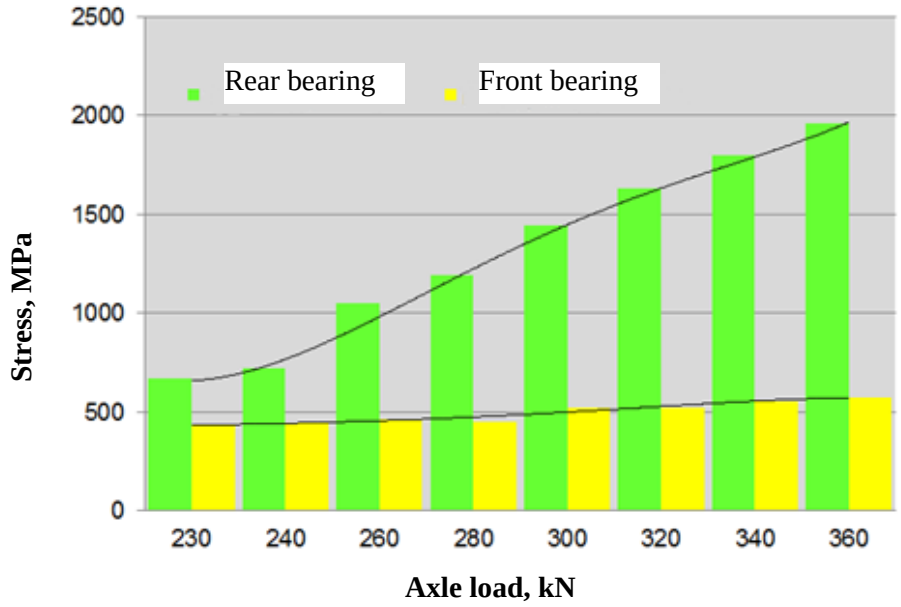

Fig. 3.47. The dependence of the change in the maximum contact stresses in the contact zone of the second roller with the outer ring for the front and rear bearings

The corresponding analytical dependences of changes in the maximum contact stresses in the zone of contact of the second roller with the inner ring have the following form:

for a rear bearing

$$\sigma_{\max}^{вн}(з) = 0{,}28\left(P^{в}\right)^4 - 6{,}42\left(P^{в}\right)^3 + 60{,}5\left(P^{в}\right)^2{}_2 - 44{,}8P^{в} + 1114 \qquad (3.65)$$

For a front bearing

$$\sigma_{\max}^{вн}(п) = 0{,}35\left(P^{в}\right)^4 - 6{,}22\left(P^{в}\right)^3 + 40{,}3\left(P^{в}\right)^2{}_2 - 49{,}3P^{в} + 512{,}2 \qquad (3.66)$$

The corresponding analytical dependences of the maximum contact stresses in the zone of contact of the second roller with the outer ring have the following form:

for a rear bearing

$$\sigma_{\max}^{зов}(з) = 1{,}24\left(P^{в}\right)^4 - 25{,}36\left(P^{в}\right)^3 + 173{,}9\left(P^{в}\right)^2{}_2 - 49{,}3P^{в} + 512{,}2 \qquad (3.67)$$

For a front bearing

$$\sigma_{\max}^{зов}(п) = -0{,}12\left(P^{в}\right)^4 + 1{,}74\left(P^{в}\right)^3 - 6{,}2\left(P^{в}\right)^2{}_2 + 18{,}7P^{в} + 416{,}8 \qquad (3.68)$$

The analysis of the obtained results shows that, regardless of the location of the roller, the zone of concentration of maximum contact stresses is located at the transition from the generating roller to the chamfer. At a load of 230 kN in

the contact zone with the inner ring for the rear bearing, the maximum stresses for the upper roller were 1330 MPa, for the next one 1100 MPa. The corresponding values for the contact zone of the upper roller with the outer ring were 727 MPa for the upper roller, and 695 MPa for the next one.

At a load of 360 kN (taking into account the coefficient of vertical dynamics) in the contact zone with the inner ring for the rear bearing, the maximum stresses for the upper roller were 2780 MPa, for the next one this value is 2320 MPa. The corresponding values for the contact zone of the upper roller with the outer ring were for the upper roller 1740 MPa, for the next one - 1880MPa.

The obtained stress values are inferior to those allowed (3500 MPa). Thus, it can be concluded that the contact strength of the rolling elements in the static mode will be ensured.

The thesis that the rear bearing is more loaded than the front one is confirmed, since the maximum stresses for the rear bearing both in the contact zone of the rollers with the outer ring and the inner ring exceed the similar values for the front bearing.

The stress distribution along the generating rollers is shown in Fig. 3.48-3.49.

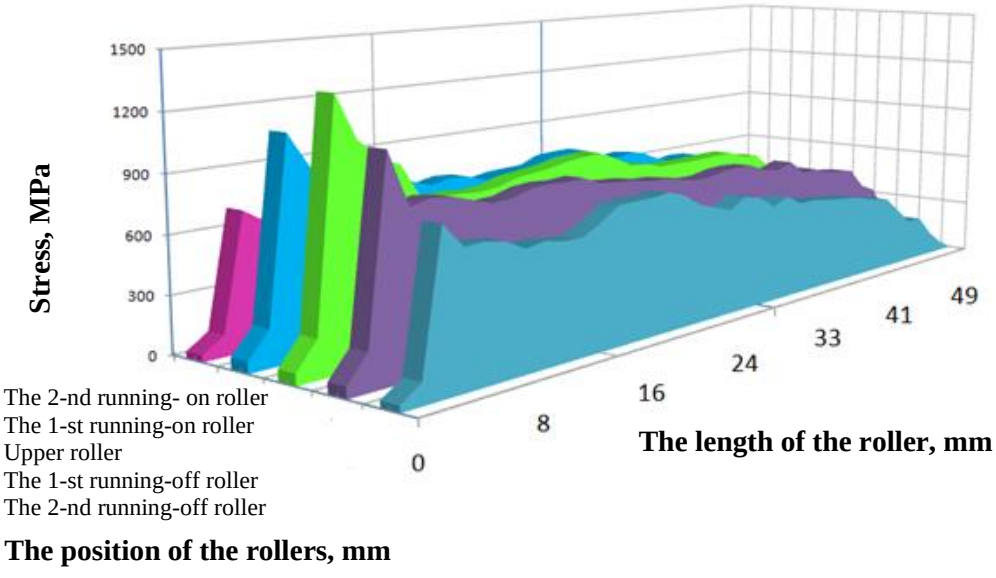

Fig. 3.48. Distribution of contact stresses along the rear bearing roller in contact with the inner ring (radial load 230 kN)

The obtained results show that for the front bearing, the distribution of stresses along the generating roller both in the contact zone with the inner and in the contact zone with the outer ring is close to the classical version: the stresses are approximately the same along the entire length of the generating roller and have maximum values in the middle of the roller (taking into account the presence of the crowned roller).

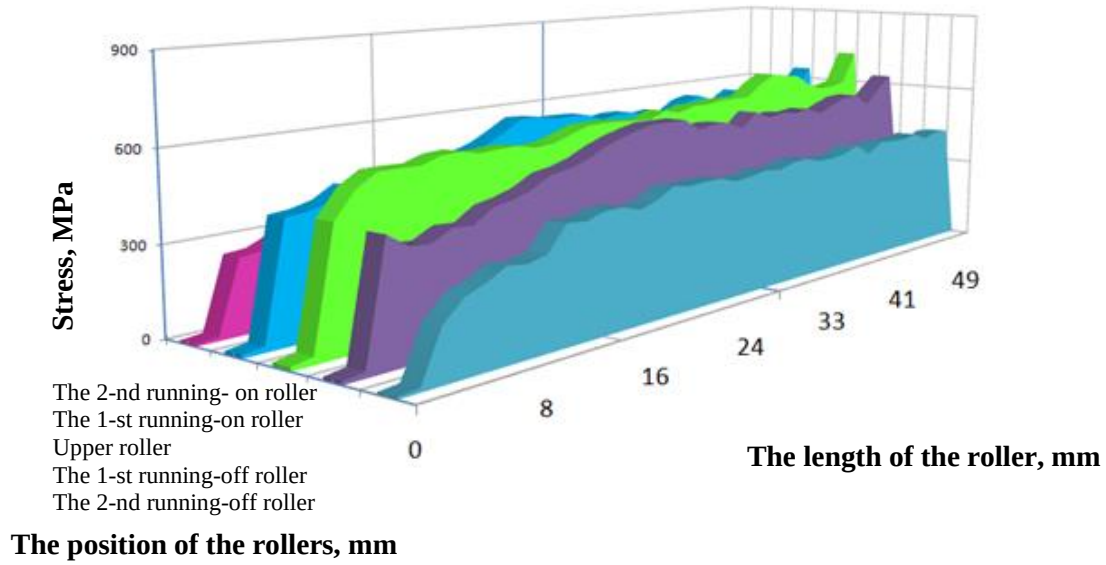

Fig. 3.49. Distribution of contact stresses along the forming roller of the rear bearing in contact with the outer ring (radial load 230 kN)

A similar pattern is observed in the rear bearing in the contact area with the outer ring. At the same time, upon contact with the inner ring, there is a significant increase in stress from one end of the roller (located near the flange of the axle neck). The maximum stresses are twice the average (that is, the so-called "edge" effect takes place).

When the radial load increases, the "edge" effect increases. This is especially noticeable for the rear bearing, where the peak values of contact stresses (up to 2700 MPa) also appeared in the contact zone of the rollers with the outer ring (Fig. 3.50 - 3.51).

The appearance of axial forces does not change the basic picture of the distribution of contact stresses: there is an "edge effect" near the ends of the rollers on the side of the axle neck (Fig. 3.52).

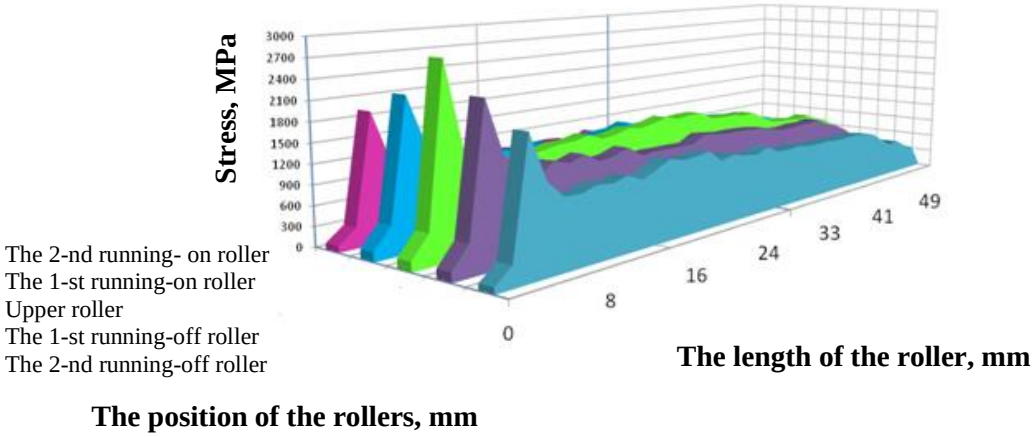

Fig. 3.50. Distribution of contact stresses along the forming roller of the rear bearing in contact with the outer ring (radial load 360 kN)

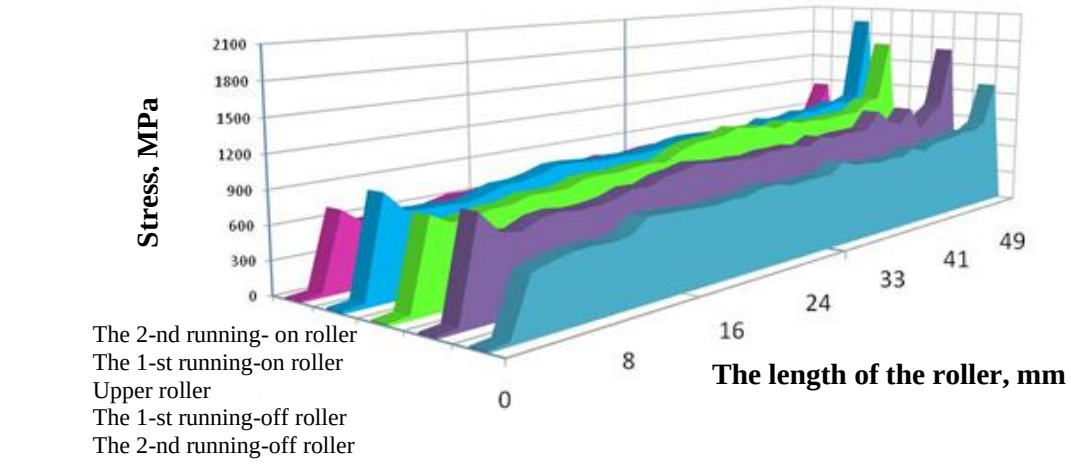

Fig. 3.51. Distribution of contact stresses along the generating roller of the rear bearing in contact with the inner ring (radial load 360 kN)

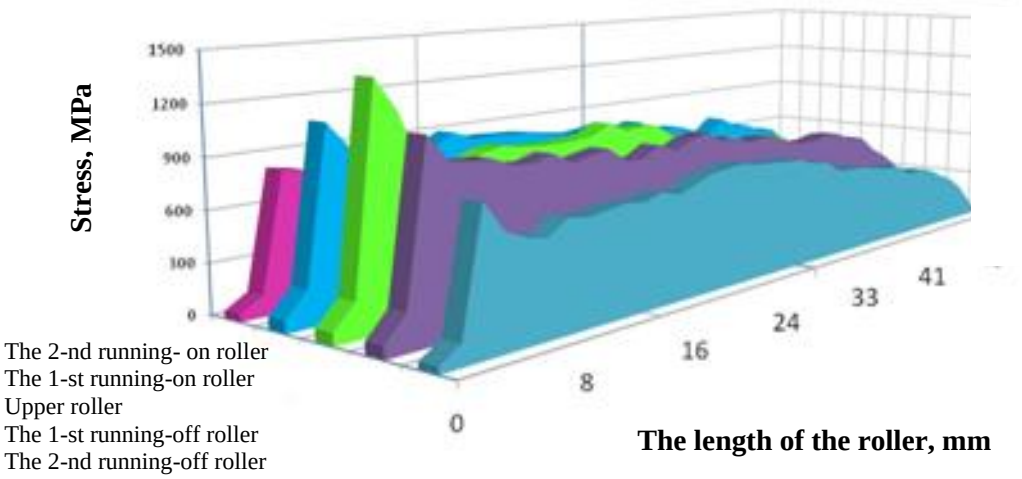

Fig. 3.52. Distribution of contact stresses along the rear bearing roller in contact with the inner ring (radial load 230 kN, axial load 50 kN)

The value of the maximum stresses after the application of the axial load in this place increased by 10%.

The results of studies of the influence of the radius of the generating rollers on the contact stresses are shown in fig. 3.53 - 3.54.

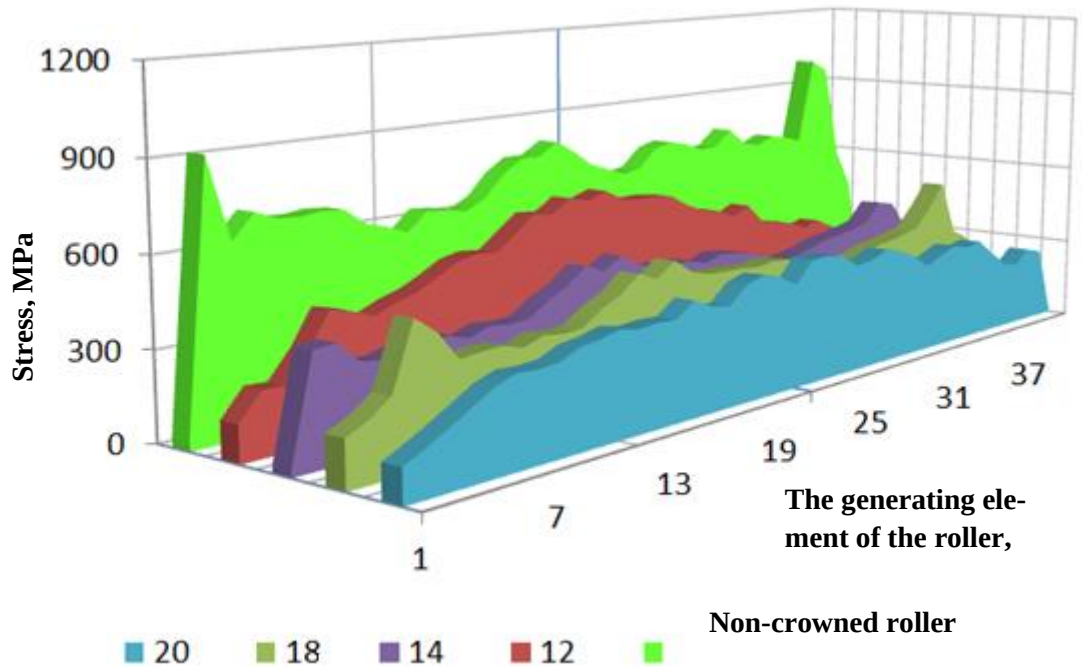

Fig. 3.53. Distribution of contact stresses along the forming roller in contact with the inner ring

With the appearance of the "bomb" the "edge" effect disappears. The value of the maximum contact stresses gradually decreases depending on the increase in the crowned roller radius. The smallest stresses occur at the crowned roller radius of 20 m. Contact stresses reach a maximum if the roller turns into a cylinder.

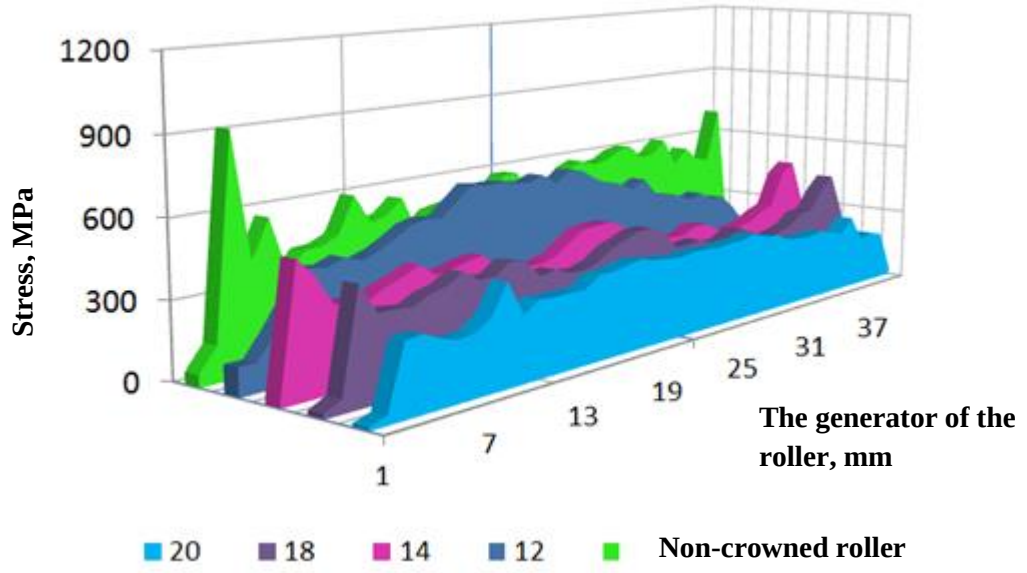

Fig. 3.54. Distribution of contact stresses along the forming roller in contact with the outer ring

4. RESEARCH OF THE RELIABILITY OF AXLEBOX ASSEMBLIES OF FREIGHT WAGONS

4.1. A probabilistic model of the reliability of axlebox cylindrical bearings

In chapter 2, it was shown that the main element of the axlebox assembly of a freight car is a cylindrical roller bearing. Its technical condition mainly affects the reliability of the vehicle as a whole. Therefore, there is a need to create a mathematical model that would allow determining the reliability indicators of cylindrical bushing bearings.

In the role of such a model, the vast majority of researchers recommend using the Weibull-Hnedenko distribution [29, 86, 87, 110].

But it should be noted that bearings, which are used in other branches of mechanical engineering, are non-renewable products. As a rule, when they fail, they are not repaired, but replaced with new ones. This makes it easier to identify their service life and determine the reasons for failure.

The operation of wagon cylindrical bearings, which is carried out in accordance with the requirements of regulatory documents [53], differs in that the terms of carrying out complete revisions (repairs) of the axlebox assembly do not have strict limitations, but are related to the technical condition of the wheel set. But the most important thing is that in the process of carrying out a complete revision, the bearing is completely disassembled and reassembled. At the same time, the bearing elements are depersonalized and, in the future, when assembling the bearing after repair and installation on the axle, in fact, we get a completely new bearing with rollers, rings and a cage that were selected randomly and previously worked as part of different bearings.

Thus, it should be noted that the obtained set of experimental data does not meet the conditions of statistical homogeneity, because all types of failures are included in the general sample. It also consists of both new bearings and those that have already undergone restoration. In this case, it is expedient to use the super positional law of distribution of working hours [45].

The results of the examination of cylindrical axle box bearings show that fatigue failures, sudden failures and corrosion failures occur among them. The corresponding failure distribution function will look like this:

$$F(t) = p_1 \cdot F_1(t) + p_2 \cdot F_2(t) + p_3 \cdot F_3(t), \quad (4.1)$$

where p_1, p_2, p_3 – respectively, the probability of the event that the failure occurred due to fatigue, sudden factors or corrosion;

$F_1(t), \cdot F_2(t), \cdot F_3(t)$ are, respectively, the distribution function for fatigue failure, sudden failure, and corrosion failure.

The probability density function of the failure distribution will look like this:

$$f(t) = p_1 \cdot f_1(t) + p_2 \cdot f_2(t) + p_3 \cdot f_3(t), \quad (4.2)$$

where $f_1(t)$,· $f_2(t)$,· $f_3(t)$ are, respectively, the density of the working life distribution for fatigue failures, sudden failures, and corrosion failures.

The task is complicated by the fact that experimental data on bearing failures or their absence are reliably known only for a certain period of time, which immediately precedes the survey. In our case, it is the time between two full audits of the axlebox assembly. We do not know the history of previous use of the bearings. Such data are a special case of truncating the sample from the left.

To solve this problem, the technique described in [74] was used, which was further developed in relation to railway bushing bearings in studies [72, 87]. According to this methodology, in the solution process, data is restored by calculating the probability of bearing failures in periods when they were not monitored.

Suppose we have u of identical bearings. The objects are sufficiently highly reliable, so the probability of two or more failures in the period θ between technical condition checks can be neglected. We believe that the inspection and possible replacement of bearings is carried out no more than once a year.

We denote the probability of bearing failure during the first period of operation $(0,1)$ by p_1, during the second by $(1,2) - p_2$, etc. (Fig. 4.1).

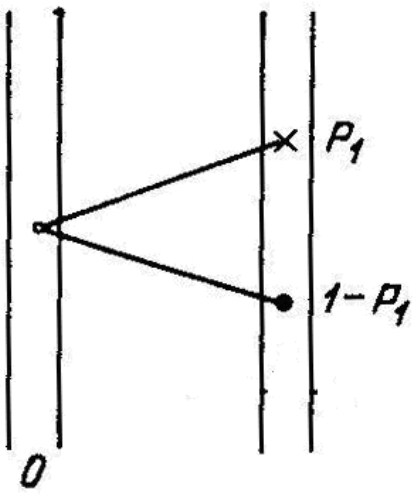

Then for the interval $(m-1, m)$ the probability of bearing failure will be p_m. The number of bearings inspected for the corresponding period will be denoted as ν_i, and the failed bearings as $-m_i$. In one (first) period, failure will occur with probability p_1, and failure-free operation with probability $1 - p_1$.

Fig. 4.1. A graph of possible states of the axle box bearing after the first interval of operation

According to the initial data, we get

$$p_1 = \frac{m_1}{\nu_1}. \quad (4.3)$$

Of the m_2 bearings that failed after two years, $p_1\_m_2$ failed a year ago. Therefore, the probability of bearing failure in the second year of operation can be determined by the following formula

$$p_2 = \frac{m_2 - p_1 \cdot m_2}{\nu_2} = \frac{m_2}{\nu_2} \cdot (1 - p_1). \tag{4.4}$$

Similarly for the third year of operation

$$p_3 = \frac{m_3 - p_1 \cdot m_3 - p_2 \cdot m_3}{\nu_3} = \frac{m_3}{\nu_3} \cdot (1 - p_1 - p_2). \tag{4.5}$$

Then in the general case we get

$$p_i = \frac{m_i}{\nu_i} \cdot \sum_{k=1}^{i-1} p_k. \tag{4.6}$$

The values of the empirical distribution function are calculated as follows:

$$\tilde{F}(0) = 0, \tag{4.7}$$

$$\tilde{F}(1) = p_1, \tag{4.8}$$

$$\tilde{F}(2) = p_1 + p_2, \tag{4.9}$$

$$\tilde{F}(i) = \sum_{k=1}^{i-1} p_k. \tag{4.10}$$

The obtained empirical distribution function is shown in Fig. 4.2.

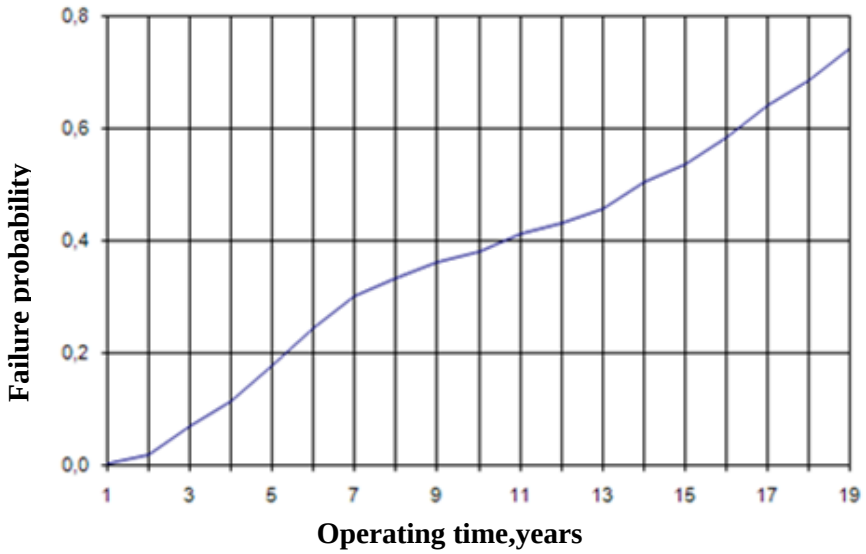

Fig. 4.2. Empirical fatigue distribution function of cylindrical axlebox bearings

Using the obtained values of the empirical distribution function, it is possible to establish the regularity of the distribution of the working life of the bearings in full.

According to [103], there are two ways of identifying the empirical distribution function:

• physical, which consists in building a failure model and investigating it by mathematical methods;

• statistical, which involves testing the hypothesis that the assumed distribution law belongs to this type.

In this case, it is advisable to use a combination of these methods.

Since we are building a model of bearing failure due to fatigue, we will mentally divide the ring design into n parts of equal volume. Then we will consider the failure as the event consisting in the appearance of the first microscopic crack (or other fatigue damage) at any point of the volume. In this regard, we will consider the following random variable η is the operating time of the structure to the first crack

$$\eta = \min(\xi_1, \xi_2, \ldots, \xi_i), \tag{4.11}$$

where ξ_i is the working time of the ith part of the ring until the first crack appears in it.

To determine the moment of appearance of the first crack in the i-the part of this structural element, the volume of this i-the part will be reduced to almost zero volume, in which no more than one crack can fit.

For this purpose, with the help of the boundary transition operation, we will simulate the process of crushing this part into a significant number of particles of practically zero volume. Then we will accept under IBR in time t

$$P\{\eta > t\} = \lim_{n\to\infty} P\{min(\xi_1, \xi_2, \dots., \xi_i) > t\}. \quad (4.12)$$

In order to obtain the final result of taking the limit (4.12) in the usual form, it is advisable to consider the so-called normalization coefficient B_n, which depends on the index n

$$B_n = n^{-\frac{1}{\alpha}}, \quad (4.13)$$

where α is some constant.

Then the expression (4.12) takes the following form:

$$P\{\eta > t \cdot B_n\} = \lim_{n\to\infty} P\{min(\xi_1, \xi_2, \dots., \xi_i) > t \cdot B_n\}. \quad (4.14)$$

Let's introduce the following assumptions:

the values $\xi_1, \xi_2, \dots., \xi_i$ are independent random variables;

the values $\xi_1, \xi_2, \dots., \xi_i$ are uniformly distributed random variables.

The function $F(t)$ can be expanded near zero into a static series

$$F(t) = 1 - c \cdot t^{\alpha} + 0(t^{\alpha}). \quad (4.15)$$

Then, using standard operations, we take the limit in expression (4.14) and obtain

$$P\{\eta > t \cdot B_n\} = exp^{-c\cdot t^{\alpha}}. \quad (4.16)$$

where a is the scale parameter;

b is a shape parameter.

The distribution density function will look like this:

$$f_1(t) = \frac{b}{a}\left(\frac{t}{a}\right)^{b-1} exp^{-\left(\frac{t}{a}\right)^b}. \quad (4.19)$$

The system of equations for determining the parameters will look like this:

$$\begin{cases} m_i^{\text{ут}} = N_1 \cdot h \cdot \frac{b}{a}\left(\frac{t_i}{a}\right)^{b-1} \cdot exp^{-\left(\frac{t_i}{a}\right)^b}, \\ m_{i+1}^{\text{ут}} = N_1 \cdot h \cdot \frac{b}{a}\left(\frac{t_{i+1}}{a}\right)^{b-1} \cdot exp^{-\left(\frac{t_{i+1}}{a}\right)^b}, \\ m_{i+2}^{\text{ут}} = N_1 \cdot h \cdot \frac{b}{a}\left(\frac{t_{i+2}}{a}\right)^{b-1} \cdot exp^{-\left(\frac{t_{i+2}}{a}\right)^b}, \\ m_{i+3}^{\text{ут}} = N_1 \cdot h \cdot \frac{b}{a}\left(\frac{t_{i+3}}{a}\right)^{b-1} \cdot exp^{-\left(\frac{t_{i+3}}{a}\right)^b}, \end{cases} \quad (4.20)$$

Where $m_i^{\text{ут}}$ – the number of failures that occurred at the i -th moment of time;

N_1 is the total number of failures due to fatigue;

h is an interval width.

If we take the value of t_i in such a way that $t_{i+1} = 2t_i$, $t_{i+2} = 4t_i$, $t_{i+3} = 8t_i$, then having received the shares $\frac{m_i}{m_{i+1}}$, $\frac{m_{i+1}}{m_{i+2}}$, $\frac{m_{i+2}}{m_{i+3}}$ and taking the logarithm, we get the following system of equations:

$$\begin{cases} ln\frac{m_i}{m_{i+1}} = \left(\frac{b}{a} - 1\right) ln\frac{1}{2} - \frac{1}{a} t_i^b (2^b - 1), \\ ln\frac{m_{i+1}}{m_{i+2}} = \left(\frac{b}{a} - 1\right) ln\frac{1}{2} - \frac{1}{a} t_i^b \cdot 2^b (2^b - 1),, \\ ln\frac{m_{i+2}}{m_{i+3}} = \left(\frac{b}{a} - 1\right) ln\frac{1}{2} - \frac{1}{a} t_i^b \cdot 4^b (2^b - 1), \end{cases} \quad (4.21)$$

Then the estimate of the parameter $\hat{b}$ is calculated as

$$\hat{b} = ln\frac{ln\frac{m_{i+1}}{m_{i+2}} - ln\frac{m_{i+2}}{m_{i+3}}}{ln\frac{m_i}{m_{i+1}} - ln\frac{m_{i+1}}{m_{i+2}}}. \quad (4.22)$$

If the estimate of the parameter $\hat{b}$ is known, then the value of the estimate of the parameter $\hat{a}$ can be obtained by substituting the estimate of the parameter $\hat{b}$ into any equation (4.21).

After performing the calculation, we get that for the Weibull-Hnedenko distribution, the value of the parameter a will be equal to 15.07, the value of the shape parameter b is 1.86. That is, formula (4.18) takes the following form:

$$F_1(t) = 1 - exp^{-\left(\frac{t}{15,07}\right)^{1,86}}. \quad (4.23)$$

Regarding the obtained data, we know that the failures at the time points t_i and t_{i+1} are sudden; accordingly, then there were $m_i^{\text{рап}}$ and $m_{i+1}^{\text{рап}}$ failures. The distribution density function for the exponential distribution describing the sudden failure pattern will look like this:

$$f_2(t) = \lambda \cdot \exp^{-\lambda t}. \quad (4.24)$$

Then the system of equations for determining the parameter λ will have the following form:

$$\begin{cases} m_i^{\text{рап}} = N_2 \cdot h \cdot \lambda \cdot exp^{-\lambda t_i}, \\ m_{i+1}^{\text{рап}} = N_2 \cdot h \cdot \lambda \cdot exp^{-\lambda t_{i+1}}. \end{cases} \quad (4.25)$$

where N_2 is the number of failures classified as sudden;

λ is an exponential distribution parameter (failure intensity).

After solving this system of equations, we get

$$\lambda = \frac{ln\frac{m_{i+1}}{m_i}}{t_i - t_{i+1}}. \quad (4.26)$$

After calculations, we determine that the parameter λ will be equal to 0.000949.

The failure distribution function for the exponential distribution will look like this

$$F_2(t) = 1 - exp^{-0,000949t}. \quad (4.27)$$

Similarly, assuming that the failures of cylindrical bearings due to corrosion damage are distributed according to the normal law, we will formulate the corresponding system of equations

$$\begin{cases} m_i^{\text{кор}} = N_3 \cdot h \cdot \dfrac{1}{\sigma\sqrt{2\pi}} \cdot exp^{-\frac{(t_i-\overline{T})^2}{2\sigma^2}}, \\ m_{i+1}^{\text{кор}} = N_3 \cdot h \cdot \dfrac{1}{\sigma\sqrt{2\pi}} \cdot exp^{-\frac{(t_{i+1}-\overline{T})^2}{2\sigma^2}}, \\ m_{i+2}^{\text{кор}} = N_3 \cdot h \cdot \dfrac{1}{\sigma\sqrt{2\pi}} \cdot exp^{-\frac{(t_{i+2}-\overline{T})^2}{2\sigma^2}}, \end{cases} \quad (4.28)$$

where N_3 is the number of failures classified as corrosive;

$\overline{T}$, σ are parameters of the normal distribution.

Solving this system with respect to $\overline{T}$, we obtain

$$\overline{T} = \frac{(t_{i+2} - t_{i+1})^2 - \frac{ln\frac{m_{i+1}}{m_{i+2}}}{ln\frac{m_i}{m_{i+1}}}\left(t_{i+1}^2 - t_i^2\right)}{2\left[\frac{ln\frac{m_{i+1}}{m_{i+2}}}{ln\frac{m_i}{m_{i+1}}} \cdot (t_i - t_{i+1}) - (t_{i+1} - t_{i+2})\right]}. \quad (4.29)$$

The value of $\overline{T}$ will be equal to 10.4, and σ is 68.95.

Finally, we obtain a distribution function for bearing failures from corrosion damage

$$F_3(t) = \int_0^t \frac{exp^{-\frac{(t-10,4)^2}{2\cdot 68,95^2}}}{68,95\sqrt{2\pi}}. \quad (4.30)$$

Then the function of distribution of working time to failure acquires its final form (Fig. 7.3)

$$F(t) = 0.873449 \cdot \left(1 - exp^{-\left(\frac{t}{15,07}\right)^{1,86}}\right) +$$
$$+0.0579 \cdot (1 - exp^{-0,000949t}) + 0.0687 \cdot \left(\int_0^t \frac{exp^{-\frac{(t-10,4)^2}{2\cdot 68,95^2}}}{68,95\sqrt{2\pi}}\right). \quad (4.31)$$

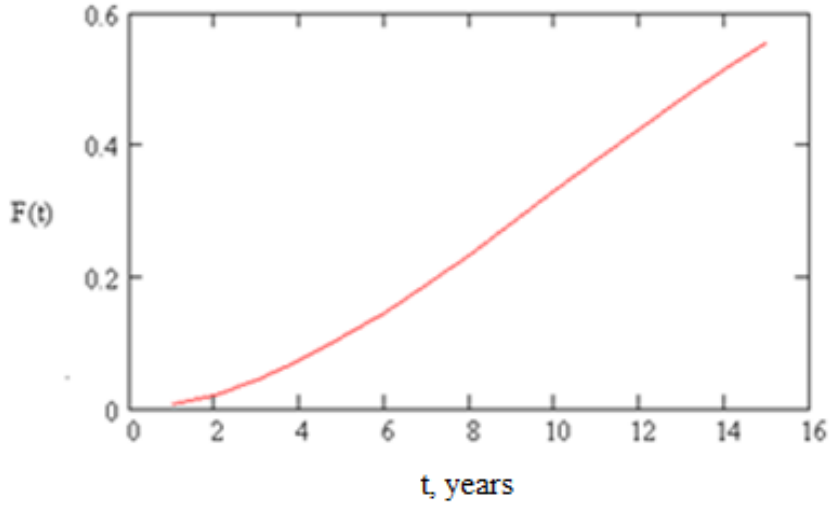

Fig. 4.3. The function of distributing the run-up of cylindrical axlebox bearings due to all types of damage

It is obvious that the 90 percent resource of cylindrical bushing bearings is 4.5 years. This correlates satisfactorily with the results of observations in operation.

The data obtained as a result of observations made it possible to determine the durability indicators of different manufacturers of cylindrical bearings. Thus, the 90-percent resource of bearings produced by KharP JSC is 3.5 years, and bearings produced by YEPK are 5.5 years.

4.2. A model for determining the reliability indicators of bearing assemblies of freight cars

The durability of the axlebox assemblies is mainly determined by the durability of the axlebox bearings. According to the requirements of the international standard ISO 281:2001, the main indicator characterizing its durability is a 90 percent resource. But the calculation of the 90-percent resource for railway bushing bearings gives results that exceed the actual by 2÷3 times. This happens because during calculations, a number of values are calculated using simplified formulas that do not take into account a number of operating operational factors.

The durability of rolling bearings L_{10} with linear contact of the rolling surfaces can be estimated using the formula

$$L_{10} = \left(\frac{Q_{c.k}}{Q_k}\right)^4, \qquad k = i,..0, \tag{4.32}$$

where $Q_{c.k}$ is the main dynamic capacity.

It is defined as the contact load that the contact surface can withstand during 106 revolutions with a probability of 90%.

The expression for this quantity can be written as follows

$$Q_{c.k} = B \cdot \lambda \frac{(1 \mp \gamma)^{\frac{29}{27}}}{(1 \mp \gamma)^{\frac{1}{4}}} \cdot \left(\frac{\gamma}{cos\alpha}\right)^{2/9} \cdot D_a^{\frac{20}{27}} \cdot l_a^{\frac{2}{9}} \cdot Z^{-\frac{1}{4}}, \qquad k = i, 0, \qquad (4.33)$$

where B i s the material constant, B =551;

λ is a correction factor that takes into account the presence of boundary stresses;

D_a is an average diameter of the roller, mm;

l_a is working length of the roller, mm;

Z is the number of rolling elements in one row;

α is the contact angle in the bearing.

To calculate the equivalent load Q_k in equation (4.33), it is necessary to first calculate the equivalent load for each contact between the roller and the raceway.

The main dynamic bearing capacity was derived based on the assumption that the risk of cracking is the same for both bodies in contact. Then it is possible to obtain the equivalent load for the contact between the roller and the surface of the raceway, considering only the probability of failure-free operation of the roller.

Assume that S is the probability of failure-free operation of a roller with an effective length dx. Then, according to [15],

$$n\frac{1}{S_k} = C \cdot H^{\frac{35}{6}} \cdot q_k^{\frac{9}{2}} \cdot D_a \cdot l_a^{\frac{9}{8}} dx, \quad k = i, 0, \qquad (4.34)$$

where C is a constant;

$$H_i = \frac{cos\varepsilon}{D_a} - \frac{cos\beta}{d_m + D_a cos\gamma}, \qquad (4.35)$$

where ε is half the angle at the top of the conical roller;

β is the angle of inclination of the raceway of the inner ring;

$d_m$is a coordinate that determines the nominal radial position of the roller.

Consider an arbitrary conical roller consisting of a large number of layers, each of length dx, for which the parameters in equation (4.35) can be considered constant. Next, we obtain from the law of the probabilities product

$$ln\frac{1}{S_k} = C \cdot L_k^{\frac{9}{8}} \cdot \int_0^{l_a} H^{\frac{35}{6}} \cdot q_k^{\frac{9}{2}} \cdot D_a \cdot l_a^{\frac{9}{8}} dx, \quad k = i, 0. \qquad (4.36)$$

Assume that q_k is the equivalent load per assembly length. Equation (4.36) can also be written as follows

$$ln\frac{1}{S_k} = C \cdot L_k^{\frac{9}{8}} \cdot H_{л}^{\frac{35}{6}} \cdot q_{ck}^{\frac{9}{2}} \cdot D_a \cdot l_a, \quad k = i, 0. \tag{4.37}$$

Then, using equation (4.37), we can write

$$q_{ck} = \left[\frac{1}{H_k^{\frac{35}{6}} \cdot D_a \cdot l_a} \int_0^{l_a} H_k^{\frac{35}{6}} \cdot q_k^{\frac{9}{2}} \cdot D_a dx\right]^{\frac{2}{9}}, k = i, 0. \tag{4.38}$$

The total equivalent load can then be written as

$$Q_{ck} = q_{ck} \cdot l_a, k = i, 0. \tag{4.39}$$

For a rotating inner raceway, the equivalent load can be written as:

$$Q_i = \left[\frac{1}{Z}\sum_{i=1}^{Z}\left(Q_{c,i}\right)^4\right]^{\frac{1}{4}}. \tag{4.40}$$

For a non-moving outer ring raceway, the equivalent load would be

$$Q_i = \left[\frac{1}{Z}\sum_{i=1}^{Z}\left(Q_{c,i}\right)^{\frac{2}{9}}\right]^{\frac{9}{2}}. \tag{4.41}$$

According to the Lundberg-Palmgren theory, for bearings in which the form of contact (linear or point) is unknown before applying the load, it is recommended to calculate the durability using the expression

$$\frac{1}{L_{10}} = \left[\left(L_{10_{зов}}\right)^{-1,11} + \left(L_{10_{вн}}\right)^{-1,11}\right]^{-0,9}, \tag{4.42}$$

where $L_{10_{зов}}$ is the durability of the outer ring; $L_{10_{вн}}$ is the durability of the inner ring.

The same authors suggest using the expression to define L_{10_i}.

$$L_{10_i} = \left(\frac{C_i}{P_{екв_i}}\right)^4, \quad (4.43)$$

where C_i and $P_{екв_i}$ are, respectively, the dynamic carrying capacity and the equivalent load for each contact of the i-th roller with the ring.

Using the concept of the fatigue stress limit P_0, we will consider the additional value X

$$X = 1 - \frac{P_{екв_i}}{P_0}. \quad (4.44)$$

Then, finally, the model for determining the durability of bushing bearings takes on the following form

$$L_{10_i} = \frac{1}{(X)^{3,3}}\left(\frac{C_i}{P_{екв_i}}\right)^4. \quad (4.45)$$

The equivalent load for each contact of the i-th roller with the ring was calculated taking into account the previous results

$$P_{екв_i} = \int_0^l q_i(x)\,dx, \quad (4.46)$$

where $q_i(x)$ is the load distribution along the generating line of each of the rollers;

l is the working length of the roller, m.

The obtained values $P_{екв_i}$ were further summarized separately for contact with the outer and inner rings. The dynamic load capacity was calculated taking into account the marginal stresses near the ends of the rollers.

The results of the calculations are shown in fig. 4.4-4.6.

Determination of the probability of failure-free operation was carried out taking into account the studies of V. E. Kanarchuk and M. M. Dmitriev [54] depending on the additional parameter

$$K_{t_j} = \frac{L_{10}}{L_{p\gamma_j}}, \quad (4.47)$$

where $L_{p\gamma_j} - \gamma$ is the γ-percentage resource that is embedded in the bearings during design.

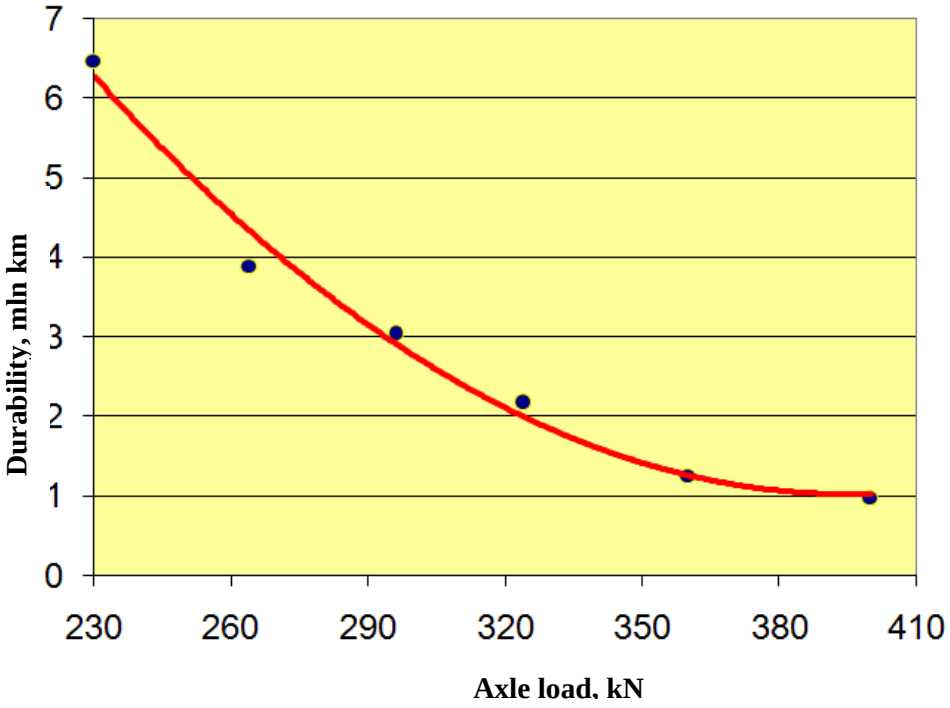

Fig. 4.4. Dependence of change of 90 percent resource without axial load

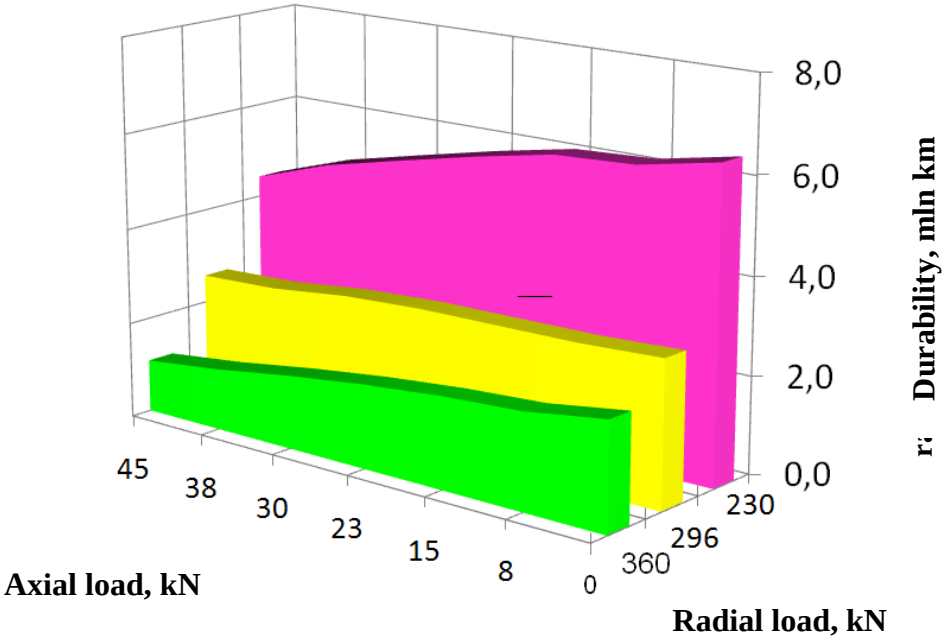

Fig. 4.5. Dependence of the change of the 90 percent resource in the presence of an axial load

The obtained results made it possible to perform a comparative assessment of the reliability of cylindrical and conical bearings.

Given that tapered roller bearings are self-sealing, it can be assumed that they will not have corrosion failures. Then the density function of the distribution of working time to failure will have the form.

$$f(t) = 0{,}942 \cdot \frac{1{,}89}{83{,}57}\left(\frac{t}{83{,}57}\right)^{0{,}89} \exp^{-\left(\frac{t}{83{,}57}\right)^{1{,}89}} + 0{,}058\lambda \cdot \exp^{-0{,}0079t}. \quad (4.48)$$

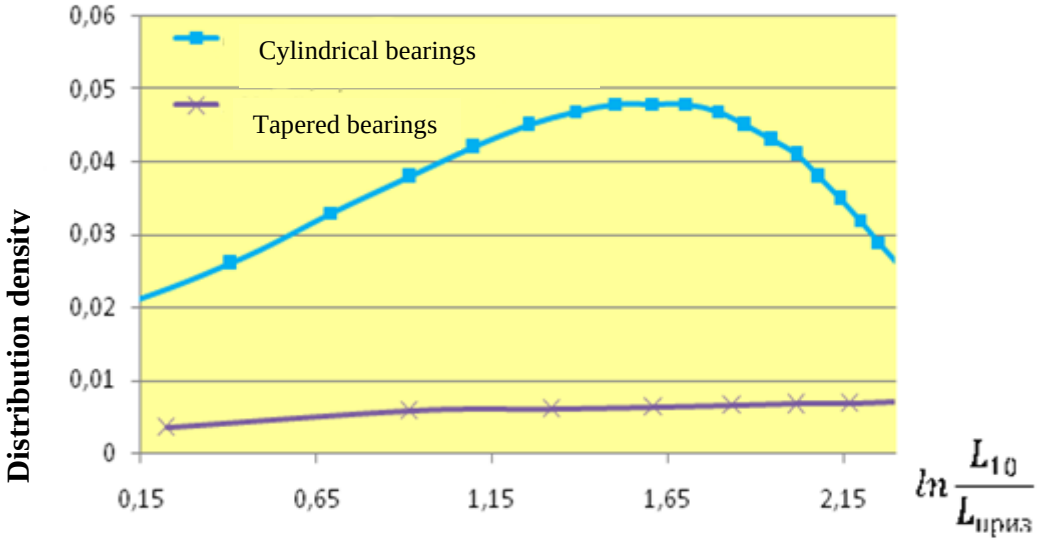

Fig. 4.6. Distribution density of work for cylindrical and conical bearings

4.3. Reliability model of axlebox bearings taking into account the probabilistic nature of operating loads

4.3.1. Peculiarities of mechanical systems from the point of view of reliability theory

By a mechanical system we will understand some object that interacts with the environment and performs certain functions related to the change in time and space of the mutual location of the elements that interact with each other. Depending on the type of these elements, the mechanical system is a system of material points, a solid body, a continuous medium, etc. According to the nature of the change in time and the interaction of its elements, the state of the mechanical system is described by the equations of statics, kinematics or dynamics. Methods of studying mechanical systems are widely used in the calculation of machines, mechanisms, building structures and structures, vehicles, aircraft, etc.

By nature, environmental loads and actions on a mechanical system are random. The random nature of the loads is determined by the random values of the load parameters, its random distribution in time and at different points of the system, the random combination of different loads and many other factors.

From a mathematical point of view, random loads are described by random variables with given distribution laws, random processes, random fields, or space-time random functions. An example of the first type of loads is statically applied loads at individual points or nodes of the structure. Random processes

describe, for example, kinematic actions on the wheels of vehicles moving along an uneven path. Loads from the technological equipment of industrial building floors can serve as an example of loads for the description of which methods of random field theory are used. Pulsations in the turbulent boundary layer acting on the surface of the aircraft are an example of spatio-temporal random loading.

Within each type of loads, the latter can be classified according to different characteristics. Thus, loads specified as random processes can be stationary or non-stationary, scalar or vector, one-dimensional or multi-dimensional, discrete or continuous, short-term or long-term, etc.

The probabilistic properties of the behavior of the mechanical system are determined not only by the random nature of external loads, but also by the variability of the mechanical properties of the materials from which individual elements are made, as well as by the change in the nature of the interaction of elements during operation, manufacturing inaccuracy, and other factors.

The stochastic nature of the variability of the mechanical properties of materials has a twofold nature. First, during operation, the parameters that determine the mechanical properties of the system change over time. These changes are associated with the aging of the material, with the deterioration of strength characteristics, with the accumulation of damage, corrosion and frictional wear, as well as with the change in properties during the restoration and repair of individual elements. Secondly, variability appears when considering this system as an element of many systems, the properties of which change stochastically when moving from one element to another.

The reliability of mechanical systems is determined by many factors, the most important of which are the action of random external loads, the properties of the system itself and its elements, the nature of the interaction of elements, structural and technological features, etc.

The reliability assessment of the mechanical system consists of the following main stages. First, using the methods of the mechanics of a continuous medium, a solid body, or material points, the calculation scheme of a real system is selected, and its mathematical model is built. The choice of the calculation scheme also includes the approximation of external loads and their probabilistic description. After that, statistical dynamics methods are used to determine the probabilistic characteristics of the parameters that determine the behavior of the system during random actions. Then the parameters characterizing the quality of the system are determined, and the permissible area is found, in which the quality parameters must be kept within the established limits.

4.3.2. Failure as the ejection of a random process from the admissible area

The bearing assembly of a freight car is a mechanical system that interacts with the environment. It is affected by certain external influences q, which can acquire random values from the space Q. The stochastic behavior of the system

will be characterized by the elements u, which are parts of the corresponding space U . The latter is chosen in such a way that the state of the system is completely described with its help within the framework of the calculation scheme . The properties of the system are characterized by the operator L, which corresponds to each realization of elements from the space of influences Q with the realization of elements in the space of states U.

$$Lu = q. \tag{4.49}$$

At the same time, the quality space V is chosen in such a way that with the help of its elements it is possible to fully characterize the quality of the functioning of the system. During normal operation of the system, its quality parameters must be within the established limits during the entire normative period of service. Mathematically, this corresponds to the finding of elements v in the admissible region Ω of the quality space V. The exit of the trajectory v(t)) from the admissible region Ω corresponds to the failure of the system (Fig. 4.7).

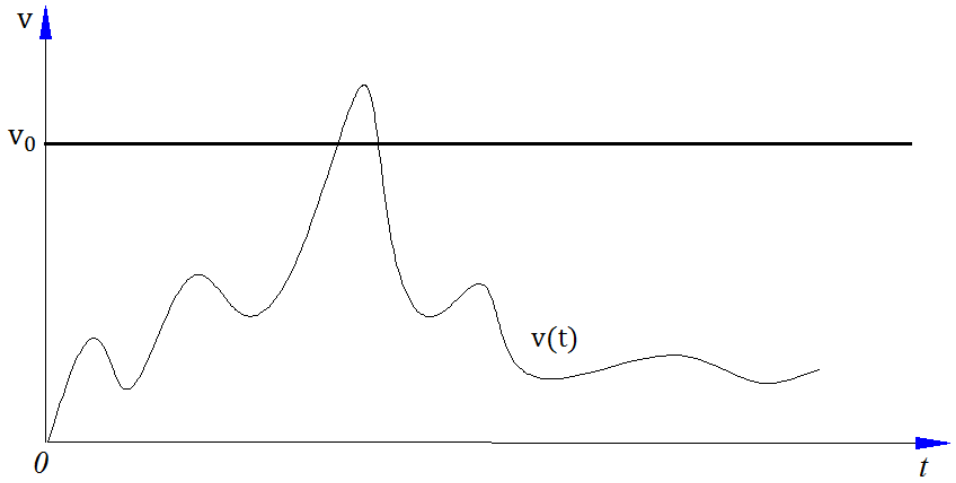

Fig. 4.7. Graphical illustration of emission theory for one-dimensional space

The main reliability indicator $P(t)$, the probability of fault-free operation on the segment $[0, t]$ corresponds to the probability of finding the quality vector in the permissible area during this time segment

$$P(t) = P\{v(t) \in \Omega;\ \tau \in [0, t]\}. \tag{4.50}$$

This expression does not take into account dispersion of physical and mechanical properties of materials and dispersion of load parameters. Provided that the random properties of the system are characterized by a vector random variable r, and the dispersion of the parameters of the external influence $q(t)$ is determined by the vector s, then the combined density of the distribution of the parameters r and s will be denoted as $p(r, s)$.

Then the probability of trouble-free operation of the system is calculated by the formula of full probability

$$P(t) = \iint P(t|r,s)\, p(r,s)\, drds\,. \qquad (4.51)$$

At the initial moment of time, the random process $v(t)$ with probability equal to 1 will be in the admissible region Ω , i.e. $P(0) = 1$. Emissions from this area in the time interval $[0, t]$ are very rare events. We denote the mathematical expectation of the number of emissions of a random process $v(t)$ in the time interval $[0, t]$ as $N(t)$. Then

$$PM[N(t)] \equiv \Lambda(t) \approx \int_0^t \lambda(t)dt\ . \qquad (4.52)$$

This relation connects the mathematical expectation of the number of emissions of a random process $v(t)$ with the intensity of failures. In the case when the corresponding mechanical system is highly reliable (and many years of experience in the operation of axle box bearing assemblies makes it possible to assert this), it is possible to use a Poisson flow of failures. Then the probability of trouble-free operation can be calculated using the following formula:

$$P(t) \approx exp[-\Lambda(t)]. \qquad (4.53)$$

The following procedure for assessing the performance of the axle box assembly is proposed, which will consist of the following stages:

- construction of a quality space for the most responsible elements of the axle box assembly;
- study of the characteristics of random load processes acting on axle box bearing assemblies;
- determination of the probability of emission of a random process of loads for the quality space;
- calculation of fail-safe characteristics of the axle box bearing assembly.

We will consider the bearing assembly as a system consisting of two main elements: a double-row conical bearing and an adapter through which all types of loads are transferred to the bearing. It is known that the durability of axle boxassemblies as a whole is determined mainly by the appearance of fatigue shells on the contact surfaces of rings and rollers. The cause of these shells is the contact stresses $\sigma(t)$ that exceed the compressive strength limit. That is, the quality of the system will be characterized by the value of the maximum contact stresses.

The quality space V in this case will be one-dimensional, and the range of admissible values is given by the constraint

$$\sigma(t) < \sigma_{\text{ст}}, \tag{4.54}$$

where $\sigma_{\text{ст}}$ is the compressive strength limit of the bearing steel.

The value of $\sigma(t)$ depends, in turn, on the magnitude of vertical loads $Q^{\text{в}}(t)$, which act on the axlebox bearing assembly. While

$$\sigma(t) = f[Q^{\text{в}}(t)], \tag{4.55}$$

where $Q^{\text{в}}(t)$ is the vertical load that causes the corresponding stresses.

Then the maximum possible stress $\sigma_{max}(t)$ can be compared to the maximum possible vertical loads $Q^{\text{в}}_{max}(t)$.

The vertical loads $Q^{\text{в}}(t)$ acting on the axle box bearing assembly depend on many factors: the magnitude of the static load, the number of axles, the state of the track superstructure, the technical condition of the running parts and the center plate arrangement, the speed of movement, etc. p. In practice, the last mentioned factors are united by a single concept, i.e., the coefficient of vertical dynamics.

Then, the probability of failure of the axle box assembly is defined as the probability of the appearance of vertical loads that cause stress in its elements that exceeds the limit of compressive strength, for the specified time

$$P(\tau) = P\{-Q^{\text{в}}_{max} < Q^{\text{в}}(t) < Q^{\text{в}}_{max};\ \tau \in [0, T]\}. \tag{4.56}$$

Then the amount of random process of change of vertical loads

$$N(\tau) = T \int_0^{\infty} f\left(Q^{\text{в}}, \dot{Q}^{\text{в}}, t\right) \dot{Q}^{\text{в}} dQ^{\text{в}}, \tag{4.57}$$

where $f\left(Q^{\text{в}}, \dot{Q}^{\text{в}}, t\right)$ is the compatible integrity of the distribution of the random process of changing vertical loads and its first derivative.

If the random process $Q^{\text{в}}(t)$ is stationary, then

$$f\left(Q^{\text{в}}, \dot{Q}^{\text{в}}, t\right) = f_1[Q^{\text{в}}(t)] \times f_2\left[\dot{Q}^{\text{в}}(t)\right]. \tag{4.58}$$

Assuming that the process of changing vertical loads is subject to the normal law of distribution

$$f_1[Q^{\text{в}}(t)] = \frac{1}{\sqrt{2\pi} \cdot \sigma_{Q^{\text{в}}}} exp\left[-\frac{(Q^{\text{в}} - M[Q^{\text{в}}(t)])^2}{2\sigma^2_{Q^{\text{в}}}}\right], \tag{4.59}$$

$$f_2\left[\dot{Q}^{\text{в}}(t)\right] = \frac{1}{\sqrt{2\pi}\cdot\sigma_{\dot{Q}^{\text{в}}}} exp\left[-\frac{\left(\dot{Q}^{\text{в}}\right)^2}{2\sigma^2_{\dot{Q}^{\text{в}}}}\right], \quad (4.60)$$

where $M[Q^{\text{в}}(t)]$ is a mathematical expectation of the random process of change of vertical loads $Q^{\text{в}}(t)$;

$\sigma^2_{Q^{\text{в}}}\sigma$ is its dispersion;

$\sigma^2_{\dot{Q}^{\text{в}}}$ is a variance of its first derivative;

$f_1[Q^{\text{в}}(t)]$ is a distribution density of the random process of changing vertical loads;

$f_2\left[\dot{Q}^{\text{в}}(t)\right]$ is a distribution density of the random process of changing the derivative of vertical loads.

The mean square deviation of the first derivative of the random process of changes in vertical loads is determined by the following formula:

$$\sigma_{\dot{P}^{\text{в}}} = \sqrt{-\left[\frac{\ddot{K}_{P^{\text{в}}}(\tau)}{K_{P^{\text{в}}}(\tau)}\right]_{\tau=0}}, \quad (4.61)$$

where $K_{P^{\text{в}}}(\tau)$ is the correlation function of the random process of changing vertical loads; $\ddot{K}_{P^{\text{в}}}(\tau)$ is the second derivative of the random process of changing vertical loads.

Finally, the formula for determining the amount of emissions will look like this

$$N(\tau) = \frac{1}{2\pi}\sqrt{-\left[\frac{\ddot{K}_{Q^{\text{в}}}(\tau)}{K_{Q^{\text{в}}}(\tau)}\right]}\cdot exp^{-\frac{(Q^{\text{в}}-M[Q^{\text{в}}(t)])^2}{2\sigma^2_{Q^{\text{в}}}}}. \quad (4.62)$$

4.3.3. Determination of probabilistic characteristics of loading processes

To determine the characteristics of the loading processes of axle box bearings, the results of operational dynamic tests of freight cars equipped with axle box assemblies with high-reliability bearings were used, which were carried out in accordance with the decision of the Center Rolling Stock Management Department of Ukrzaliznytsia by specialists of SE “UkrNDIV” (Kremenchuk). Five four-axle open-top cars of model 12-783 manufactured by JSC KVBZ with axle box assemblies, equipped with different types of bearings, were tested.

Prior to the start of dynamic tests, experimental open wagons underwent operational tests for some time on the experimental route of Ukrzaliznytsia Rokovata - Uzhhorod. So that the results that will be obtained during the dynamic running tests can be compared with each other in the future, the open-top cars were equally loaded, and also had approximately the same diameters, wheel profiles and characteristics of the spring groupings.

During running dynamic operational tests, typical equipment for recording dynamic processes was used, which was based on the use of the strain measure-

ment method. All the equipment used during the tests met the requirements of current regulatory documents.

During the preparation of the tests, which were carried out in the Nyzhnodniprovsk wagon depot of the Prydniprovsk railway, open-top cars bogies, the wheel pairs of which were equipped with test bearings, were disassembled and the places for gluing the strain gauges were cleaned. Further, in the selected places, according to the test method, they were installed on the side frames and the upper beam, connected to the measuring circuits. To ensure the possibility of carrying out tests during adverse weather conditions, strain gauges were isolated from moisture.

All measuring circuits were connected to the main apparatus, which registered all measurements and was located in the passenger-laboratory car.

In order to determine the scale of the recordings, before driving test trips, all measuring schemes were graduated with a static load.

The tests took place during daylight hours at an ambient temperature of minus 1 to minus 15°C.

Tests were carried out both in empty and loaded mode. When traveling in a loaded mode, the car's load-carrying capacity was fully used.

Train test runs with experimental open wagons were carried out on a straight section of the track with a length of 14.577 km. The speed range was from 40 km/h to the maximum allowed 120 km/h.

Curved track sections with a radius of 800 meters were located on the second and third kilometers of the test area, and on the fifth, ninth and fifteenth kilometers - a curve with a radius of one thousand meters. When passing the curves, the speed range was from 40 km/h to 100 km/h (with speeds up to the realization of unquenched acceleration equal to 0.7 m/s^2).

Switches located at stations Novomoskovsk-Dniprovsky and Balivka, the train with experimental open wagons proceeded at the maximum permitted speed of 40 km/h.

Registration of dynamic processes was carried out in two directions relative to the directions of movement.

Recording of experimental data was carried out by sequentially setting processes to the hard disk of the on-board computer. Also, the designations of the channels that corresponded to the recording of the device on which the sensors were installed were recorded in a special log. The serial number of the experiment, the name of the test route, the speed of movement in kilometers per hour (km/h) on the speedometer scale, the test mode, information about the equipment and test cars, as well as the date of the tests were recorded in the log.

The primary analysis of the obtained data during dynamic running tests was carried out using a personal computer and standard mathematical software for statistical processing of dynamic processes was used. The method of processing and evaluating test results is performed in accordance with the requirements of regulatory documents [78].

Dynamic processes of wagon loading, which were recorded on a magnetic medium, were processed by a program for calculating the instantaneous values of process amplitudes. Records of implementations were kept in both directions of train movement with a total duration of at least 300 s in each speed range. The sampling frequency of the recordings of dynamic processes was chosen to be more than 128 Hz, which made it possible to determine the indicators in the necessary frequency range.

Each random process was considered, calculations were made and the maximum values of the probability of vertical loads were determined. Next, average values for individual implementations were selected for each speed range. Then, as a result, one value of the indicator was determined within each speed range, starting with a speed of 40 km/h.

The results obtained during the experimental trips were later used to determine the characteristics of the load processes. In fig. 4.8-4.11 show some of the obtained realizations.

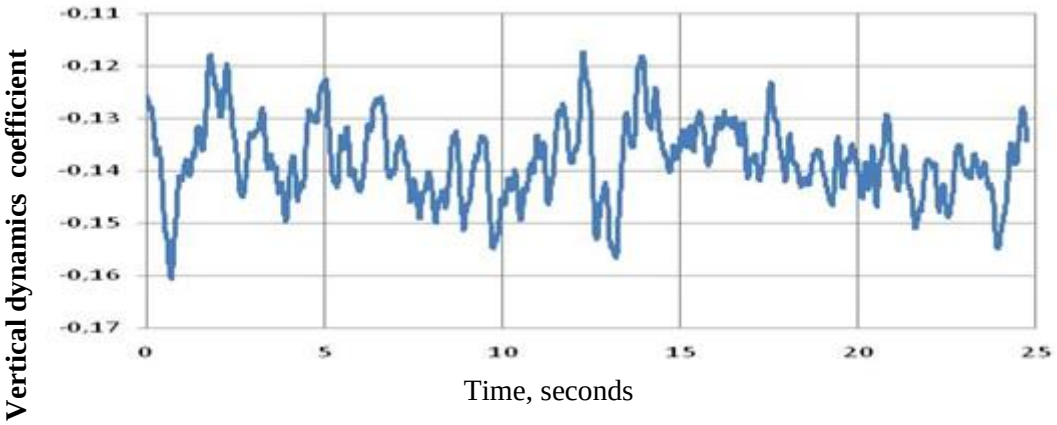

Fig. 4.8. Change in the coefficient of vertical dynamics at a speed of 40 km/h on a straight track section

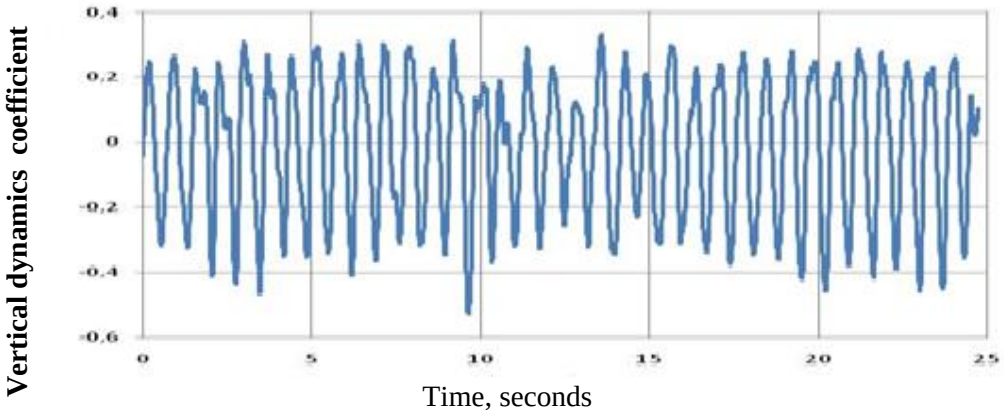

Fig. 4.9. Change in the coefficient of vertical dynamics at a speed of 120 km/h on a straight track section

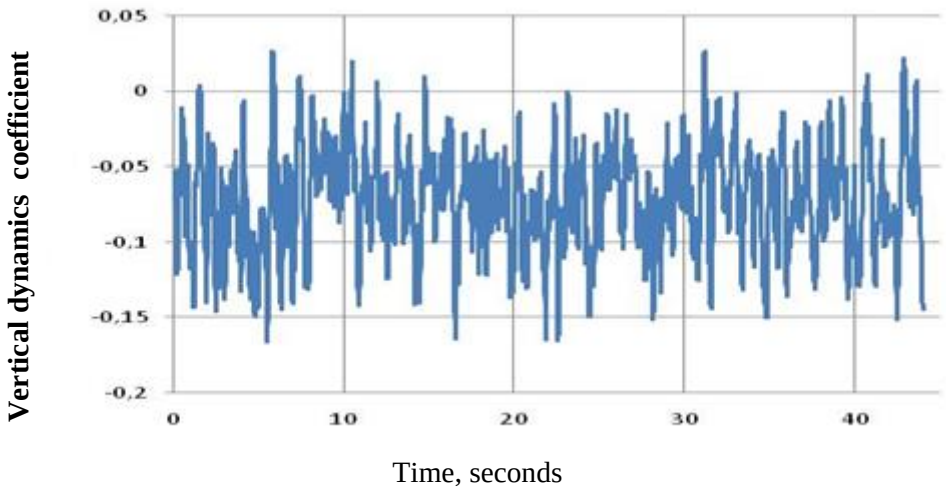

Fig. 4.10. Change in the coefficient of vertical dynamics at a speed of 40 km/h on a curved track section

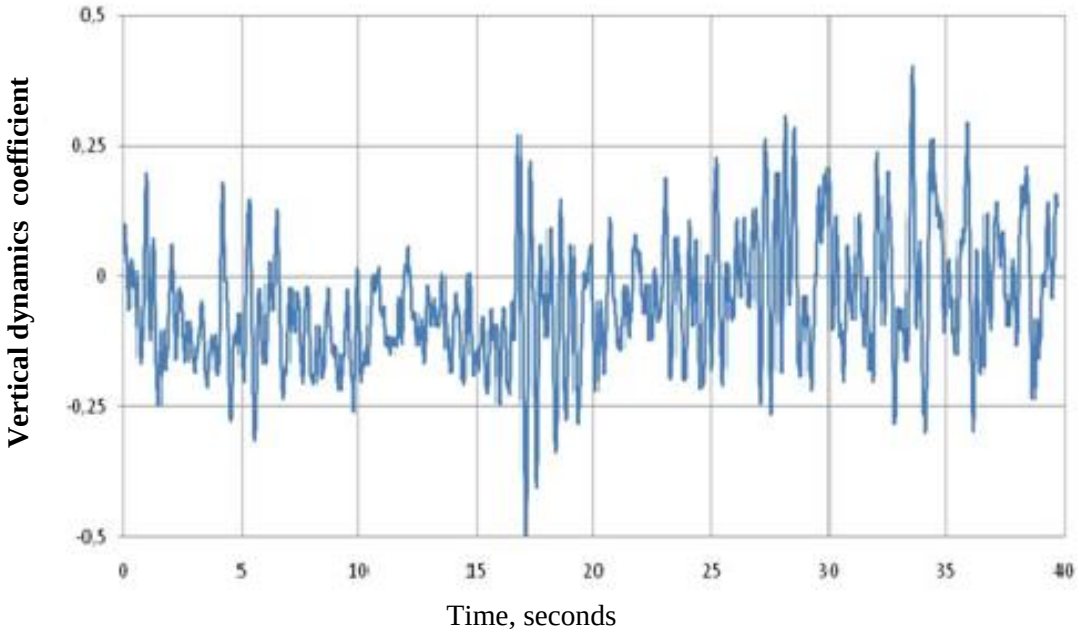

Fig. 4.11. Change in the coefficient of vertical dynamics at a speed of 100 km/h on a curved section of the track

It is obvious that the process of change in time of the coefficient of vertical dynamics is a random process with a pronounced sinusoidal component.

In order to determine the characteristics of the random processes that characterize the loading processes of the unreinforced masses of freight carts, the obtained arrays of values of the coefficient of vertical dynamics were subjected to statistical processing using the Microsoft Excel program package.

At the same time, the following parameters were determined: the amount of mathematical expectation, dispersion, as well as the minimum and maximum values of efforts.

The results of statistical processing show that the random processes that characterize the coefficient of vertical dynamics are distributed according to the normal law (Fig. 4.12).

Obtained parameters characterizing this law (table 4.1).

Dependencies characterizing the change in the mathematical expectation and maximum values of the random process on the speed of movement on straight and curved sections of the track are shown in Fig. 4.13-4.14.

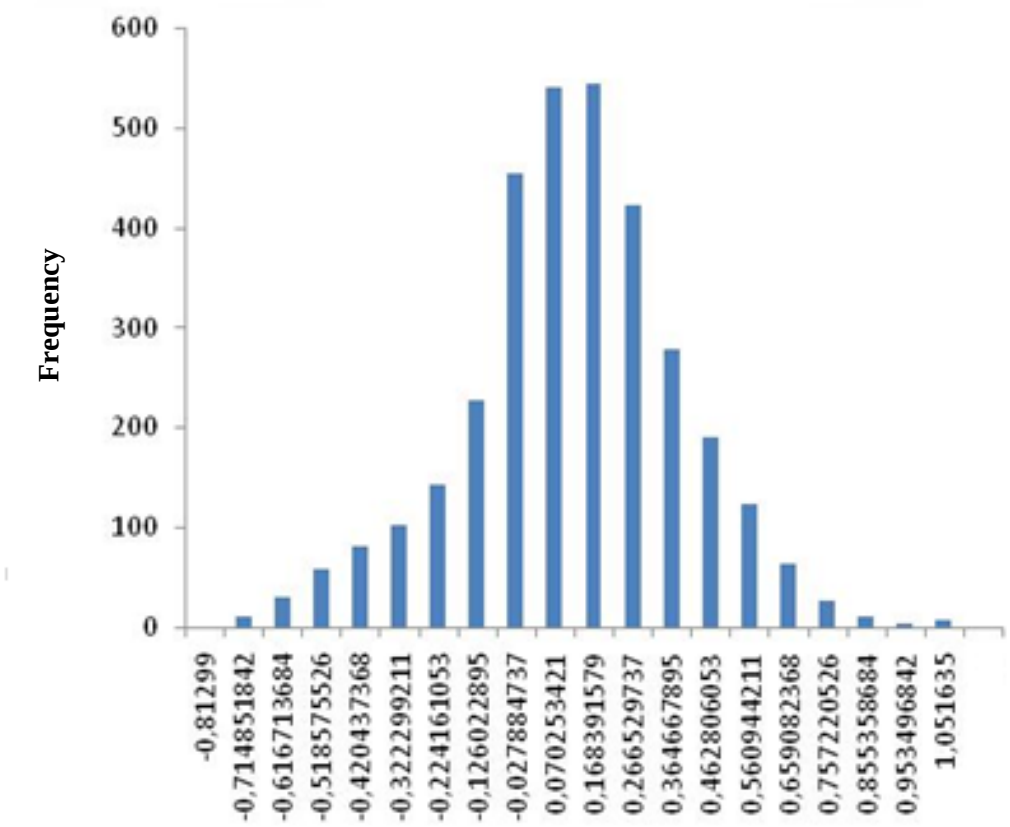

Fig. 4.12. Distribution of instantaneous values of the coefficient of vertical dynamics at a speed of 100 km/h on a straight section of the track

Table 4.1

The value of the distribution parameters

Speed, km/h	Driving mode	Mathematical expectation	Dispersion
40	Straight track section	-0,13793	0,00005
	Curved track section	-0,04602	0,00164
60	Straight track section	-0,05368	0,008313
	Curved track section	-0,15031	0,000177
80	Straight track section	-0,00278	0,008367
	Curved track section	-0,0558	0,013517
100	Straight track section	-0,05368	0,008313
	Curved track section	-0,05259	0,014342
120	Straight track section	-0,01878	0,046714
	Curved track section	-	-

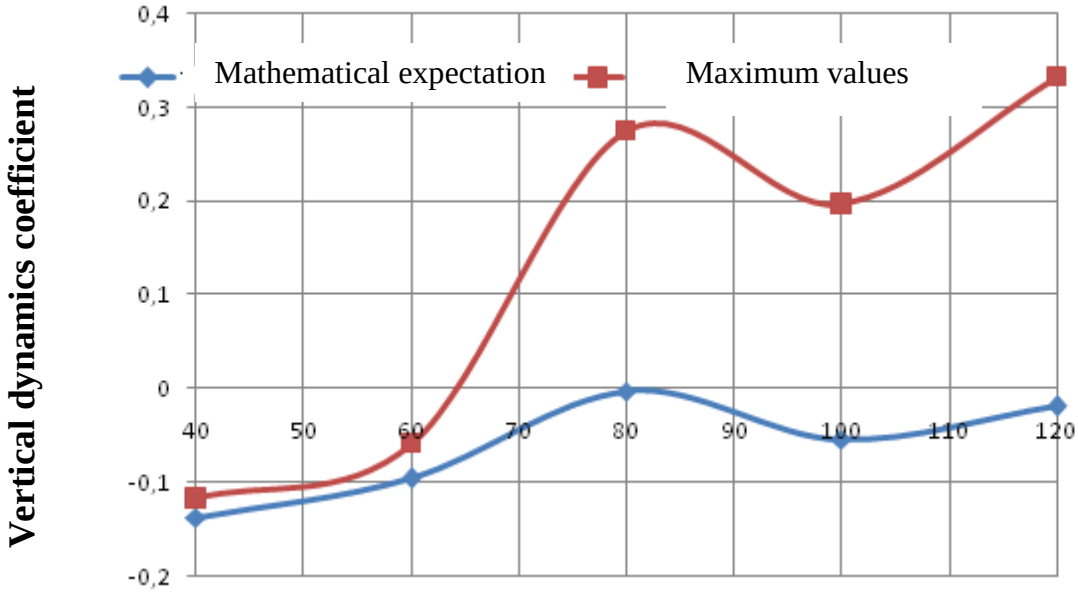

Fig. 4.13. Change of mathematical expectation and maximum values of the random process from the speed of movement on straight sections of the track

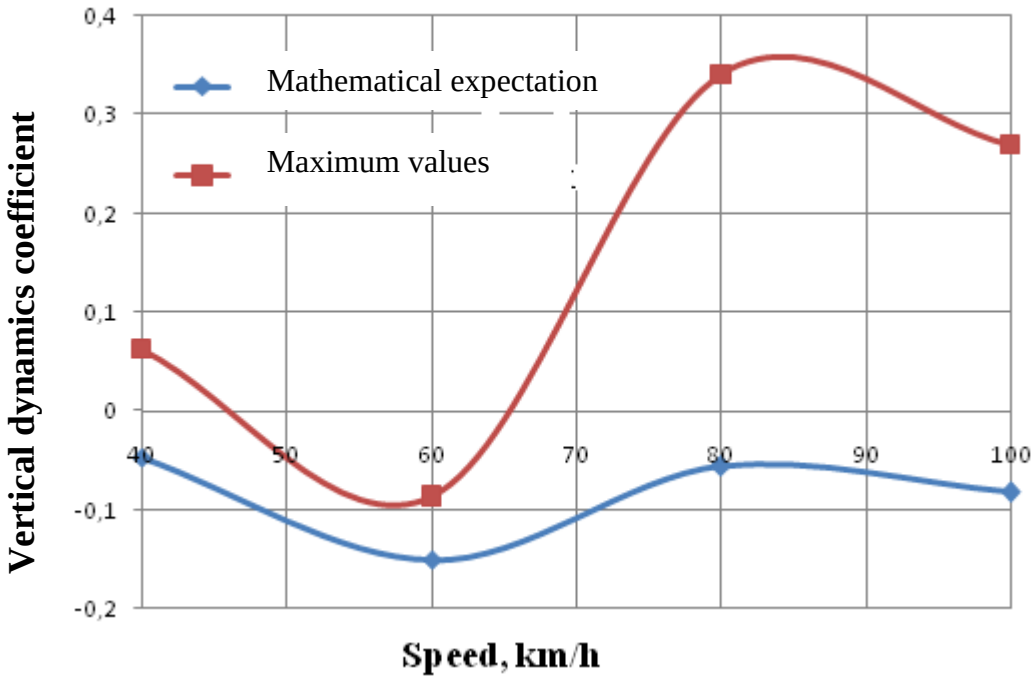

Fig. 4.14. Change of mathematical expectation and maximum values of the random process from the speed of movement on curved sections of the track

The values of the correlation function $K_{K_д^в}(\tau)$ were calculated as follows:

$$K_{\overline{K}_д^в}(\tau) = \frac{1}{n-m}\sum_{i=1}^{n}\left[K_д^в(t_i) - \overline{K}_д^в I K_д^в(t_{i+1}) - \overline{K}_д^в\right], \qquad (4.63)$$

where n is the number of points in the implementation; m is an integer defining the correlation interval $\tau = m\Delta t$, m =1,2,...).

In practice, the normalized correlation function is often used instead of the correlation function $K_{\overline{K}_д^в}(t)$.

$$R_{\overline{K}_д^в}(\tau) = \frac{K_{\overline{K}_д^в}(\tau)}{D_{\overline{K}_д^в}}. \qquad (4.64)$$

For ergodic processes, the condition must be satisfied

$$\lim_{i\to\infty}\left|R_{\overline{K}_д^в}(\tau)\right| = 0. \qquad (4.65)$$

It is usually replaced by an inequality of type

$$\left|R_{\overline{K}_д^в}(\tau)\right| \le R_{\overline{K}_д^в\sigma}(\tau_K), \quad \tau \ge \tau_K, \qquad (4.66)$$

where $R_{\overline{K}_{Д}^{в}}(\tau_K)$ is some arbitrary small, predetermined value; τ_K is a correlation interval that practically limits the maximum value of τ.

Usually $R_{\overline{K}_{Д}^{в}\sigma}(\tau_K)$ is accepted

$$R_{\overline{K}_{Д}^{в}}(\tau_K) \approx 0{,}1R(0). \tag{4.67}$$

Expressions of the type are often used to approximate empirical estimates of normalized correlation functions

$$R_{\overline{K}_{Д}^{в}}(\tau) = \mathrm{e}^{-\alpha|\tau|} \times \cos\beta|\tau| \tag{4.68}$$

where α, β are empirical coefficients determined by methods of mathematical statistics.

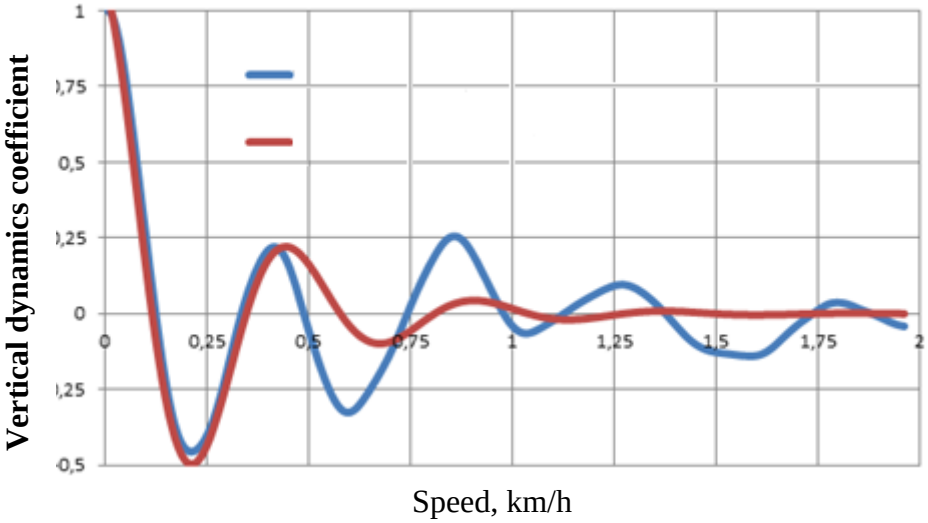

Fig. 4.15. Correlation function for movement on a straight section of the track at a speed of 100 km/h

The convergence of experimental and theoretical correlation functions was about 90%, which is quite satisfactory.

It was established that the process of changing the coefficient of vertical dynamic loads of unreinforced masses is a random process. It is proved that this process has a stationary and ergodic character.

The performed analysis made it possible to state that the random process of changing the coefficient of vertical dynamic loads of unreinforced masses obeys the normal law distribution The main parameters characterizing these processes depending on the speed and mode of movement are determined.

Correlation functions were calculated for the obtained random processes of change in the coefficient of vertical dynamics of freight cars and the parameters characterizing them were determined.

Calculations of the probability of failure-free operation were performed taking into account the results obtained in the previous section. The main disad-

vantage of correlation functions of the form (7.68) is the impossibility of differentiating them. Therefore, the second derivative of the correlation function was calculated using numerical methods.

During the calculations, according to [47], the time of the car being loaded and empty with the recommended speeds was taken into account. As a result, dependences were obtained that characterize the probability of trouble-free operation of the axlebox assembly depending on the speed and mode of movement on a straight section of the track (Fig. 4.16).

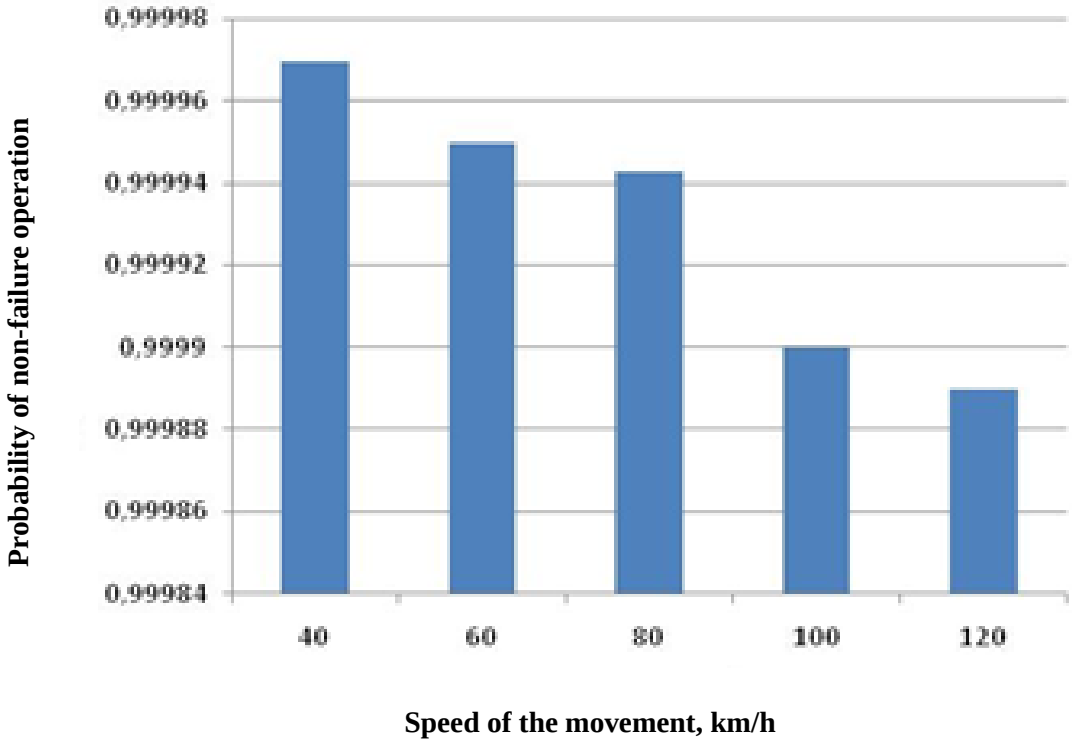

Fig. 4.16. The results of calculating the probability of non-failure operation of axlebox bearings while moving on a straight section of the track.

REFERENCES

1. Andereason, S. (1973). Load Distribution in Taper Roller Bearing Arrangment Considering Misalighment. *Tribology*. Vol. 6, 3, 84-92
2. Boussininesq, J. (1895). *Application des potentials a letude de leguilibre et du mouvement des solids elastigues*. Paris
3. Brandlein, J. (1972). The fatigue life of axial loaded cylindrical roller bearings. *Ball and roller bearing engineering*, 7-11
4. Broszeit, E., & Zwirlein O. (1986). "Internal Stresses and Their Influence on Material Stresses in Hertzian Contacts Calculations with Different Stress Hypothesis". *ASME J. of Tribology*. Vol. 108, 387-393
5. Gabelli, A., Ioannides E., & Miglietta E. (1996). "*Increased Life Performance of Rolling Elements Bearings in Gearboxes and Transmissions" International Conference on Gears, Dresden May '96, VDI Benchte* Nr.1230. P. 631-645.
6. Harris, T. (2006). *Rolling bearing analysis*. New York.
7. Harris, T. A. (1971). An analytical method to prevent skidding in trust loaded angular contact ball bearing. *ASME Trans*., Vol. 93, 17-24.
8. Hertz, H. (1895). Über die Berührung fester elastischer Körper. *Journal für die reine und angewandte. Mathematik* , 92, 156-171. Leipzing
9. Ioannides, E., Harris T. (1985).A new fatigue life model for rolling bearings. *ASME J. of Tribology*. Vol. 107, 3, 367-378.
10. Ioannides, E., Berling G., Gabelli A. (2001). The SKF formula for rolling bearing lifetime. *Evolution*, 1, 25-28.
11. Kakuta, K., Kohno T., Ota H. (1996). Generating Mechanism of Forces Acting on Retainer of Ball Bearings Supporting Unbalanced Rotating Shaft. *Transactions of the Japan Society of Mechanical Engineers*, 62-600, 3210–3215.
12. Kalker, J. J. (1977). The surface displacement of elastic, half-space loaded in slender, bounded,curved surface region with application to the calculation of a contact pressure under a roller. *Journal of instrumental matemathic application*,Vol. 19, 2.
13. Kleckner, R.,. Pirvics I., Castelli V. (1985). High-speed cylindrical rolling element bearing analysis CYBEAN – analytical formulation . *ASME Trans.*, 3, 277–287.
14. Kobayashi, T. H., Fujiwara H. (2001). Dynamic Analysis of Needle Roller Bearings in Connecting Rod Big-EndApplications. NTN Technical Review, 69, 89–96.
15. Lju, J. Y. (1976). Analyses of Tapered roller Bearings Considering High Speed and Combined Loading *Transaction of ASME. Ser. F*. Vol. 98, 4. –.
16. Losche, T. (1989). New aspects in the realistic prediction of the fatique life of rolling bearings. *Wear*, 134, 357–375.
17. Sakaguchi, T., Harada K. (2006). Dynamic Analysis of Cage Stress in

Tapered Roller Bearings. *Proc. ASIATRIB.* Kanazawa, 649–650.
18. Takuya, O. (2006). High Load Capacity Cylindrical Roller Bearings. NTN technical review, 74, 90-95.
19. Timoshenko, S. P. (1924). The Approximate Solution of Two-Dimensional Problems in Elaticity Phil. Mag., S.6, Vol. 282, 1005-1104.
20. Martynov I. E. Axlebox assembly of a railway vehicle 1574502 (USSR), class. B61 F15/12, 05/19/88, No. 442783/27-11; Appl. May 5, 1988; publ. June 6, 1990, Bull. No. 24, 3 p.
21. Abashkin, V.V., V.F.Devyatkov (1978). Axlebox assembly with elastic elements. *Improving the reliability and durability of roller bearings in the axle boxes of cars: VNIIZhT* , 583, 13-23. M.: Transport
22. Akbashev, B. Z., Losev A.V. (1982). Research on increasing the axial load capacity of axle bearings of locomotives, *Intercollegiate thematic collection of scientific works,* 167, 27-34. Rostov-on-Don.
23. Andrievsky, V. G. Yakhin B. A., Gaidamaka A. V. (1987). Influence of roller misalignment on the wear of a roller bearing cage 42726. *Bulletin of mechanical engineering*, 1, 32−34.
24. Andrievsky, V. G., Borzilov I. D., Fedorets E. V. (1981). *Study of axial loading of roller bearings of freight cars.* Dep. at the Central Research Institute of TEI MPS,1566.
25. Andrievsky, V. G. (1985). Fatigue failure of bearing cages, in which the rolling elements perceive the axial load. Dep. at the Central Research Institute of TEI MPS, 2959.
26. Batenkov S.V. (1980). Influence of mounting misalignments on the durability of radial roller bearings with short cylindrical rollers. *Proceedings of VNIPP*, 2, 54−58.
27. Batenkov, S.V. (1979). Analysis of the effect of misalignment on the durability of cylindrical roller bearings. *Proceedings of VNIPP*, 3, 111−121.
28. Batenkov S. V. (1982). Study of the influence of misalignments on the durability of cylindrical roller bearings. *Candidate's thesis*: *05.22.07*. Moscow.
29. Beizelman, R. D., Tsypkin B. V., Perel L. Ya. (1975). *Rolling bearings. Directory*. Moscow: Mashinostroenie.
30. Berezhinsky, V. M. (1982). Increasing the durability of tapered bearings used in the hubs of the front wheels of trucks *Research and development of progressive bearing designs: VNIIPP*, 3, 54-73. Moscow
31. Berestaev, O. V., Goman A. M., Yakimovich A. A. (1990). To the solution of the problem of contact interaction of conical rollers with intersecting axes. *Bulletin of Universities. Engineering*,1, 3-7.
32. Claude Sonner (1977). *An axlebox for wheelsets of railway rolling stock*. Patent 583727 USSR, MKI3 B 61F 15/14 / (France); the applicant and patent holder is a foreign firm "Societe Nouvel de Rulerman". No. 1834293/27-11. Appl. September 29, 1972, publ. December 5, 1977, Bull. No. 45.
33. Bhardvaj, M. A. (1977). Systematic approach to determining the actual misalignments and load distribution for cylindrical roller bearings in serial

gears. *Problems of friction and lubrication*,1, 44-54.
34. Virabov, R. V. (1978). On the issue of misalignment of roller guides. *Bulletin of mechanical engineering*, 2, 12−15.
35. Volkov N. N., Rodzevich N. V. (1972). *Rolling bearings of wheelsets of wagons and locomotives*. Moscow: Mashinostroenie.
36. Gaidamaka, A.V.(2017). Methodology for the advancement of the technical level of roller bearings in axle boxes for railway vehicles. *Candidate's thesis*: 05.02.02. Odessa
37. Gaidamaka, A. V. (2009). *Roller bearings. Basic knowledge and areas of improvement*. Kharkiv: Publ. House "Fort"
38. Gaidamaka, A. V. (1988). Increase in load capacity and reduction of resistance to rotation of heavily loaded roller bearings by changing the design and material of the cage: 05.02.02 / A. V. Gaidamaka. - Kharkiv,. - 23 p.
39. Gaidamaka, A. V. (2011). Roller bearings of axleboxes of wagons and locomotives: modeling and improvement. *Monograph.* Kharkiv: Publishing House "Cursor"
40. Galakhov, M. A. (1974). Influence of misalignment of rings on the distribution of pressure along the generatrix of a cylindrical roller. *Proceedings of VNIPP*, 5, 73-80.
41. Galakhov M. A., Flaksman Ya. Sh. (1977). Choice of roller-ring contact geometry for axle box bearings of rolling stock. *Intercollegiate thematic collection*, 140, 56-60. Rostov-on-Don
42. Galakhov, M.A. (1976). Optimal form of the crowned roller. *Vestnik mashinostroeniya*, 7, 36-37.
43. Galakhov, M. A., Flaksman Ya. Sh. (1978). Pressure distribution in the contact of a profiled roller with a bearing ring. *Bulletin of mechanical engineering*, 2, 34-37.
44. Galin, L. A. (1949). *Basic problems of the theory of elasticity*.Moscow: Mashgiz.
45. Gnedenko, B. V., Belyaev Yu. K., Soloviev A. D. (1982). *Mathematical methods in the theory of reliability*. Moscow: Nauka.
46. Johnson, K. V. (1989). *Mechanics of contact interaction*. Moscow: Mir.
47. Freight wagons. General requirements to rebuilding and designing of new and modernized cars with a gauge of 1520 mm (non-self propelled). *DSTU 7598:2014 from the 1-st* July 2015. Kyiv: Minekonomrozvytku Ukrainy.
48. Dunaev P. F., Lelikov O. P. (1976). Determination of the limit angles of misalignment of rolling bearing rings. *Bulletin of mechanical engineering*, 2, 3-7.
49. Esipov, V. V., Vendrovsky O. P. (1982). Improving the efficiency of cylindrical roller bearings of axle boxes of electric locomotives under the influence of axial loads. *Intercollegiate thematic collection*, 167, 42-50Rostov-on-Don.
50. Zaikin, G. I. (1982). The main directions of improvement of railway roller bearings in order to increase their operational reliability and durability. *Intercollegiate thematic collection*, 167, 3-8. Rostov-on-Don

51. Study of unevenness of the wheels of passenger cars. (1979). *Proceedings of VNIIZhT*, 608.
52. Varfolomeev V. A., Motovilov K. V., Martynov I. E. (1990). *The study of axial forces acting on the axle assemblies of freight cars*. Ministry of Railways of the USSR, Moscow State University of Railway Transport Engineers after F. E. Dzerzhinsky. Moscow: Dep. in the Central Research Institute of TEI of the Ministry of Railways, No. 5279 railway.
53 Instructions for the operation and repair of axlebox assemblies of wheel pairs of freight cars. (2014). *TsV-0143*. Kyiv: Ukrzaliznytsia.
54. Kanarchuk, V.E., Polyanskyi S.K., Dmitriev M.M. (2003). *Reliability of machines*. Kyiv: Lybid
55 Kvasov, V. I., Tsikhanovich L. G. (1972). Influence of misalignments on the durability of cylindrical roller bearings. Contact-hydrodynamic theory of lubrication and its practical application in engineering. *Proceedings of the 1st All-Russian Conference: abstracts.* (pp. 29−30). Kuibyshev
56. Kvasov, V. I., L. G. Tsikhanovich (1972). Some questions of alignment of contact pressures along the generatrix of the rolling bodies of axlebox cylindrical roller bearings. *Intercollegiate thematic collection,* 89, 66-79. Rostov-on-Don.
57. Kvasov, V. I., Tsikhanovich L. G. (1972). Estimation of the stress state and durability of cylindrical roller bearings at misalignments. *Intercollegiate thematic collection,* 89, 52−65. Rostov-on-Don.
58. Classification and catalog of defects and damages of bearings. (2005). *Departmentsl regulatory document of the State Administration of Railroad Transport of Ukraine*. Kyiv: Ukrzaliznytsia.
59. Kovalev, E. A., Kvasov V. I. (1982). Operational durability of axle box bearings for cars and locomotives, *Intercollegiate thematic collection*, 167, 8-13. Rostov-on-Don.
60 Komissar A.G. (1987). *Rolling bearings in heavy operating conditions*. Reference book. Moscow: Mashinostroenie.
61 Lukin V. V., Shadur L. A., Koturanov V. N., Khokhlov A. A., Anisimov P. S. (2000). *Design and calculation of wagons*. Textbook for universities railway. transp. V. V. Lukin (Ed.). M.: UMK MPS of Russia.
62 Krasenkov V.I. (1958). On the applicability of Hertz's theory to one spatial contact problem *News of universities. Engineering*, 1, 16-26.
63 Krasyukov, A.P. (1982). Efficiency of using hollow rollers for axle boxes of rolling stock. *Intercollegiate thematic collection*, 167, 57-66. Rostov-on-Don
64 Kudryavtsev, N. N., Belousov V. N., Saskovets V. M. (1981). Influence of short unevenness of wheels and rails on dynamic forces and accelerations of running parts of cars. *Proceedings of VNIIZhT*, 610, 4-23.
65 Kudryavtsev, N. N., Belousov V. N., Ivanov S. G. (1984). Investigation of vibrations of roller bearings of axlebox assemblies of cars. *Bulletin of VNIIZhT*, 3, 30-33.
66. Kannel, I. V. (1974). Comparison of calculated and measured axial pressure

distributions between cylinders. *Problems of friction and lubrication*. Vol. 96, 3, 231-237
67 Leykakh L. M. (1978). Correction of the crossing of the axes of rollers and rings in roller bearings. *Vestnik mashinostroeniya*, 10, 27-29.
68 Lelikov, O. P. (2006). Shafts and supports with rolling bearings. Design and calculation. Moscow: Mashinostroenie.
69 Losev, A.V. (1974). Changing the design of roller bearings for high-speed movement. *Railway transport*, 12, 47-49.
70 Losev, A. V. (1972). Study of the work of cages of railway roller bearings at high speeds. *Candidate's thesis*. Moscow.
71 Martynov, I. Ye. (2007). Determining the durability of the tapered bearings for railway rolling stock. *Collection of scientific works of UkrDAZT*, 86, 56-61.Kharkiv.
72 Martynov, I. E. (2000). Analysis of the operating experience of cylindrical roller bearings of axle boxes of freight cars. *Bulletin of SNU named after V.Dahl*, 5 (27), 157-159. Lugansk.
73 Melnichuk, V. A., Donchenko A. V., Martynov I. E. (2002). On the issue of increasing the reliability of axlebox assemblies with rolling bearings. *Railway transport of Ukraine*, 5, 34-37.
74 Belyaev, Yu. K., Bogatyrev V. A., Bolotin V. V. et al. (1985). *Reliability of technical systems.* Handbook. I.A. Ushakov (Ed.). Moscow: Radio and communication.
75 Novikov, V.F., Krasyukov A.P. (1977). Influence of distortions of rings on the durability of cylindrical roller bearings with hollow rollers. *Intercollegiate thematic collection*, 140, 74-82. Rostov-on-Don.
76 Novikov, V. F., Krasyukov A. P. (1975). Study of load distribution in bearings with hollow rollers and analysis of their stress state. *Intercollegiate thematic collection*, 112, 63-69. Rostov-on-Don.
77 Novikov, V. F. Study of the distribution of axial load between the rolling elements of a cylindrical roller bearing. *Intercollegiate thematic collection*, 140, 48-56. Rostov-on-Don.
78 *Norms for the calculation and design of railway cars of the Ministry of Railways of the 1520 mm gauge (non-self-propelled)*. (1996). Moscow: GosNIIV-VNIIZhT. Moscow.
79 Spitsyn, N. A., Mashnev M. M., Kraskovsky E. Ya. et al. (1970). Supports of axles and shafts of machines and devices. Moscow: Mashinostroenie.
80 Orlov A. V. (1985). *Rolling bearings with surfaces of complex shape*. Moscow: Mashinostroenie.
81 Tsurkan I. G., Kogan M. S., Samoshin V. A. et al. (1973). Features of the behavior of an extreme pressure additive in a lubricant for axlebox roller bearings. New oils and lubricants for rolling stock assemblies. *Coll. of scientific works of VNIIZhT*, 490, 38-48. Moscow: Transport.
82 Petrov, V. A., Amelina A. A. (1984). Analysis of the choice and development of axle box structures for equipment of wagons of the main railways of the

USSR. *Proceedings of VZIIT*, 122, 4-25. Moscow.
83. Pikovsky, V. A. (1970). Some issues of calculation and application of roller bearings with hollow rolling elements. *Collection of scientific works*, 82, 39-45. Perm.
84 Pinegin, S. V. (1965). Contact strength in machines. Moscow: Mashinostroenie.
85 Pini, V. E. (1982). Force interaction of parts of a cylindrical roller bearing under combined load. *Intercollegiate thematic collection*, 167, 71-77. Rostov-on-Don.
86 Pokrovskij, B. N. (1979). On the issue of γ-percentage service life of rolling bearings, taking into account the history of their damage identification. *Proceedings of VZIIT*, 122, 48-51. Moscow.
87 Pokrovskij, B. N. (1979). On the issue of assessing the reliability of rolling bearings of axle boxes of cars. *Proceedings of VZIIT*, 101, 5-8. Moscow.
88 Pokrovskij, B. N. (1978). On the formulation of the question of assessing the reliability of rolling bearings of axle boxes of cars. Proceedings of VZIIT, 97, 41-49. Moscow.
89 Polyakov, A.I., Devyatkov V.F. (1982). Results of testing bearings of increased strength and durability from steel ShKh4. *Ways to improve the design of axlebox assemblies of cars with rolling bearings: Coll. of VNIIZhT*, 654, 31-37.
90 Prilepov, N. N. Petrov, V. A. (1976).What the analysis of failures of rolling bearings showed. Railway transport, 4, 55-57.
91 Motovilov, K. V., Martynov, I. E., Perov, S. V. et al. (1989). Results of life tests of axlebox assemblies of the MIIT design. No. 5028 railway. Moscow: Dep. in the Central Research Institute of TEI of the Ministry of Railways
92 Rodzevich, N.V. (1986). Selection and calculation of the optimal generatrix for rolling elements of roller bearings. *Engineering science*, 1, 90-99.
93 Rodzevich, N.V. (1970). Choice and calculation of the optimal form of rollers for bearings. *Bulletin of mechanical engineering*, 7, 29-33.
94 Rodzevich, N.V. (1960). Elimination of the concentration of contact pressures in bearings. *Mechanical engineering*, 7, 67-76.
95 Russkikh, S. P., Berezhinskiy, V. M. (1981). Determination of linear load in the contact of a roller with a ring in a bombed roller bearing. *Improving the design and increasing the service life of rolling bearings: Coll. of VNIIPP*, 4, 17-25. Moscow.
96 Saversky, A.S. (1976). *Influence of misalignment of rings on the performance of rolling bearings: review*. Moscow: NIIavtoprom.
97 Spektor, A. A. (1963). Optimization of internal geometry and calculation of characteristics of contact interaction of parts of cylindrical roller bearings. *Proceedings of VNIIPP*, 1 (33), 60-74. Moscow
98 Spitsyn, N. A., Andrievsky, V. G. (1980). Effect of radial load on the forces acting on the cage of a radial bearing. *Bearing industry*, 8, 3-7.
99 Spitsyn, N. A. (1963). Theoretical research in the field of determining the optimal shape of a cylindrical roller. Proceedings of VNIPP, 1, 10-15.

100 Tallian, T. (1976). Evaluation of durability under contact fatigue under rolling conditions in a contaminated lubricant. Part 1. Mathematical model. *Problems of friction and lubrication*, 2, 64-73.
101 Tallian, T. (1976). Evaluation of durability under contact fatigue under rolling conditions in a contaminated lubricant. Part 2. Experiment. *Problems of friction and lubrication*, 3, 35-46.
102 Tallian, T. (1978). Predicting the effect of friction coefficient and surface microgeometry on rolling fatigue life. *Problems of Friction and Lubrication*, 2, P.12–24.
103 Ustich, P. A., Karpychev,V. A., Ovechnikov, M. N. (1999). *Reliability of railway non-traction rolling stock.* Moscow: IG "Variant".
104 Filatova, E. M., Martynov, V. S. (1977). Resistance to rotation of a cylindrical roller bearing under combined load. *Intercollegiate thematic collection,* 140, 66-74. Sat. - Rostov-on-Don.
105 Filatova, E. M., Martynov V. S. (1978). Comparative evaluation of the resistance to rotation of a cylindrical roller bearing with flat and convex roller-board contacts. *Proceedings of VZIIT*, 97, 72-84. Moscow.
106 Filatova, E. M., Matyushin S. I. (1982). Improvement and development of new methods for calculating axle bearings, *Intercollegiate thematic collection,* 167, 50-56. Rostov-on-Don.
107 Khasman, I. A. (1967). Improving the reliability and durability of rolling bearings in axle boxes of railway rolling stock. Moscow: NIINAvtoprom.
108 Tsurkan, I. G., Kogan M. S. (1970). The principle of operation and effectiveness of extreme pressure additives in axlebox lubricants. *Operation of wagon axle boxes with roller bearings at high-speed movement. Proceedings of VNIIZhT,* 405, 110-116. Moscow: Transport.
109 Tsyurenko, V. N., Yurakov P. S. (1978). Methods of experimental studies of the kinematics and temperature regime of rolling bearings in wagon axle boxes. Improving the reliability and durability of roller bearings in wagon axle boxes. *Proceedings of VNIIZhT*, 583, 90-97.
110 Tsyurenko, V. N., Petrov V. A. (1982). Reliability of roller bearings in axle boxes of wagons. Moscow: Transport.
111 Tsyurenko, V. N., Shavshishvili A. D. (1978). Determination of the optimal shape of the outline of the ends of the rollers of cylindrical bearings. *Proceedings of VNIIZhT*, 583, 41-48.
112 Tsyurenko, V. N. (1982). Experience in the operation of wagons with axleboxes on rolling bearings. Ways to improve the design of axleboxes of cars with rolling bearings. *Proceedings of* VNIIZhT, 654, 4-26. Moscow: Transport.
113 Tsyurenko, V. N. (1978). Causes of cracks in the sides of the rings of cylindrical roller bearings. Improving the reliability and durability of roller bearings in the axle boxes of cars. *Proceedings of VNIIZhT*, 583, 36-41. Moscow: Transport.
114 Chebanenko, V. M. (1952) On the issue of choosing a rational design for a carriage roller axle box. *Railway engineering*, 7, 11-16.

115 Shavshishvili, A.D. (1981). Investigation of the operability of rolling bearings of axleboxes of wagons intended for operation at speeds up to 200 km/h. *Candidate' thesis.* Moscow.
116 Shavshishvili, A. D. (1982). Operation of cylindrical roller bearings in contact between the end of the roller and the bead of the ring. *Proceedings of VNIIZhT*, 654, 90-97.
117 Shadur, L. A., Chelnokov, I. I., Nikolsky L. N et al (1980). Railway cars. Moscow: Transport.
118 Ekholm, K. F., Devyatkov V. F. (1953). Car axle boxes with roller bearing. Moscow: Transzheldorizdat.
119 Yavlensky, A. K. (1978). Theory of dynamics and diagnostics of rolling friction systems. Leningrad: Publishing house of Leningrad.

State Enterprise "Ukrainian Scientific Railway Car Building Research Institute"

(SE "UkrNDIV")

I.E. MARTYNOV, A.V. TRUFANOVA,
O.M. SAFRONOV

AXLEBOX ROLLER BEARINGS FOR RAILWAY VEHICLES: DESIGN AND CALCULATIONS

Recommended for publication by the Scientific and Technical Council of the State Enterprise «Ukrainian Scientific Railway Car Building Research Institute" (Minutes No. 2 dated December 22, 2022)

Paper format: 60x84⅛, Circulation: 100 copies.

Publishing house SE "UkrNDIV"

Publisher's editorial address:

33, I. Prykhodka Str., Kremenchuk, Poltava region, 39621

www.ukrndiv.com.ua

Certificate of entry into the State Register of publishers, manufacturers and distributors of printed products No. 5515 dated August 10, 2017

SE "UkrNDIV" 2022 – 121 p.

ISBN 978-966-97716-7-4